# Technical Memorandum

# Identification of Flash Flood-Prone Areas that Warrant Outdoor Warning Sirens

*Submitted by*: Water Engineering Research Center
@ The University of Texas at Arlington
In collaboration with AtkinsRéalis

February 26, 2026

TEXAS WATER
DEVELOPMENT BOARD

# EXECUTIVE SUMMARY

## Purpose and Authority

In July 2025, severe flash flooding led to a state disaster declaration for 30 counties within Texas. In response, during the second called session, the 89th Texas Legislature passed, and Governor Abbott signed, Senate Bill 3 (SB3), establishing requirements for outdoor warning sirens in areas identified within the 30-county, flash flood-prone area; and Senate Bill 5 (SB5), providing funding through a state-administered grant program to assist local governments with the cost of installing outdoor warning sirens (OWS) required under SB3.

This report explains how the Texas Water Development Board (TWDB) identified areas within the 0.2 percent annual chance floodplain with elevated risk of flash flooding in the 30 disaster-declared counties affected by SB3. The TWDB will provide the designated elevated risk segments to local stakeholders to assist them in selecting locations for installation of outdoor warning sirens.

## Foundational Efforts

In recent years, the TWDB has made significant strides in flood planning, flood science, and flood research. Most notably in terms of flood planning, the first State Flood Plan for Texas was released in 2024, which was supported through Regional Flood Planning Group (RFPG) efforts to develop regional flood plans through the first regional planning cycle from 2020 to 2023 (TWDB, 2024). The development of this plan relied on the creation of many foundational datasets. In terms of flood science, TWDB has supported initiatives to improve flood modeling, which includes statewide coverage and improved availability of Base Level Engineering (BLE) models.

## Study Approach

Flash floods develop rapidly and pose significant risks to life and property. To determine where sirens are most needed, the TWDB developed an index called the Flash Flood Hazard Index (FFHI). Flash Flood Hazard Index provides a quantitative measure of likelihood of flash flood occurrence. This index combines terrain, geomorphic, hydrologic, land cover and meteorologic factors into a single score to quantify flash flood potential. To identify areas of potential flash flooding, a threshold for Flash Flood Hazard Index was estimated based on literature review and sensitivity analyses. Areas above the threshold indicate areas where flash flooding is most likely—which when combined with structures and people exposed support identification of Flash Flood Risk Areas (FFRA) where installation of outdoor warning siren systems may be warranted.

The FFHI estimation was based on 13 different physical factors representing terrain, geomorphic, hydrologic, land cover and meteorological categories that influence flood potential. Peer-reviewed literature, available data, and regional expertise were utilized to develop the FFHI. FFHI results were validated through comparisons with available flood hazard models and maps, as well as data showing areas that have a history of severe flooding.

The Analytic Hierarchy Process (AHP) was used to estimate Flash Flood Hazard Index. The Analytic Hierarchy Process is based on a weighting system that is a widely used, well documented and structured method for weighing multiple factors. AHP, although an approximate methodology, provides a highly scalable and credible approach that estimates relative hazard rather than deterministic flood conditions to assess flood hazard at the scale of this study area (30 counties) and meet the schedule for implementation of SB3 and SB5.

The Flash Flood Hazard Index is combined with exposure data such as camp locations, parks, and buildings to identify areas that are likely subject to damage from flash flooding. The delineation of flash flood risk areas is thus an intersection of flash flood hazard potential areas (areas above the Flash Flood Hazard Index thresholds) and exposure within the 0.2 percent annual chance floodplain from the TWDB 2024 Flood Quilt. The 2024 Flood Quilt was the most recent, readily available, and planning level dataset backed by hydrologic and hydraulic modeling.

The workflow implemented for this initiative used readily available data related to terrain, rainfall characteristics, population density, and building locations to conduct the assessment. Areas with the highest flash flood risk were generally characterized by steep slopes, rapid runoff, and concentrated development, particularly in urban settings. However, areas where people are anticipated to congregate outdoors with the intent of an overnight stay, such as camps or campgrounds, were also identified. Rural areas with residential or agricultural-related development were also identified as high risk in certain locations.

Flash Flood Hazard Index results were validated using historical flood records and flood hazard models, including Base Level Engineering (BLE) outputs. The use of Flash Flood Hazard Index helps address the limitations of historical observation and records, which are often incomplete, temporally limited, and have limited spatial coverage. Historical observations show where flash flooding has occurred, but physical watershed characteristics provide comprehensive spatial coverage to identify where flash flooding has the potential to occur.

Typically, flood hazards and risks are analysed and mapped using hydrologic and hydraulic models like those employed in Base Level Engineering (BLE). However, development or implementation of such models was not feasible for this study due to the need for expedited delivery to support timely SB3 compliance. A standard approach would have required development of new guidance, storm-duration analyses, and model configuration or retrofitting across approximately 48 HUC-8 watersheds, along with evaluation of flash flood characteristics. Because this approach would have significantly delayed implementation, the team developed an alternative, approximate approach that estimates and combines the hazard index with exposure data to identify areas of flash flood risk that may benefit from implementation of outdoor warning sirens. Though new hydrologic and hydraulic (H&H) models were not developed, existing BLE model outputs were used to validate the study's hazard results.

The study methodology uses widely-accepted geomorphic and other parameters supported by peer-reviewed literature to establish hazard and risk values based on proven, defensible methodologies that provide a consistent determination of flash flood hazard potential in a timely manner. The inclusion of exposure through the consideration of campgrounds, parks, and buildings helps to target the locations where outdoor warning sirens may be needed based on the presence of people and buildings. Combining these factors into the study is an appropriate and feasible approach for efficient implementation.

As a last step, the TWDB conducted a post-processing review that used results of the flash flood hazard analysis to intersect with exposure data and the 0.2 percent (500-year) annual chance floodplain to identify where outdoor warning sirens may be needed. This step was designed to include not only places with stable populations, but also areas with transient populations (e.g. tourists, seasonal visitors, temporary residents), such as parks and campgrounds, which are harder to map precisely. As part of this review, the data were then filtered, as explained in Section 6, to identify outdoor areas with elevated hazard levels and exposure through campgrounds, parks, and buildings. Finally, the results were further refined by evaluating the number and types of buildings within the 0.2 percent annual chance floodplain.

## Geographic Scope

The study area encompasses Bandera, Bexar, Burnet, Caldwell, Coke, Comal, Concho, Edwards, Gillespie, Guadalupe, Hamilton, Kendall, Kerr, Kimble, Kinney, Lampasas, Llano, Mason, Maverick, McCulloch, Menard, Real, Reeves, San Saba, Schleicher, Sutton, Tom Green, Travis, Uvalde, and Williamson counties as identified in the governor's disaster declarations associated with the 2025 flooding tragedy.

## Mapping Deliverables

The study identified flash flood prone areas within the 30-county area that may warrant outdoor warning sirens to alert people that flash flooding is imminent. Deliverables include geospatial data and maps that can be used to identify locations where outdoor warning siren system installation may be warranted. Local communities are anticipated to use the mapped areas to plan for OWS system placement and operations. Local communities are also expected to utilize knowledge on the ground to refine and determine final locations for placement of the outdoor warning sirens. These areas are represented as polygons along identified stream reaches, with lateral boundaries defined by mapped 0.2 percent (500-year) annual chance floodplain extents from the TWDB 2024 Flood Quilt. This mapping product constitutes the primary deliverable for identifying areas that may require OWS systems as specified in SB3 § 16.502(g). For these areas to be "final and binding," as indicated in SB3 § 16.502(g), the board will also consider community input and local knowledge as a second step after the mapping deliverables from this effort are released.

## Statutory Elements

The methodology used to identify flash flood risk areas within the 30-county study area directly addresses the following SB3 criteria:

- **History of Flooding (§ 16.502(a)(1)):** The approach addresses both consistent and severe flooding through incorporation of the National Oceanic and Atmospheric Administration (NOAA) Storm Events data, which includes locations of storms, fatalities, and injuries, and through independent validation using locations of known and historic flooding events, with extra attention given to recent major flood sites.
- **Other Relevant Factors (§ 16.502(a)(2)):** SB3 provides flexibility for the consideration of any other factor that the TWDB considers relevant, which allowed consideration of additional technical factors when generating areas that may warrant outdoor warning sirens. Some factors for the hazard index, as identified in Section 3, fall within "other relevant factors," as they are not explicitly stated in the relevant statute; however, these factors are supported by literature and influence the flashy aspect of hydrologic and hydraulic responses. Additionally, outputs from the BLE models developed by the Federal Emergency Management Agency (FEMA) and the TWDB were used for validating hazard factors and supported the establishment of hazard thresholds. This flexibility also allows the TWDB to consider local knowledge and community input before finalization. Accordingly, the TWDB will incorporate local knowledge and community input as a post-processing step for the determination of areas that may warrant outdoor warning sirens before deeming them "binding."
- **Human Exposure Factors (§ 16.502(b)):** The methodology explicitly considers potential loss of human life, existence of residences and dwelling structures, and potential property damage through inclusion of exposure data such as building footprints, population counts, campgrounds, and open areas such as parks. Incorporation of these factors ensures that the outdoor warning sirens target where people are demonstrably at risk.

## Regulatory Foundation

The methodology provides the TWDB with a transparent, reproducible, and defensible basis for identifying flash flood-prone areas under SB3 § 16.502. The approach directly addresses each statutory criterion, incorporates multiple lines of evidence, and produces spatial products. The methodology was developed in coordination with the TWDB to ensure alignment with agency priorities and implementation needs.

## Summary of Key Limitations

This flash flood hazard assessment was developed at a regional scale appropriate for identifying general patterns across the 30-county study area and enabling timely access to the grant funding authorized by SB5. Like all regional-scale mapping efforts, this analysis provides a comprehensive first assessment that captures major flash flood risk patterns while recognizing that no regional study can capture every site-specific terrain feature, localized drainage pattern, or individual property condition.

The study methodology integrates multiple physical factors using the Analytic Hierarchy Process (AHP). Factor selection and weighting were informed by extensive literature review and expert interpretation and validated using available outputs from flood models such as Base Level Engineering (BLE). A sensitivity analysis was conducted to understand how different weighting scenarios for the hazard index influence the results, demonstrating that the overall hazard patterns are robust across a range of plausible weighting assumptions.

The resulting mapping is intended to function as a provisional product that establishes regional context and supports resource allocation across the 30-county area. Local officials and emergency managers are encouraged to enhance this regional assessment with local knowledge, field observations, and site-specific considerations when making final siren placement decisions. This combined approach balances statewide methodological consistency with local expertise, ensuring that community-specific needs are addressed while enabling timely access to program funding.

## Broader Implications

Future updates should include new data, methods, and local knowledge to improve the accuracy of the mapped deliverable. Beyond the implementation of SB3, this study establishes a framework for flash flood hazard and risk assessments applicable to other regions of Texas. The multi-stage approach combining analyses of physical and meteorological characteristics with historical validation and systematic exposure refinement that was designed and implemented for this initiative provides a template that can support the broader mission of the TWDB—to protect life and property through risk- and evidence-based flood preparedness and mitigation strategies.

## Disclaimer

This product is a screening level assessment intended to identify areas that may be susceptible to flash flooding and where outdoor warning sirens may be warranted. It is based on a regional scale analysis of physical watershed characteristics, available exposure data, and historical information, and does not predict the occurrence, timing, or severity of flash flooding during any specific storm event. This product should not be used as a predictive or forecasting tool related to flooding. The mapped areas primarily reflect riverine and channel adjacent flash flood susceptibility and may not capture all forms of localized or pluvial flooding, including flooding away from mapped streams or floodplains. Absence from the mapped areas should not be interpreted as absence of risk. Results are dependent on the quality, resolution, and recency of available datasets, and are generalized at a 1 kilometer scale. Therefore, they are not intended for site specific or parcel level determinations. This product should not be used for regulatory determinations. Identification of areas that may warrant sirens does not ensure siren audibility or effectiveness under all conditions, nor does it replace the need for local knowledge, additional warning methods, or professional judgment. Final decisions regarding outdoor warning siren placement should incorporate local review, field verification, and community specific considerations.

Data in the Provisional Flash Flood Risk Areas Map represents the best information available to the TWDB at the time. The information is not represented in real-time and should not be considered as exact conditions in your area. The TWDB provides information via this website as a public service. Neither the State of Texas nor the TWDB assumes any legal liability or responsibility or makes any guarantees or warranties as to the accuracy, completeness, or suitability of the information for any particular purpose.

Please contact flood_sirens_program@twdb.texas.gov for any questions.

# ACKNOWLEDGEMENTS

This memorandum was prepared for the TWDB by the project team (shown below), who recognize this opportunity to support flood-risk reduction and public safety efforts that benefit communities across Texas. This project reflects a shared commitment to applying sound science and engineering to inform decision-making in service of the people of Texas. The work was made possible by the sustained contributions of scientists, engineers, and technical specialists who committed significant time and expertise under a condensed schedule.

## Project Team

Texas Water Development Board

Water Engineering Research Center at the University of Texas at Arlington

AtkinsRéalis

WEST Consultants

Torres & Associates

# LIST OF ACRONYMS

| Acronym | Definition |
|---|---|
| AHP | Analytic Hierarchy Process |
| AUC | Area Under the Curve |
| BLE | Base Level Engineering |
| CI | Consistency Index |
| CN | Curve Number |
| CR | Consistency Ratio |
| DD | Drainage Density |
| DEM | Digital Elevation Model |
| DR | Distance to Rivers |
| DV | Depth–Velocity |
| EL | Elevation |
| FA | Flow Accumulation |
| FAHP | Fuzzy Analytical Hierarchy Process |
| FEMA | Federal Emergency Management Agency |
| FFHI | Flash Flood Hazard Index |
| FFRA | Flash Flood Risk Areas *(provisional)* |
| FIS | Flood Insurance Studies |
| FL | Flashiness Index |
| GIS | Geographic Information Systems |
| gSSURGO | Gridded Soil SURvey GeOgraphic database |
| H&H | Hydrologic and Hydraulic |
| HAND | Height Above Nearest Drainage |
| HEC-RAS | Hydrologic Engineering Center River Analysis System |
| HSG | Hydrologic Soil Group |
| HUC | Hydrologic Unit Code (watershed boundaries) |
| HUC-8 | Hydrologic Unit Code (8-digits) |
| IA | Individual Assistance |
| LiDAR | Light Detection and Ranging |
| LULC | Land Use/ Land Cover |
| MCDA | Multi Criteria Decision Analysis |
| NAD | North American Datum |
| NAVD | North American Vertical Datum |
| NDVI | Normalized Difference Vegetation Index |
| NFIP | National Flood Insurance Program |
| NHD | National Hydrography Dataset |
| NLCD | USGS National Land Cover Dataset |
| NOAA | National Oceanic and Atmospheric Administration |
| NRCS | USDA Natural Resources Conservation Service |
| NWS | National Weather Service |
| OWS | Outdoor Warning Sirens |
| PCA | Principal Component Analysis |

| | |
|---|---|
| ***PLC*** | Plan Curvature |
| ***PRC*** | Profile Curvature |
| ***QA/QC*** | Quality Assurance and Quality Control |
| ***RF*** | Rainfall |
| ***RFPG*** | Regional Flood Planning Group |
| ***ROC*** | Receiver Operating Characteristic |
| ***RV*** | Recreational Vehicle |
| ***SB3*** | Senate Bill 3 (89th Texas Legislature, Second Called Session) |
| ***SB5*** | Senate Bill 5 (89th Texas Legislature, Second Called Session) |
| ***SED*** | Storm Events Database |
| ***SHAVE*** | Severe Hazards Analysis & Verification Experiment |
| ***SL*** | Slope |
| ***SPI*** | Stream Power Index |
| ***TPI*** | Topographic Position Index |
| ***TWDB*** | Texas Water Development Board |
| ***TWI*** | Topographic Wetness Index |
| ***TX*** | Texas |
| ***USA*** | United States of America |
| ***USDA*** | United States Department of Agriculture |
| ***USGS*** | United States Geological Survey |
| ***UT*** | University of Texas |
| ***WERC*** | Water Engineering Research Center |
| ***WEST*** | WEST Consultants |

# TABLE OF CONTENTS

# 1. Introduction

## Study Area

Senate Bill 3 (SB3) was enacted during the 89th Legislature Second Special Session (2025) in response to severe flash flooding that resulted in state disaster declarations for 30 counties primarily located in central Texas. SB3 directs the Texas Water Development Board (TWDB) to identify areas within these flash flood-prone counties that may warrant outdoor warning sirens pursuant to Texas Water Code § 16.501-502. This technical memorandum documents the methodology developed and applied to identify and delineate flash flood-prone areas that may warrant outdoor warning siren installation within the 30-county area.

The scope of the analyses conducted in support of identifying potential outdoor warning siren areas is limited to the 30-county disaster-declared area shown in Figure 1-1 and specified in SB3. While the technical approach and workflows developed for this initiative may be applicable to other geographic locations within Texas, this effort focuses exclusively on satisfying the requirements of SB3 for these 30 counties. This 33,632-square-mile, 30-county area includes Bandera, Bexar, Burnet, Caldwell, Coke, Comal, Concho, Edwards, Gillespie, Guadalupe, Hamilton, Kendall, Kerr, Kimble, Kinney, Lampasas, Llano, Mason, Maverick, McCulloch, Menard, Real, Reeves, San Saba, Schleicher, Sutton, Tom Green, Travis, Uvalde, and Williamson counties. The deliverables from this study include draft geospatial data and provisional maps in digital format that identify flash flood risk areas where installation of outdoor warning sirens may be warranted, and this report documenting the approach and findings. These deliverables are expected to be refined through stakeholder cooperation and revision.

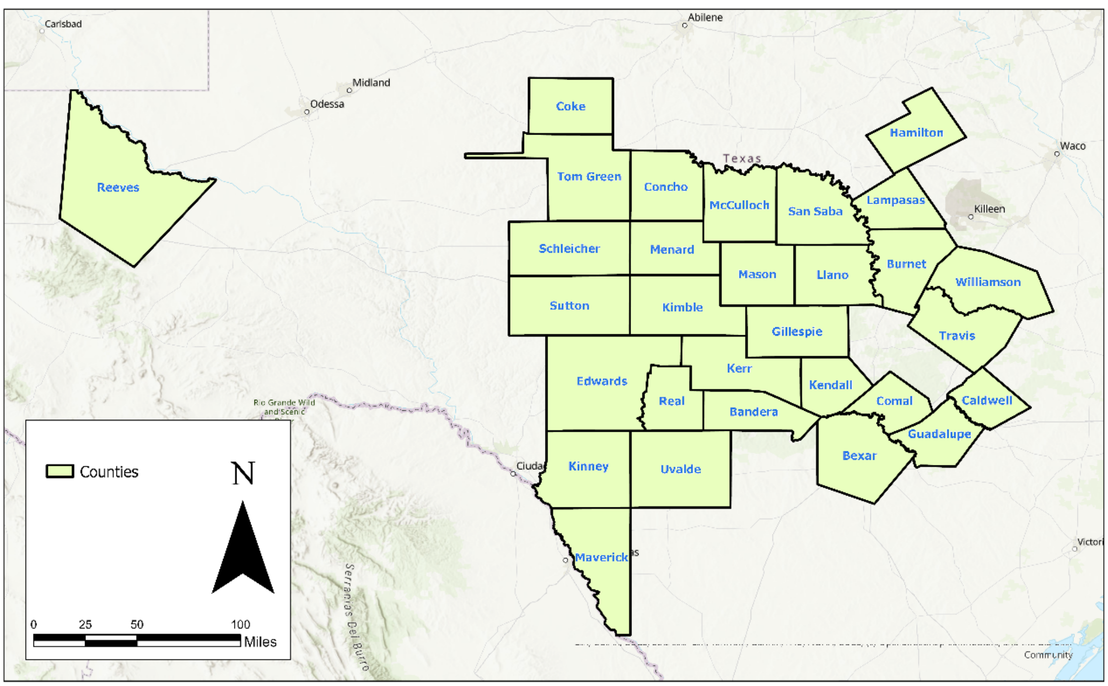


**Figure 1-1. Study area showing the "Flash Flood-Prone Area," as defined in SB3.**

## Background

The Hill Country region of Central Texas—encompassing Bandera, Kerr, Kendall, Bexar, Comal, Gillespie, Llano, Mason, Travis, Williamson counties, and others—has a long and well-documented history of flash flooding. The area sits within "Flash Flood Alley," a crescent of steep, rugged terrain with shallow soils overlaying bedrock. This geography promotes rapid runoff into several creeks that funnel into major rivers like the Guadalupe River and

Colorado River. The 2024 State Flood Plan highlights the "Flash Flood Alley" area, where the steep terrain, shallow soil, and intense rainfall rates contribute to flash flooding (TWDB, 2024).

In July 2025, a mesoscale convective vortex generated an extraordinary amount of rainfall by drawing tropical moisture from both the Gulf of America and the Pacific Ocean. The resulting flash flooding caused the Guadalupe River in Kerrville, TX (USGS Gage #08166200) to surge 26 feet in just 45 minutes. According to NOAA Storm Events data and subsequent analysis by Yale Climate Connections, the event resulted in over 135 fatalities statewide, making it the deadliest inland flood event in the United States since the Big Thompson River Flood in 1976.

The Balcones Escarpment—a steep fault zone running from near Dallas to southwest of San Antonio—intensifies the risk of flash flooding in counties along the escarpment, including Travis, Hays, Comal, and Uvalde. As warm, moist air from the Gulf is forced upward along the escarpment, it cools rapidly and results in heavy rainfall. The underlying thin soils and shallow bedrock provide little capacity to absorb deluges, causing excess rainfall to runoff and accumulate in creek beds and converge through narrow canyons into rivers draining the Edwards Plateau. These rapid flows, often in low-lying areas and narrow floodplains, are difficult to predict due to their speed and intensity. Figure 1-2 illustrates the Balcones Escarpment and the Edwards Plateau with the 30 counties.

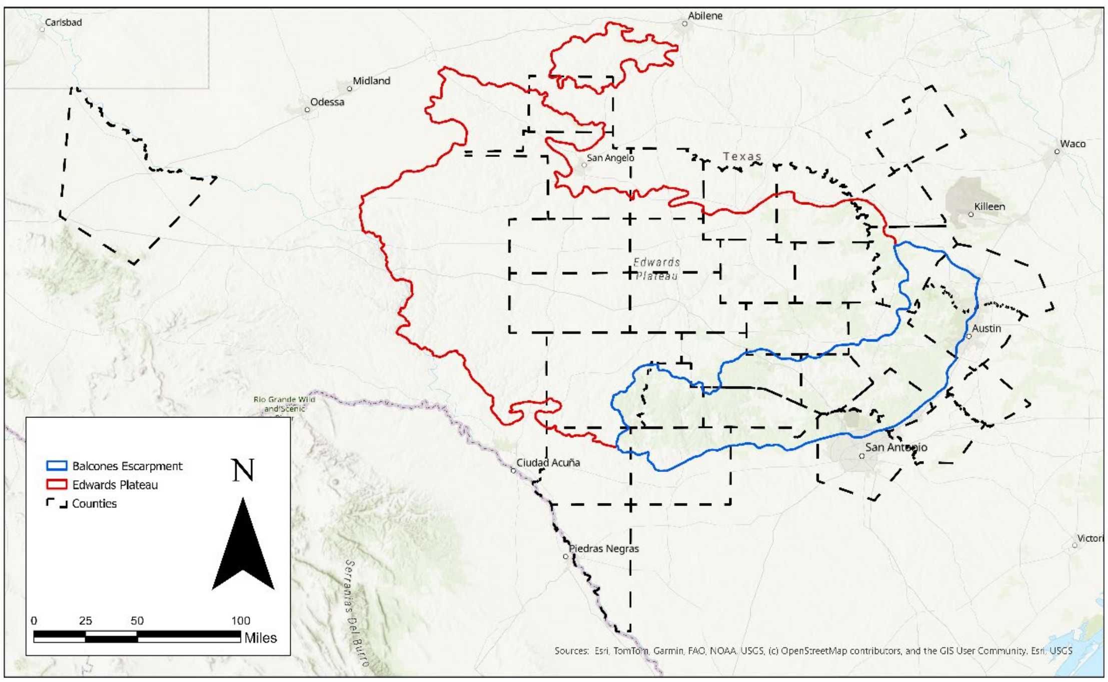


**Figure 1-2. 30-county study area with the Balcones Escarpment and the Edwards Plateau.**

The National Weather Service emphasizes that slow-moving, training thunderstorms—common in this region, particularly when moisture combines from the Gulf, Eastern Pacific, and remnants of tropical storms—are a key meteorological trigger. These storms stall over the rugged central Texas landscape, dumping 2–4 inches of rain per hour. This pattern has repeatedly produced flash flood warnings across nearly all counties in the region, including the 30-county study area. These large, intense, and localized rainfall events, combined with limited soil absorption and topographical funneling of stormwater runoff, make the region a hotspot for deadly flash floods.

## Literature Review

Traditional flood hazard mapping methods used in Texas, such as Federal Emergency Management Agency (FEMA) Flood Insurance Studies (FIS), and Base Level Engineering (BLE) analyses produced by FEMA and the TWDB, typically estimate flood flows and flood inundation extents for large storm events with standard durations of 24 hours. In contrast, flash flooding is generally caused by localized storms with durations much shorter than 24 hours. While traditional flood hazard maps are effective at identifying flood-prone areas, they do not identify which of these flood-prone areas also have elevated risk for flash flooding.

Therefore, a literature review was conducted to identify peer-reviewed, defensible factors that contribute to flash flood risk, and to identify appropriate analytical methods to calculate flash flood risk consistently across the 30-county study area and validate the results. The literature review examined more than 50 published flood risk studies and analytical methods, with emphasis on 30 studies that were flash flooding focused. The review resulted in an organized inventory of commonly used methodologies to identify hazard and exposure factors that contribute to flash flood risk and identify validation strategies that informed the subsequent steps in the analysis. More details on the literature review can be found in Appendix A.

The literature reviewed in this study shows that flood and flash flood risk assessment methods have been widely used in real-world case studies and evaluated using observed evidence. Across diverse geographic regions, researchers have used historical flash flood records, locations where torrential valleys were carved by powerful stream flow, post-event damage reports, and field observations to identify areas of elevated flood and flash flood hazard. In these studies, commonly used factors such as slope, drainage density, distance to channels, land cover, soil characteristics, rainfall, terrain curvature (e.g., along or across terrain features), and others were combined using frameworks based on geospatial analysis, multi-criteria decision analysis, statistics, or machine-learning. The resulting flood hazard maps consistently aligned with known flash flood-affected locations, previously damaged infrastructure, or areas with high flood frequency.

The performance of these contributing factor-based approaches was evaluated using systematic validation methods by comparing mapped flash flood-risk patterns with observed flash flood events and documented impacts. Many studies assessed how well the resulting mapped risk areas aligned with recorded flood damage, disaster loss databases, or post-event on-site surveys, often supported by remote sensing and aerial imagery. Across these validation efforts, areas classified as high or very high risk were consistently associated with more frequent flash flooding, greater damage, or higher exposure. Together, these findings provide strong evidence that contributing factor-based methods reliably capture meaningful patterns of flash flood risk.

Collectively, these studies show that contributing factor-derived flood-risk assessment methods developed from prior research are grounded in real-world evidence and can effectively identify flood-prone areas across a wide range of climates, landscapes, and community settings. While individual studies used different modelling techniques and validation approaches, they consistently reached similar conclusions demonstrating that spatial flood-risk patterns based on established indicators and weighting schemes are robust and transferable. The present study builds upon this validated body of work by adopting similar, evidence-supported methodologies to identify relative flash flood-risk patterns for spatial identification and planning-level assessment.

# 2. Overview of Study Methodology

Identification of flash flood-prone areas that may warrant outdoor warning siren systems requires determination of flash flood risk. Flood risk is defined in the 2024 State Flood Plan as: “a combination of the probability (likelihood or chance) of a flood event happening and the impact if it occurred” (TWDB, 2024). The components of flood risk are:

- Hazard, which reflects the magnitude and extent of flooding
- Exposure, which represents who and what might flood

The methodology used in this approach considers the relative likelihood of flash flooding (*hazard)* acting on people and buildings present (*exposure)*. While vulnerability (denoting the susceptibility of those people and to harm) has not been considered within this study, data on vulnerability is available from the State Flood Plan information for consideration at the community level, if desired (TWDB, 2024).

Standard workflows used for flood hazard mapping (floodplain mapping) employ hydrologic and hydraulic (H&H) modeling. These workflows estimate the probability of flooding in any given year, which is referred to as the percent annual chance floodplain). The flood hazard data are then combined with structure and population data to estimate flood risk in terms of monetary value (dollars) and other metrics. FEMA’s Flood Insurance Studies or BLE employ these methods to identify flood extents of various annual chance events such as 0.2, 1, 4, 10 percent, etc. but do not intend to explicitly identify areas susceptible to flash flooding.

Flash floods are a subset of floods that differ from other types of flooding. They result from a combination of various factors such as high intensity precipitation, rapid changes in terrain elevations, thin soil depths and others that lead to rapid hydrologic responses. Flash floods are generally associated with dangerous conditions with high velocities and depths; they are distinguished by their sudden onset rather than gradually rising water levels. While flash flooding is often characterized by streamflow peaking within a few hours of causative rainfall, the critical characteristic is the speed at which flooding transforms from minimal flow to life-threatening conditions, often appearing as a sudden wall of water that provides little warning time for those in the flood path.

Therefore, assessment of flash flood hazard should incorporate factors indicative of rapid watershed response (i.e., where rainfall is likely to run off quickly) and general flooding propensity (i.e., where floods may occur in response to rainfall). Because flash flood hazard is rarely assessed at the local level and no single standardized methodology has emerged as a widely adopted national standard of practice, a focused literature review was undertaken to identify peer-reviewed and defensible technical approaches—including associated hazard and exposure factors, and methods for validating the outputs produced.

To support delineation of Flash Flood Risk Areas (FFRA) within the 30-county area, an H&H modeling-based approach was initially considered but was determined to be infeasible due to time constraints. Implementing such an approach would have required development of new technical guidance, design of new storm scenarios, and extensive computational time and resources to execute flash flood simulations for watershed areas within the study area.

The literature review revealed several feasible approaches for flash flood hazard assessment, including multi-criteria weighting and machine learning techniques in place of H&H modeling. These approaches were evaluated based on feasibility of implementation, transparency, and interpretability. Based on this evaluation, a multi-criteria weighting methodology was selected over machine learning methods due to its transparency and interpretability, and reduced reliance on large, high-quality datasets necessary for machine learning training.

Implementation of this methodology involves four major steps:

1. **Estimation of Hazard Index**: Multiple hydrologic and topographic factors were combined to produce an index to quantify the flood hazard, called the **Flash Flood Hazard index (FFHI)**. The factors used for Flash Flood

Hazard Index estimation are listed in Appendix A, Table A-2. The hazard index process was tailored to focus on incorporating factors that lead to flashy watershed responses.

2. **Estimation of Exposure at Risk**: Exposure-related factors—such as structures, population, campgrounds, and open areas such as parks—where people congregate, were combined with Flash Flood Hazard Index to identify locations with flash flood hazard that may benefit from outdoor warning sirens to support reduction of flood risk.
3. **Depiction of Flash Flood Risk Areas**: Finally, the hazard index and exposure locations are combined to determine where hazard levels intersect with known or potential outdoor exposure locations. Through a filtering process, provisional Flash Flood Risk Areas (FFRA) are established based on hazard thresholds and locations with buildings, campgrounds, parks, and locations of historic impact identified by past damages and/or fatalities. The provisional map produced through this effort provides a strong foundation for further refinement through community and public involvement.
4. **Stakeholder Refinement**: Following release of the provisional FFRA, the TWDB may work with stakeholders to ensure that the risk areas are practical and warranted for communities to implement outdoor flash flood warning sirens. Refinement by stakeholders will ensure the regional-scale mapping product sufficiently reflects local knowledge.

Generation of the indices requires a method to develop weights for each factor to be used in an overall equation. The Analytic Hierarchy Process (AHP) was selected due to its strengths and widespread use in flood and hazard-mapping studies. The Analytic Hierarchy Process is a specific Multi-Criteria Decision Analysis method that can be used to combine various factors into an overall index. The Analytic Hierarchy Process was used independently on the hazard and exposure factors to generate the hazard index. The Analytic Hierarchy Process provides a flexible framework that enables the incorporation of findings from existing literature as expert judgement and supports efficient implementation at the scale of this study. The Analytic Hierarchy Process is well suited for regulatory and decision-support applications because of its transparency (e.g., the ability to identify which factor(s) contributed to a high hazard) and the flexibility to incorporate regional knowledge to select factors and adjust factor weighting (Lin et al., 2020; Majeed et al., 2023). Additional details on the Analytic Hierarchy Process method are provided in Appendix C.

Unlike typical flood risk analyses that estimate hazard and risk in terms of Annual Exceedance Probability and expected annual average losses, the methodology applied in this study estimates the relative hazard and risk as indices scaled from 0 to 1. The hazard index is developed by iteratively weighting physical, meteorological, hydrologic, and geomorphic factors, with initial weights informed by literature and refined through sensitivity analysis. Hazard index estimation is then combined with exposure factors (structures, population, campgrounds, parks, etc.) to determine Flash Flood Risk Areas (FFRAs).

The resulting Flash Flood Risk Areas represent relative flash flood hazard and exposure that serves as the initial basis for delineating the flash flood-prone areas on maps that were subsequently refined through areas of known and outdoor exposure. The hazard index component of this process was tailored to flash flooding specifically by incorporating indicators of flashy watershed responses into the contributing factors. After refinements based on a hazard threshold, the resulting spatial index and exposure data were used to generate maps of flash flood risk areas within the 0.2 percent annual chance floodplain that may warrant outdoor warning sirens.

To guide the readers through the analytical approach, the workflow and structure of this document are organized as outlined in Figure 2-1. The approach used conforms with best practices identified in the literature review to generate foundational data that are combined with post-processing to identify flash flood-prone areas that may warrant outdoor warning sirens. Further details on each step are provided in subsequent sections.

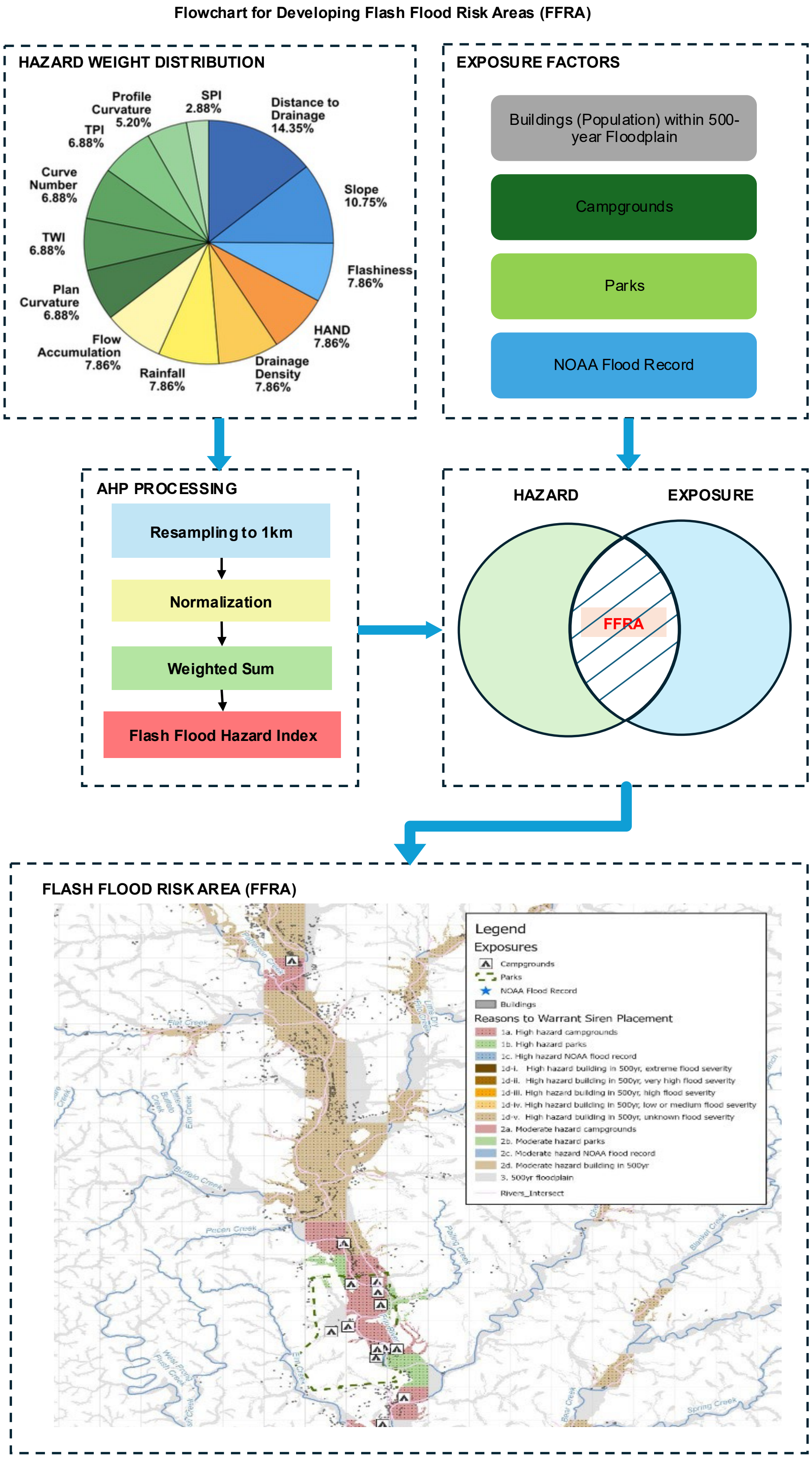


**Figure 2--1. The workflow and structure of this project.**

# 3. Factors Contributing to Flash Flood Hazard

A list of recommended factors for implementing the project methodology was generated by compiling and assessing hazard and exposure factors identified in the literature review and the availability of relevant datasets for the region. Selected parameters were widely represented in the reviewed literature and were chosen for their direct influence on runoff generation, flow acceleration, and flood intensity, while avoiding redundancy by eliminating factors that are already incorporated into other factors. More details on the literature review used to inform the selection of factors can be found in Appendix A.

Thirteen different representative factors were chosen to estimate the flash flood hazard index. These 13 factors were derived from geospatial datasets including digital elevation models (DEMs), land cover data, soil characteristics, NOAA Atlas 14 precipitation frequency estimates, and hydrologic parameters such as curve numbers which allows the flash flood hazard index to reflect local variations in terrain, geomorphology, and meteorological conditions across the study area. The factors generally fell into three categories: physical factors, meteorological factors, and flashiness. Each of these factors are drivers of flood potential or flashiness potential (e.g., rapid hydrologic response), or both as demonstrated in Figure 3-1..Collectively, the factors are combined to generate the first iteration of flash flood hazard locations. Each factor is described in more detail in the following sections.

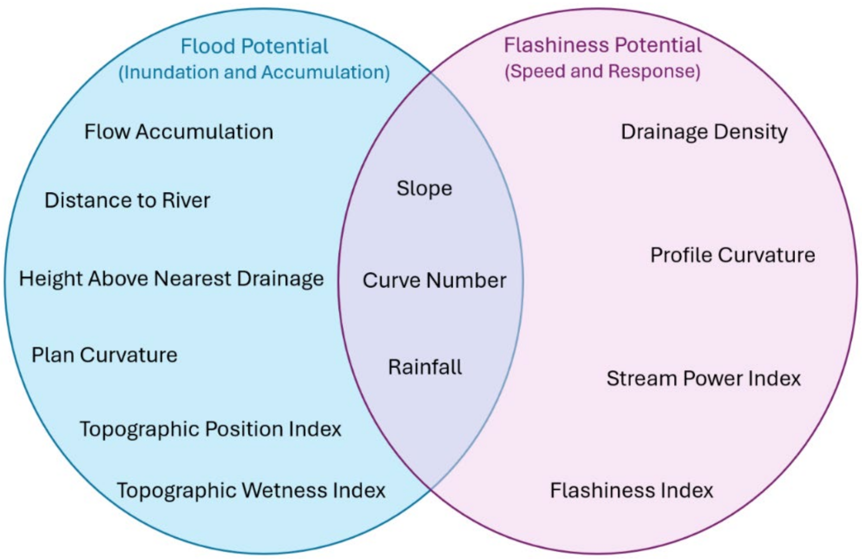


**Figure 3-1. Venn Diagram of hazard factors contributing to flood and/or flashiness potential**

Several datasets were utilized to process the contributing factors and to quantify them, including:

- U.S. Geological Survey (USGS) digital elevation model (DEM) data which link results to local terrain,
- National Oceanic and Atmospheric Administration (NOAA) Atlas-14 precipitation frequency estimates which link study results to local precipitation potential,
- land use/land cover (LULC) data from the USGS National Land Cover Dataset (NLCD) which link results to local hydrologic runoff potential, and
- soil data from the U.S. Department of Agriculture (USDA): Gridded Soil Survey Geographic (gSSURGO) database which link results to local soil conditions.

The best available datasets were used, all of which were obtained from official federal sources and considered for quality and coverage. More details on the data collection and processing can be found in Appendix B.

## Physical Factors

Physical factors used for flash flood assessment were selected to capture topographic controls on runoff generation, flow concentration, flow propagation and flood-prone areas. Most of the selected physical factors are terrain based and were developed using regional Digital Elevation Model (DEM) data. The process for quantifying these factors is based on well-established geographic information system (GIS) workflows for delineating watershed and catchment boundaries to identify areas contributing surface runoff and streamflow to a downstream outlet.

For a consistent, region-wide elevation source, the USGS 30-meter LiDAR-derived DEM, which provides a three-dimensional picture of terrain—including hills, valleys, and slopes—was used as the foundational terrain dataset. This resampled version of the 1-meter resolution DEM provides an appropriate balance between computational efficiency and representation of key topographic features relevant to flash flood processes at the study scale.

Prior to calculation of specific factors, the 30-meter DEMs were pre-processed to prepare the data for further analyses and for extracting the physical factors. First, the source DEM data was projected to a consistent spatial reference called NAD 1983 (2011) Texas Centric Mapping System Albers (Meters) projection system. Second, the projected DEMs were clipped to the outlines of all 48 hydrologic unit code (HUC)-8 watersheds with any overlap with the 30-county study area. Figure 3-2 shows the 48 HUC-8 watersheds with the 30 counties. Clipping the DEMs to HUC-8 watershed boundaries facilitated the processing of multiple areas in parallel. The unit of measurement of the ground elevations is meters, and the resolution was maintained at 30-meter by 30-meter pixels (or cells) across the study area.

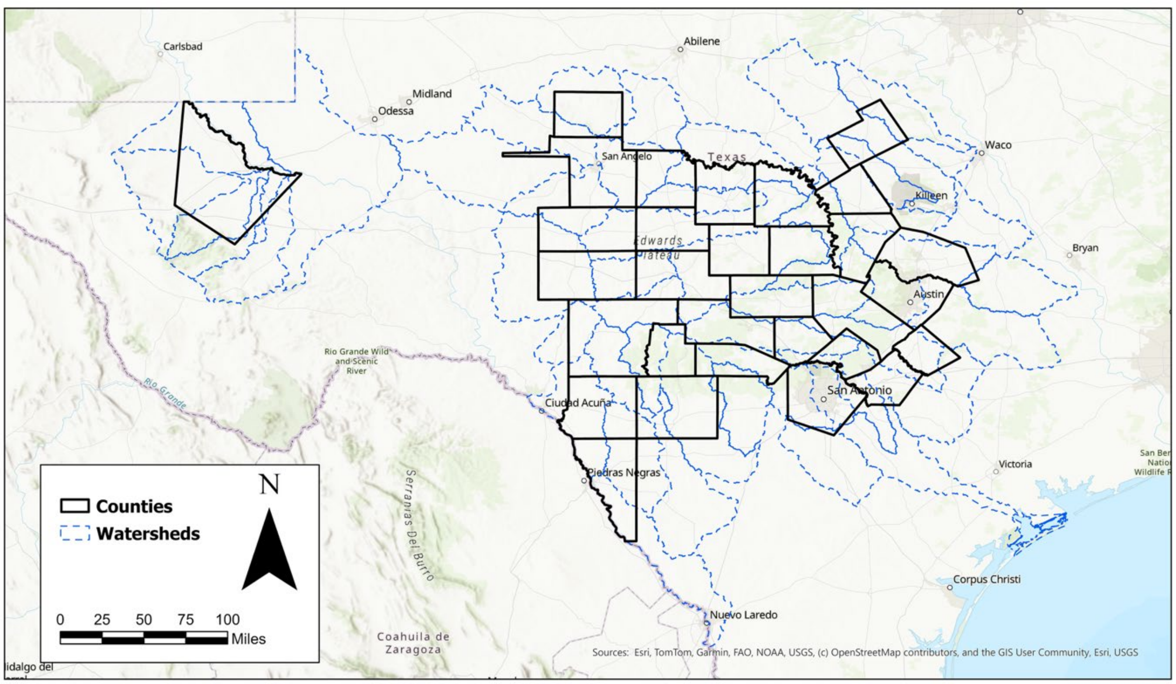


**Figure 3-2. 48 HUC-8 watersheds with the 30-county study area.**

To support extraction of factors such as flow accumulation (i.e., the number of upstream cells contributing to a given cell) and extraction of stream or drainage network and other terrain-based factors, further processing of the 30-meter DEMs was required. The additional processing steps included hydrologic conditioning of DEMs (e.g., fill sinks) and generation of flow direction grids (e.g., the directional flow of water based on the largest elevation change from the DEM). Further details on the processing steps for the hazard factors are given in Appendix B.

While the DEM and related products described above were processed at 30-meter grid resolution, the physical factor extraction and the technical analyses were conducted at 1-kilometer (km) resolution. The entire study area of 30 counties and the contributing watersheds were divided up into 1km cells. Using the pre-processed DEM and its products, land use/land cover, and soil data, the following physical factors were calculated for every 1km cell within the watershed-based study boundary:

1) **Flow Accumulation** represents the number of upstream cells contributing flow to each grid cell. In other words, it is a representation of the amount of area contributing water toward a point in a watershed based on flow direction. Flow accumulation values are calculated as the number of upstream cells (not the area). Flow accumulation was selected to indicate areas where runoff converges, such as streams and channels, and to capture ephemeral channels that can quickly accumulate flow during extreme rainfall events. **A higher flow accumulation indicates higher flood potential.**

2) **Distance to Drainage/River (DR)** is the horizontal distance from the centroid of a cell to the nearest stream cell. In other words, it is the horizontal distance from a point in a watershed to the nearest stream, river, or channel. In reviewed studies, **DR** is consistently the highest weighted factor. Because DR is directly related to flood hazard, this factor helps identify areas where flooding may occur. In this study, the drainage network is derived from the DEM-based stream grid, which indicates channels and drainage paths based on topography and does not include urban stormwater infrastructure. **A smaller distance to drainage/river indicates closer proximity to a channel and higher flood potential.**

3) **Drainage Density** is a measure of how well a watershed is drained, calculated as the length of rivers and streams divided by a unit area. Higher drainage density indicates more numerous or closely spaced channels in a watershed and a limited distance for infiltration to occur before entering the drainage network, leading to flashier responses. Water moves quickly from hillslopes into channels in areas with higher drainage density. Urban stormwater drainage systems are not included in the drainage density calculation, as the calculation was based on the DEM-based stream grid representing surface topography only. This factor was selected to quantify the efficiency of the channel networks. **Higher drainage density indicates higher flashiness potential.**

4) **Height Above Nearest Drainage (HAND)** represents the difference in vertical elevation between one DEM grid cell and the DEM value of the nearest drainage (stream) cell measured along the flow path. In other words, it is the elevation difference that water would have to rise from the nearest river, stream, or channel to a designated point in a watershed, in this case the area-averaged DEM value for the pixel. In this study, HAND was included to incorporate elevation data while avoiding areas in low elevation being emphasized regardless of hydrologic position in a watershed. **A lower HAND indicates higher flood potential.**

5) **Plan Curvature** describes the lateral shape of the land-surface measured across the slope. It is calculated based on the DEM and controls flow convergence and divergence: positive values indicate divergent flow, and negative values indicate convergent flow. Plan Curvature governs lateral flow convergence and divergence across the landscape. It was selected to capture the horizontal geometry of terrain, where the spatial expansion of surface water is enhanced in concave surfaces during high-flow conditions. **A lower plan curvature indicates higher flood potential.**

6) **Profile Curvature** describes the vertical shape of the land surface along the direction of steepest descent, based on the DEM. It controls acceleration and deceleration of streamflow: negative values indicate convex surfaces (flow acceleration), while positive values indicate concave surfaces (flow deceleration). Profile curvature was selected to quantify the zones along the direction of maximum slope where flow accelerates which helps identify the zones prone to accelerated runoff. For this factor, the raw (unfilled) DEM was used instead of the hydrologically conditioned one to preserve topographic features. **A lower profile curvature indicates higher flashiness potential.**

7) The **Topographic Position Index (TPI)** describes the relative elevation of a cell with respect to surrounding cells. The TPI is the difference between a cell's elevation and the mean elevation of a surrounding neighborhood, calculated from the DEM. Positive values indicate ridges, negative values indicate valleys, and values near zero indicate flat or mid-slope positions. This index is included to distinguish between valleys and ridges. **A lower TPI indicates higher flood potential**.

8) **Slope**, specifically terrain slope, is the gradient or steepness of a cell based on a window or neighborhood of nearby cells. It is calculated based on the DEM. Among topographic variables, slope provides the most direct and physically meaningful measure of gravitational acceleration affecting surface runoff. Slope is the most repeated factor included in previous studies. High slopes increase gravitational acceleration of overland flow, increasing peak discharge generation in small upstream catchments. **A higher slope value indicates higher flash flood potential.**

9) The **Stream Power Index (SPI)** combines slope and flow accumulation to represent the erosive and transport capacity of flowing water. A high SPI value indicates a higher hazard during floods. Because the SPI is calculated from both terrain slope and upstream contributing area, it helps quantify how vulnerable a specific location is based on its position in the watershed. This factor was included to quantify the areas where runoff from upstream contributing areas can intensify flash flood impacts. **A higher SPI indicates higher flashiness potential.**

10) The **Topographic Wetness Index (TWI)** represents the spatial distribution of saturated zones in a watershed. It is calculated based on the flow accumulation and slope grids. The TWI also identifies runoff concentration zones. This index is used in this study to represent the flood-prone areas where water from upstream drainage is likely to pool. **A higher TWI indicates higher flood potential.**

11) The **Curve Number (CN**) represents the combined effect of soil hydrologic properties and land use/land cover on surface runoff generation. While it is not based on DEM data, it is a widely used empirical parameter developed by the U.S. Department of Agriculture (USDA) Natural Resources Conservation Service (NRCS) to estimate direct runoff response to rainfall events. In this study, Curve Number was derived by integrating land use/land cover data from the National Land Cover Dataset (NLCD) with hydrologic soil group (HSG) information from the Gridded Soil Survey Geographic (gSSURGO) Dataset following standard NRCS guidelines. Curve number was used as a spatial indicator of relative runoff potential, recognizing that higher Curve Number values generally correspond to greater runoff generation under similar rainfall conditions. Curve number is a dimensionless numerical value on a scale of 30 to 100, with higher values corresponding to higher runoff potential. **A higher Curve Number indicates higher flash flood potential**.

## Meteorological Factor

In addition to physical factors, meteorological factors can also impact flash flooding. The most important meteorological factor influencing flash flooding and flooding is precipitation, or rainfall.

**Rainfall** is a triggering factor for flash floods. While topographic factors determine where and how water flows, precipitation determines how much water enters the system. Precipitation frequency estimates (in inches) were obtained as gridded products from the National Oceanic and Atmospheric Administration (NOAA) Atlas-14. In this study, the 100-year 24-hour precipitation frequency estimates (i.e., depths) were selected to capture the relative spatial distribution of rainfall across the study area. Frequency-based rainfall (e.g., 100-year, 24-hour) is used as a proxy for extreme precipitation rather than for event-specific flood simulation. It represents the spatial potential for intense rainfall capable of triggering flash flooding and serves as a climatic driver of conditions where rapid runoff generation and short response times are more likely. When combined with terrain, land-surface, and drainage-related factors, the rainfall frequency layer contributes to identifying areas that are susceptible to high-magnitude, low-probability rainfall events that typically drive flash flood initiation. **A higher precipitation depth indicates higher flash flood potential**.

The rainfall input represents 24-hour precipitation and does not explicitly represent short-duration, high-intensity rainfall bursts that often drive flash flooding. As a result, some areas susceptible to very rapid runoff from short-duration storms may be underrepresented.

## Flashiness Factor

In addition to the physical and meteorological factors described above, the literature review also revealed the existence of a readily available flashiness index from Saharia *et al*., 2017. The flashiness index was included alongside the other factors to increase the overall balance of flash flood and flood-related factors in the analysis. Additionally, the referenced paper included some analysis and discussion of locations within the 30-county study area (part of "Flash Flood Alley"), making it relevant for this effort.

The **flashiness index** introduced by (Saharia et al., 2017) is a hydrologic metric developed to quantify the severity of flash flooding based on long-term observations of streamflow or discharge from stream gages. The data was made available as a spatially continuous dataset at a 1-kilometer by 1-kilometer resolution. Conceptually, "flashiness" (as defined in the reference) represents the rate at which discharge rises above the action stage normalized by watershed area, thereby characterizing the efficiency and rapidity of basin response per unit contributing area. Rather than relying on terrain properties alone, it provides a complementary indicator of rapid response potential. **A higher flashiness index indicates higher flashiness potential**.

Once processed using their native or available resolution, all factors were first resampled to consistent 1km grids to ensure spatial alignment across the watershed. Following resampling, the factors were normalized using the inverse hyperbolic sine transformation to accommodate negative values present in some factor distributions. The transformed layers were then scaled to a common 0-1 range using minimum-maximum (min-max) normalization based on the minimum and maximum values observed across the study area.

A 1km analysis grid was selected to match the resolution of the coarsest input data and to keep the workflow computationally feasible across the 30-county domain. For example, a close-up view of the South Fork Guadalupe River with the 1km grid is illustrated in Figure 3-3. The selected 1km resolution also aligns with the goal of identifying areas that may warrant outdoor warning siren systems within the 30-county area and given that identifying the precise locations of sirens is outside the scope of this study. Several foundational datasets used in the study, such as the design-storm rainfall depth layer and flashiness index, are provided at approximately 1km native resolution (or effectively behave as 1km products after standard preprocessing) and adopting a finer grid would not produce genuinely higher-resolution information. For these reasons, a 1km grid was selected to ensure consistency across inputs while maintaining acceptable computational times for processing and mapping.

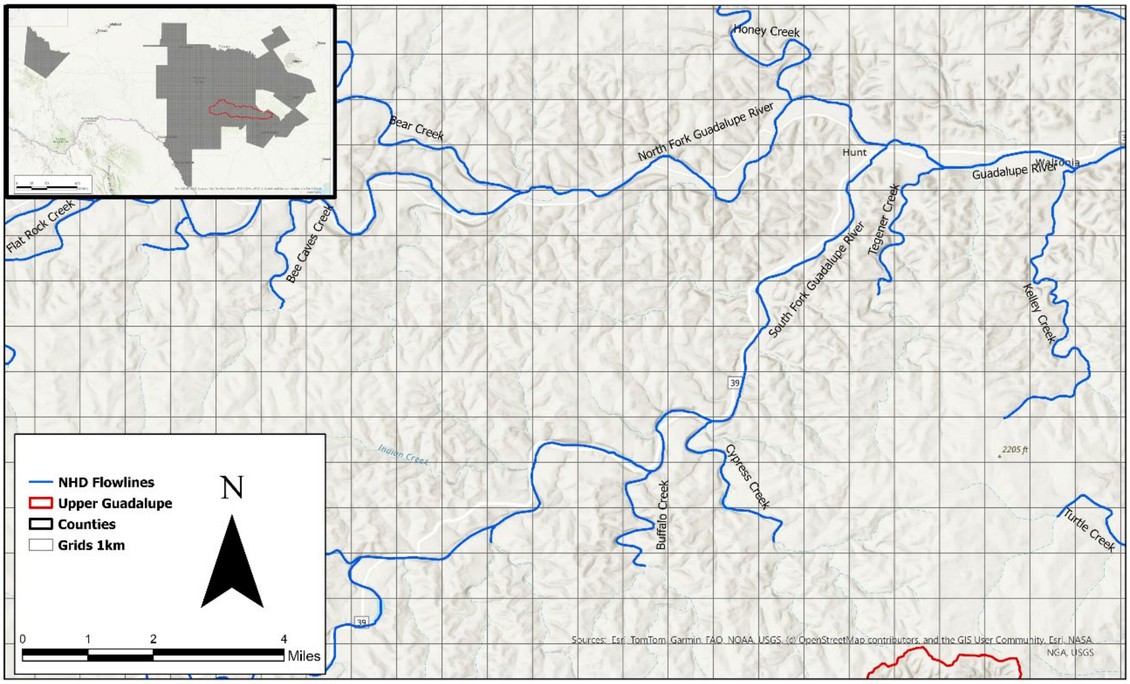


**Figure 3-3. Close-up view of the South Fork Guadalupe River with the 1km grid.**

All selected parameters are widely validated in flood hazard studies and were chosen for their direct influence on runoff generation, flow acceleration, and flood intensity—while avoiding redundancy by using integrated indices such as the Curve Number (CN). For more details on the factors contributing to flash flood hazard identified through the literature review and the considerations for their inclusion in this study, see Appendix A. Identifying areas where these features co-occur is necessary to represent elevated flash flood hazard.

The Analytic Hierarchy Process employed in this study was used to determine the weight of each factor, which was then combined using a weighted sum. This process of combining the hazard factors described in this section is detailed in the following section and identifies locations where multiple features are present that lead to higher flash flood hazard and reflect areas of flash flood risk.

# 4. Combining Flash Flood Hazard Factors into the Hazard Index

The flash flood hazard at a specific location depends on the combined influence of watershed physical and meteorological characteristics that interact in complex ways. To account for these interactions, researchers have applied a wide range of weighting and modelling approaches to quantify the relative importance of contributing factors to flash flooding. Among these, the AHP is one of the most frequently used tools in the literature for flood and flash flood hazard mapping. It provides a structured framework for comparing the relative importance of multiple contributing factors and typically relies on expert judgement. In this study, weights from the literature were leveraged to act as expert judgement for relative importance of each factor compared to other factors. The relative importance values were adjusted to incorporate the flashiness index as a factor after sensitivity analysis, the resulting weights were calculated, and a resulting hazard index value was calculated for each cell.

## Hazard Index from the Analytic Hierarchy Process

The studies reviewed did not always agree on which factors are most important for flash flooding or how much influence each factor should have. Substantial variation exists in both the methods used to identify watershed factors relevant to flash flooding and in the assignment of relative weights to those factors included in flash flood hazard assessments. Approaches ranged from expert-based techniques such as the Analytic Hierarchy Process to statistical models, as well as hybrid and machine learning techniques. Because the selected parameters and their assigned weights vary across studies, directly adopting a weighting scheme from any single source would not adequately represent the broader range of flash flood hazard factors reported in the literature. Therefore, weights were synthesized by combining factor importance information from multiple studies, providing a more balanced and representative basis for the hazard index. The resulting min-max-normalized relative weights derived from this synthesis are detailed in Appendix C.

An additional consideration was the inclusion of the flashiness index (Saharia et al., 2017), which is not commonly incorporated in existing flash flood and flood susceptibility weighting approaches. The flashiness index captures how quickly streams respond to rainfall, and its relative importance is more uncertain than that of more commonly used factors. To include this factor without introducing bias, a sensitivity analysis was performed. While the weights for all other Analytic Hierarchy Process (AHP) criteria were based on median values reported in the literature, the importance of the flashiness index was evaluated separately to examine how sensitive the results were to its assigned weight.

Within the AHP framework, the relative weights of all the parameters were systematically varied with respect to flashiness while maintaining reciprocal consistency and acceptable consistency ratios. This process produced a range of plausible weighting combinations that reflect uncertainty in pairwise comparisons. For each valid combination, the flashiness weight was recomputed and its distribution was examined. Slope and Curve Number were assigned equal importance relative to flashiness because of their similar influence on runoff response, while other parameters—such as elevation, drainage density, rainfall, and flow accumulation—were constrained to median importance levels reported in the literature. In simple terms, this approach tested many reasonable weighting scenarios to ensure that the results were not driven by a single assumption. As a result, the final Analytic Hierarchy Process (AHP) matrix reflects both rapid flash flood related factors and factors associated with the broader flooding potential. Additional details on the flashiness sensitivity analysis, the full pairwise comparison matrix, and the Analytic Hierarchy Process (AHP) calculations are provided in Appendix C.

The resultant weights for each hazard factor are given in Table 4-1. The most influential factor is an area's distance to river, accounting for approximately 14.35 percent of the hazard index, followed by slope with approximately 10.75 percent. The least influential factors are Stream Power Index and Profile Curvature, accounting for approximately 2.88 percent and 5.20 percent of the hazard index, respectively. Most factors are given near-equal weighting of 7.86 percent and 6.88 percent, aligning with the median and mean weighting.

**Table 4-1. Resultant weights for each hazard factor.**

| Factor | Hazard Weight |
|---|---|
| Distance to River (DR) | **14.35%** |
| Slope (SL) | **10.75%** |
| Flashiness Index (FL) | **7.86%** |
| Height Above Nearest Drainage (HAND) | **7.86%** |
| Drainage Density (DD) | **7.86%** |
| Rainfall (RF) | **7.86%** |
| Flow Accumulation (FA) | **7.86%** |
| Plan Curvature (PLC) | **6.88%** |
| Topographic Wetness Index (TWI) | **6.88%** |
| Curve Number (CN) | **6.88%** |
| Topographic Position Index (TPI) | **6.88%** |
| Profile Curvature (PRC) | **5.20%** |
| Stream Power Index (SPI) | **2.88%** |

Once the weights were established for each hazard factor using the Analytic Hierarchy Process method, the hazard index for each cell within the watershed-based study area was calculated using the weighted sum of the hazard factors. For technical details on the weights and the Analytic Hierarchy Process method calculations for hazard input factors and index, see Appendix C. Hazard index values for the 30-county study area ranged from 0.317 to 0.671, with mean and median values near 0.487.

## Validation of the Hazard Index with Base Level Engineering Depth-Velocity Product

The hazard index established through the prior methodology focused on determination of relative values of potentially dangerous conditions caused by the combined impacts of flashy responses with flood potential that contribute to an overall flash flood hazard. Validation of the hazard layer required knowledge of the flashiness, flood potential, and/or combined effects from flash flood potential. Because the hazard index itself is not limited to where flash flooding has already occurred nor where there are impacts on people or property, the validation of this product with historical data alone is not appropriate. Instead, the validation of hazard also included information obtained through results from HEC-RAS 2D hydraulic models developed for watersheds within the study area. The records of historical flooding can give some indications of where flashy responses have been observed, but not where flash flooding is possible. Other historical data, such as flash flood records and information about flood-related fatalities, was later utilized for validation of the risk product, as these types of historical data indicate where humans were impacted by historical storms.

As mentioned briefly in the introduction, traditional flood hazard mapping approaches, including FEMA Flood Insurance Studies and Base Level Engineering (BLE) analyses, produce comprehensive and technically sound flood hazard information. These products are well suited for showing where flooding occurs and how deep and fast the water may be during large, standardized storm events. They are effective for characterizing flood extent, depth, and velocity associated with design storms; however, they are not specifically intended to distinguish areas prone to flash flooding. In particular, standardized mapping of the 100-year, 24-hour storm available from Flood Insurance Rate Maps and BLE does not uniformly reflect flash flooding potential. These analyses typically represent longer duration design storms that assume rainfall distributed over a relatively large area. They represent the likelihood of a low probability, high magnitude flood event occurring along a channel. In contrast, flash flooding can be associated with large flood magnitudes but is often triggered by short duration, high-intensity rainfall occurring over localized portions of a watershed, rather than by prolonged rainfall over a large area. Such events can produce rapid runoff generation and short response times even when total storm rainfall is relatively limited—conditions that are not well represented by standardized 24-hour design storms used in Flood Insurance Rate Maps and Base Level Engineering (BLE) analyses.

Readily available 2D BLE outputs—such as flood depth, flow velocity, and timing information—can be informative for identifying flash flood behavior in small watersheds and headwater streams, where rapid hydrologic response and limited channel storage dominate flood dynamics. However, for large river systems like the Guadalupe or Colorado, these same outputs primarily reflect floodplain inundation and channel hydraulics rather than flashiness. As a result, directly leveraging Base Level Engineering (BLE) model outputs alone for flash flood map production would not consistently distinguish between flashy and non-flashy flood hydrologic response across the 30-county study area.

An alternative approach involving the generation of new hydrologic and hydraulic model simulations specifically tailored to flash flood conditions was considered. Such an approach would allow short-duration, high intensity rainfall events to be represented more explicitly; however, this approach was determined to be infeasible within the project schedule. Developing flash flood-specific model runs would require additional technical guidance, customized storm definitions targeting short-duration, high-intensity rainfall, and extensive computational effort to simulate and post-process results across numerous watersheds and catchments ranging in size from those associated with small channels to large river systems. Ensuring consistency and comparability of results across the entire 30-county study area would further increase the complexity of this approach. Implementing such modelling at a regional scale was therefore not practical for this initiative.

Instead, BLE HEC-RAS 2D model outputs, where available, were used extensively for validation of the Analytic Hierarchy Process (AHP)-derived flash flood hazard index rather than as direct hazard inputs. The Base Level Engineering (BLE) model outputs were used to validate but not identify flash flood susceptibility along channel reaches. Base Level Engineering (BLE) models are well suited for this role because it provides spatially and temporally explicit, physics-based estimates of flooding, including flood extents and depth-velocity outputs derived from validated hydrodynamic simulations of both design storms and observed events. Based Level Engineering (BLE) model outputs provide an appropriate and independent benchmark against which to evaluate whether areas identified as highly susceptible to flash flooding also correspond to locations with the potential to experience flooding that also brings the deep and/or fast-moving water that characterizes flash flooding.

From the Based Level Engineering (BLE) models, spatial rasters of water depth and flow velocity for the 100-year, 24-hour storm were extracted and resampled to a common 300-meter resolution to support comparison with the 1km hazard grid. For each pixel within the model domain, the maximum value of the depth–velocity product was computed over the full duration of the simulation to capture the most hazardous conditions experienced at each location. This was accomplished by combining depth (D) and velocity (V) grids into a single grid, referred to herein as the depth-velocity raster. Although depth and velocity were also examined independently, the depth-velocity raster product was emphasized because it integrates both flood depth and velocity, providing a meaningful indicator of flood intensity. Higher depth-velocity raster values correspond with conditions associated with increased hydrodynamic forces, greater damage potential, and elevated safety risks. The depth-velocity raster product is well suited for estimating the destructive potential of flooding and for validating the AHP-derived flash flood hazard index.

BLE depth-velocity raster results were readily available for 22 watersheds at the initial time of analysis, and these depth-velocity raster results were compared with the hazard product from the Analytic Hierarchy Process. Results for individual watersheds are presented in Appendix B.

The depth-velocity raster was subsequently classified into five hazard categories using the FEMA Flood Depth and Analysis Grids Guidance (2018) (Figure 4-1 and Table 4-2). The flood hazard criteria were previously defined based on the safety of vehicles, people, and buildings, which gives some indication of the impacts of each flood severity level, though the classification thresholds vary between publications (Smith et al., 2014). The FEMA classification of low flood severity (indicated by classification of 1 in this study), is in line with generally being safe for vehicles, people and buildings; medium (2) flood severity is in line with being unsafe for vehicles, children, and the elderly; and high (3) flood severity is in line with being unsafe for all vehicles and people (Smith et al., 2014). Beyond this category (i.e., in the very high (4) and extreme (5) classifications), the flood severity is unsafe for vehicles and people, and buildings will be vulnerable to structural damage (Smith et al., 2014). The depth-velocity raster results from the BLE models were categorized into five numerical classes representing flood severity, which were then used to evaluate spatial agreement with the Analytic Hierarchy Process-based flash flood hazard index for the study area (Figure 4-2). Figure 4-3 shows a close-up view of flash flood hazard index for the Upper Guadalupe watershed. Strong agreement between areas of elevated Analytic Hierarchy Process hazard and high depth-velocity raster values increases confidence in the flash flood hazard assessment, while discrepancies highlight areas where additional refinement may be warranted. In this way, BLE outputs play a critical role in validating, rather than defining, the flash flood hazard framework developed in this study.

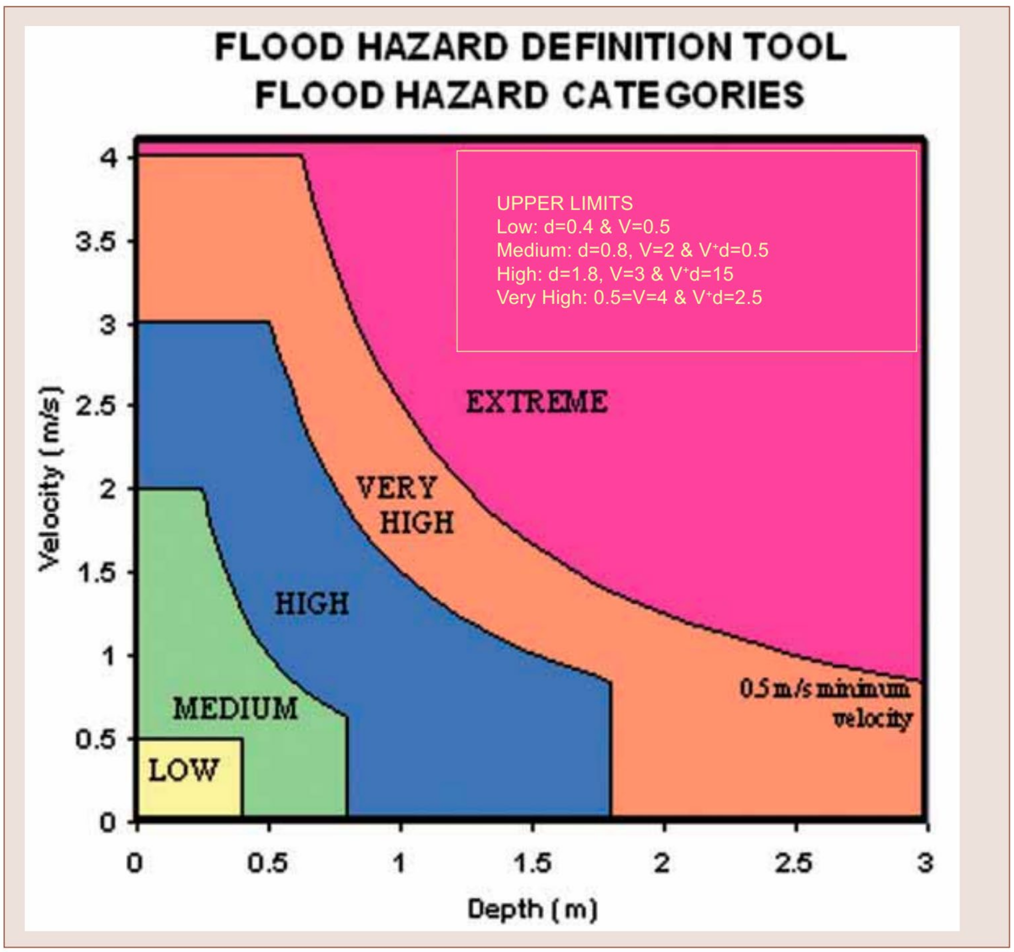


**Figure 4-1. Flood hazard categorization using depth, velocity, and depth-velocity product (Adapted from the FEMA Flood Depth and Analysis Grids Guidance (FEMA, 2018)).**

**Table 4--2. Simplified flood depth and velocity severity grid symbolization categories (Adapted from the FEMA Flood Depth and Analysis Grids Guidance (FEMA, 2018)).**

| Flood Severity Category | Depth * Velocity Range ($ft^2/sec$) | Depth * Velocity Range, metric ($m^2/sec$) |
|---|---|---|
| Low (1) | < 2.2 | < 0.2 |
| Medium (2) | 2.2 – 5.4 | 0.2 – 0.5 |
| High (3) | 5.4 – 16.1 | 0.5 – 1.5 |
| Very High (4) | 16.1 – 26.9 | 1.5 – 2.5 |
| Extreme (5) | >26.9 | >2.5 |

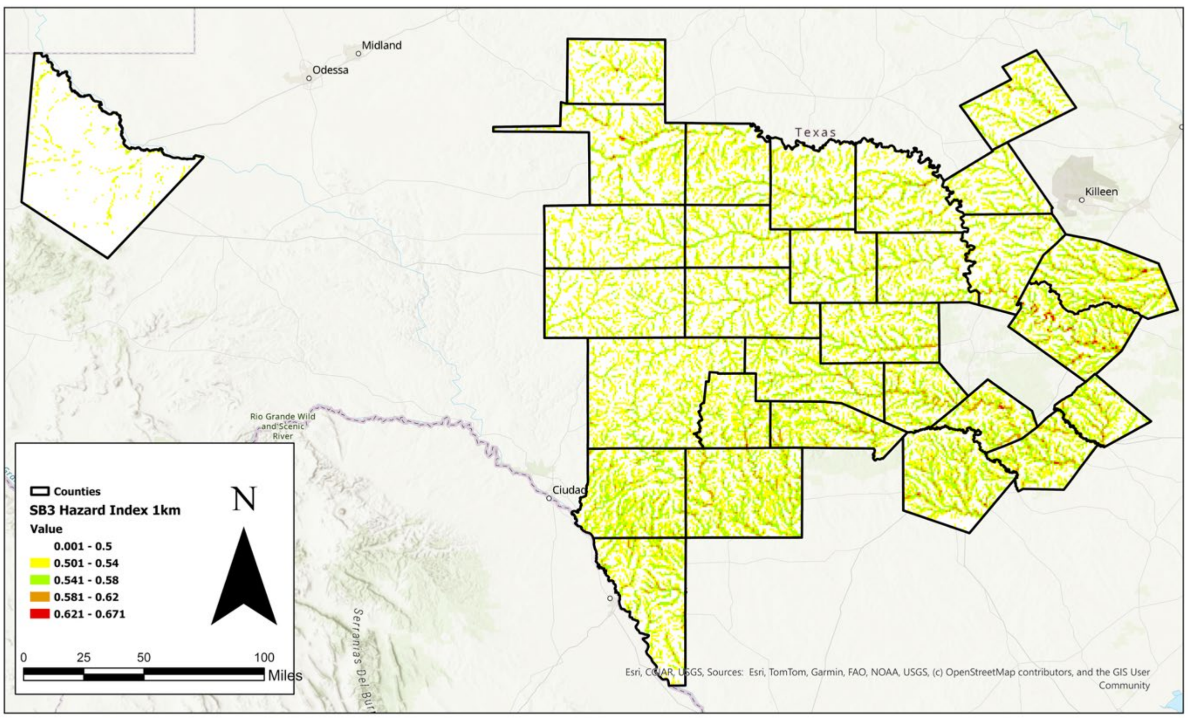


**Figure 4-2. Draft hazard information for the 30-county area**

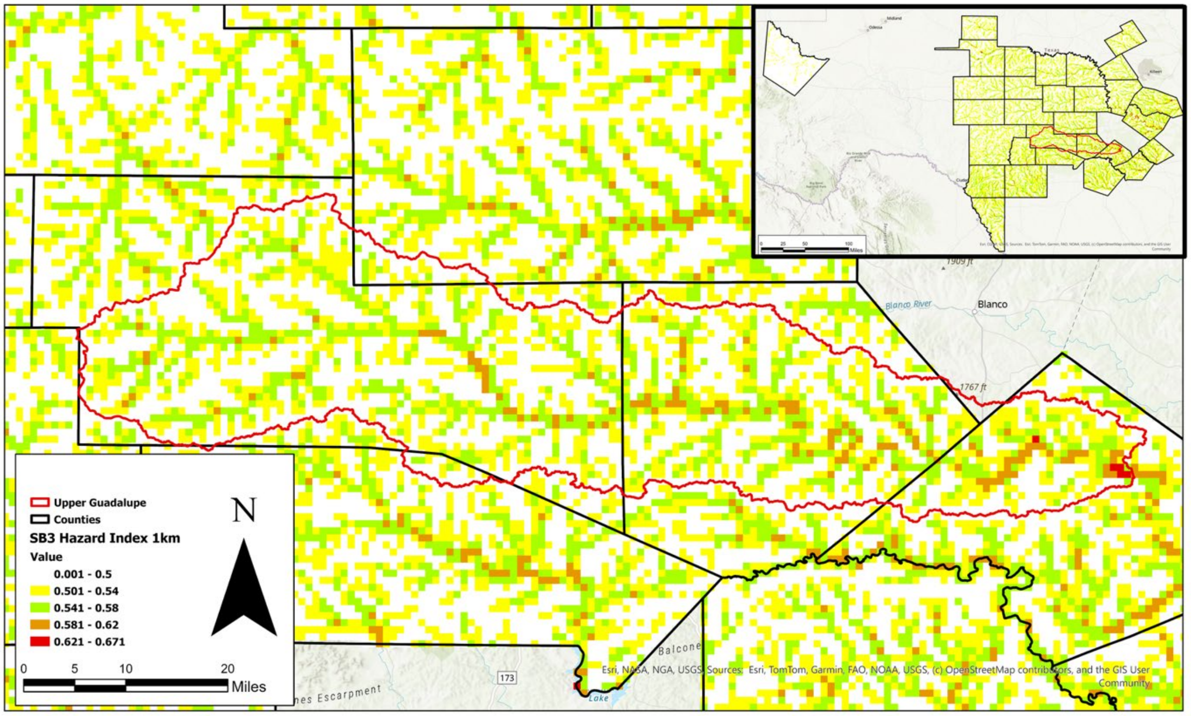


**Figure 4-3. Close-up view of flash flood hazard index over the Upper Guadalipe watershed.**

## Quantitative Measures of Hazard Index Performance

Depth-velocity results can be compared with receiver operating characteristic (ROC) curves to quantitatively evaluate the performance of flood hazard models, as supported by literature. ROC curves provide a quantitative, threshold-independent measure of model performance by comparing the proportion of areas correctly identified as high hazard (true positives) against areas incorrectly identified as high hazard (false positives) across a range of hazard thresholds when compared to the depth-velocity raster based on BLE model outputs. In this application, the receiver operating characteristic (ROC) analysis is used to evaluate how well the Analytic Hierarch Process-derived hazard index distinguishes between locations experiencing flooding from those experiencing flash flooding. Here, locations with high depth-velocity values representing deep, fast-moving floodwaters (and therefore higher flood hazard conditions) are treated as the observed "positive" condition, while areas with low depth-velocity values represent the "negative" condition. The area under the curve (AUC), in this case the receiver operating characteristic (ROC), summarizes the model's ability to discriminate between hazardous and non-hazardous areas—with higher AUC values indicating stronger agreement between the hazard layer and the depth–velocity–based flood hazard representation. This approach provides an objective and statistically robust validation of the flash flood hazard assessment.

The area under the curve (AUC) provides a single, threshold-independent measure of model performance by summarizing the overall ability of the hazard layer to discriminate between hazardous and non-hazardous conditions. An AUC value of 0.5 indicates performance no better than random classification, while values approaching 1.0 indicate strong discriminatory skill. In this context, the AUC represents the probability that a randomly selected location with high depth-velocity values is assigned a higher hazard score than a randomly selected low-hazard location. In simple terms, a higher AUC means the hazard index more consistently ranks dangerous locations above less dangerous ones (as expected). The resulting AUC therefore provides an objective and statistically robust assessment of how well the Analytic Hierarchy Process (AHP)-based flash flood hazard layer aligns with physically-based flood hazard estimates derived from the BLE model.

Validation based on the 100-year, 24-hour event was performed for 22 watersheds according to the availability of 2D BLE models and directly accessible results due to project time constraints. Figure 4-4 shows the 22 watersheds that were used for validation among the 48 HUC-8 watersheds within the study area. Example validation results for the Upper Guadalupe for the 100-year, 24-hour storm and AUC values for all analyzed watersheds are provided in Appendix C. The purpose of the ROC analysis is not to assess the exact cutoff between hazardous and non-hazardous areas, nor to achieve a specific target AUC value. Rather, it is used to evaluate whether the hazard index captures meaningful spatial patterns—such as those areas anticipated to experience higher depth and faster velocities during a flood receiving higher hazard scores than areas anticipated to experience lower depths and slower velocities.

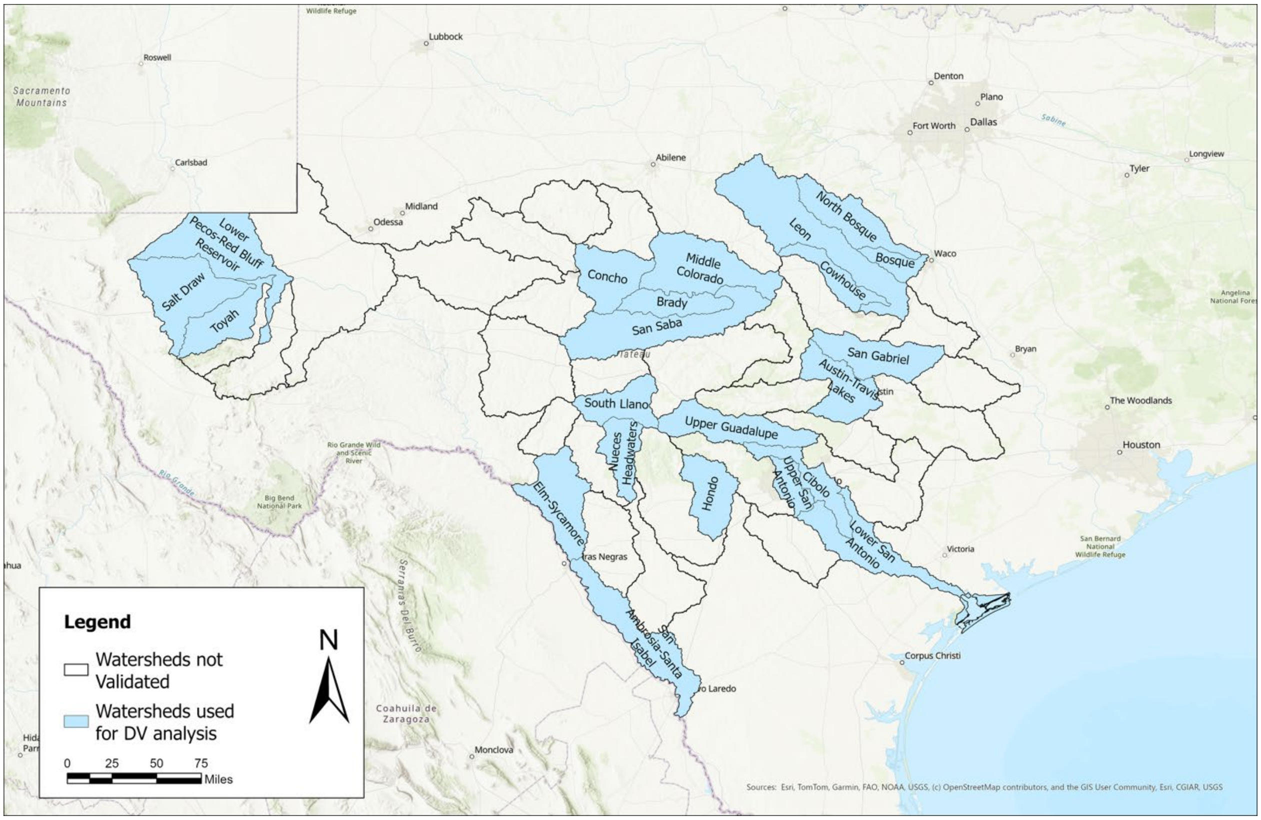


**Figure 4-4. 22 watersheds (blue) used for the depth-velocity hazard validation among the 48 HUC-8 watersheds within the study area.**

Validation against the 100-year, 24-hour rainfall scenario produced an acceptable AUC of 0.671 for the Upper Guadalupe watershed, reflecting moderate but meaningful discriminatory ability. AUC values from other watersheds ranged from 0.52 to 0.85, with a mean of 0.685 and a median of 0.69. A full table of AUC values for the 22 watersheds is given in Appendix C. This range indicates that model performance varies across watersheds but generally exceeds what would be expected by chance alone (e.g., 0.5). Such variability is expected given the inherent limitations of the validation datasets, including the conservative spatially distributed characteristics of the design-storm. In other words, the design storm within the BLE models is not designed to represent the intensity of a flash flood rainfall event or the potential impacts of the movement of a flash flood storm across watersheds. While the validation with depth-velocity raster from the BLE models is not expected to be a perfect comparison to the developed hazard index, the AUC values exceeding 0.5 demonstrate that the framework is effective for screening-level identification and prioritization of areas more likely to experience high-impact flooding. Accordingly, AUC values are interpreted diagnostically and comparatively, recognizing the imperfect nature of the validation data.

While ROC and AUC provided a quantitative, threshold-independent measure of the overall ranking performance of the hazard index, they do not directly illustrate how flash flood hazard index values are distributed across different levels of physics-based hazard levels. In addition, ROC analysis summarizes discriminatory ability using a single metric but does not convey how flash flood hazard index values vary within and between depth-velocity hazard classes. To complement the ROC-based evaluation and provide additional insight into the physical consistency of the hazard index, a class-based comparison was further performed by examining the distribution of flash flood hazard index values within the five DV hazard classes derived from BLE model outputs.

Figure 4-5 presents a combined box plot showing the distribution of flash flood hazard index values for each depth-velocity hazard class (1-5) across all analyzed watersheds. This figure was created based on aggregated raster cells from the watersheds used in the receiver operating characteristic (ROC), allowing a comprehensive assessment of how the flash flood hazard index values vary with increasing flood hazard levels. The plot summarizes the median, interquartile range, and spread of flash flood hazard index values within each depth-velocity class, providing insight into both central tendency and variability.

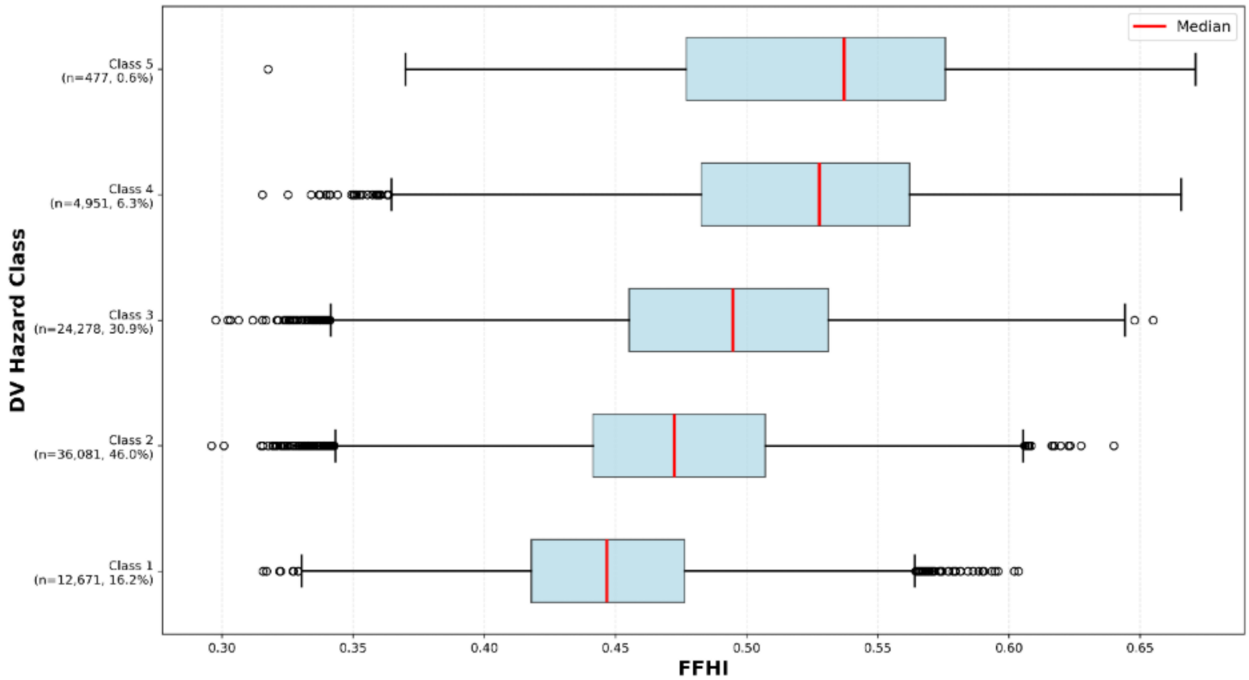


**Figure 4-5. Flash flood hazard index distributions by Depth-Velocity (DV) hazard classes for all watersheds**

A clear and systematic increase in flash flood hazard index values is observed in Figure 4-5 with increasing depth-velocity hazard classes. Median flash flood hazard index values rise progressively from Class 1 through Class 5, indicating locations experiencing deeper and faster floodwaters are consistently aligned with higher hazard scores by the Analytic Hierarchy Process framework. This monotonic trend across depth-velocity hazard classes provides strong evidence that the flash flood hazard index values capture meaningful physical gradients in flood severity rather than responding to random spatial patterns. The median values for the depth-velocity hazard Classes 4 and 5 were 0.527 and 0.537, respectively, which were used to support selection of an elevated hazard threshold described in the later sections for defining which areas were potentially included in the provisional mapping product.

This class-based comparison complements the receiver operating characteristic (ROC) by providing an interpretable, distribution-based validation that does not have to rely on binary classification thresholds alone. While ROC curves evaluate ranking performance across all possible thresholds, the depth-velocity hazard class analysis directly demonstrates that flash flood hazard index values increase systematically with increasing flood depth and velocity. Together, these two validation approaches provide complementary evidence that the Analytic Hierarchy Process-derived hazard index aligns with physically-based flood hazard representation from BLE models.

# 5. Factors Contributing to Exposure

Exposure represents the people and properties that may be affected by flooding. Because outdoor warning sirens are intended to warn people of a flash flood, exposure in this study focuses on indicators of human presence rather than property impacts. Typical exposure factors from the literature include variables such as population density, building density, and/or road density to represent the concentration of people in flood hazard areas. Exposure factors are necessary in this study to ensure the identification of locations that may need outdoor warning siren coverage due to the presence of people. For more details on the factors contributing to exposure identified through the literature review, see Appendix A.

## Outdoor Exposures

Outdoor exposures describe areas where people congregate outdoors or areas that draw transient populations (e.g. tourists and visitors). It is important to capture where people may sleep overnight outside, such as in campgrounds and recreational vehicle (RV) parks, since outdoor warning sirens are most effective at warning people outside. Campground and RV park locations were compiled by TWDB, obtained through data requests, address listings, or publicly available downloads, as described in Appendix B. Since the best spatial data available for campgrounds were in coordinate format, the area of extent is estimated with a threshold of 1,460-foot (500-meter) proximity. This is considered reasonable because the campground dataset does not discern for spatial variability of where people may be positioned relative to the point location.

Open spaces like parks can also attract large concentrations of people in the outdoor environment, potentially for recreation or sometimes for sleeping overnight. The Texas Parks and Wildlife Department (TPWD) delineated the area extents or footprints of parks within the state, as described in Appendix B. The spatial distribution of populations within the parks are not depicted, but people are expected to congregate within the boundaries of the delineated parks.

Outdoor sirens are designed to warn people outdoors, where audio is less obstructed. Low water crossings were considered but ultimately not prioritized since outdoor warning sirens would not be as impactful at warning or improving safety to people within vehicles. People within vehicles would likely be mobile and more capable of responding to alerts than people sleeping overnight in more exposed outdoor locations, like campgrounds or parks.

## Building Exposures

The 2025 version of the building dataset developed by Regional Flood Planning Groups (RFPG) was utilized to identify and quantify exposure. This dataset was in geospatial format that included building footprint geometries and attributes such as daytime and nighttime populations and building category type. While population was identified as the dominant exposure factor, the available building population data may not capture transient populations (e.g., tourists or temporary occupants). Accordingly, this data served as the primary spatial representation of locations where people are (through population) or may be (through buildings) located across the study area and thus formed the base of all exposure data for this study. Three features from this data that contribute to known building exposures are: locations of buildings, population count, and building count.

Building counts were summarized within a 1-kilometer by 1-kilometer cell to obtain counts of the number of building footprints that intersect a cell or the 0.2 percent (500-year) annual chance floodplain. The building data included six categories: residential, agricultural, vacant or unknown, commercial, public, and industrial—with residential representing the overwhelming majority. To be conservative in the identification of where people could be located during flash floods, all categories of buildings were included in the exposure data, and attributes are available for each category. For population, the maximum values of daytime or nighttime population were calculated for each building and then summed for each 1km cell within the watersheds included in the study area.

In addition, historic flash flood events with recorded exposures can be applied to identify additional building exposures. Data from the NOAA NWS Storm Events Database was captured where fatalities, injuries, or monetary building damages were recorded to prioritize areas with historical flash flood exposures, with the assumption it may occur again. Where the area extent of historic flash flood events are not captured in this dataset, the potential outdoor exposure is indicated with a 1,460-foot (500-meter) proximity of the event location to account for the spatial variability of where flooding may have occurred.

Additionally, urban areas may have readily available, widespread access to other sources of flash flood warning or alert information—so, it is important for these communities to consider if outdoor warning sirens would meaningfully improve notification during flash flood events when operated in conjunction with other alerting methods. Further discussions with cities are needed to determine where flood warning sirens could be most effective.

## Other Considerations

More details on the data collection and processing of exposure factors can be found in Appendix B.

# 6. Determining Flash Flood-Prone Areas that May Warrant Outdoor Warning Sirens

Initial results from the Flash Flood Hazard Index (FFHI) maps were refined to aid in determining where outdoor flood warning sirens may be warranted, such as locations where people live, work, visit, navigate, or congregate in flash flood-prone areas. Using the FFHI, locations were refined with additional consideration for outdoor, historic, urban, and rural exposures for high and moderate hazard areas. The areas of overlapping hazard and exposure provide the basis for this product and bring awareness to the reason why different areas may warrant sirens.

The provisional Flash Flood Risk Areas (FFRA) provides context for areas that potentially warrant outdoor flood warning systems through a hierarchy of criteria, based on flash flood hazard and exposure to flooding. The flash flood hazard threshold identifies a "moderate to high" hazard category established through FFHI validation. Additional categorizing considers the presence of exposure by accounting for buildings, campgrounds, parks, and historic flash flood events with recorded fatalities, injuries, or damages.

The product is visualized using the 0.2 percent (500-year) annual chance floodplain spatial data with attribution at 1km resolution of associated hazard and exposure data. Pixels from the 0.2 percent (500-year) annual chance floodplain are identified with an elevated flash flood risk, according to the hierarchy of hazard and exposure criteria, as shown in Figure 6-1.

The visualization field provides the provisional FFRA product information intended for public understanding. See Appendix E for more detailed information related to these fields. This field provides a simple attribution for the dataset that is easily digestible from an end user perspective. The attribute provides background information for the areas that are considered at risk of flash flooding and help establish the priority of concern. With this information, stakeholders can identify areas that may warrant siren placement based upon flash flood risk analysis in a floodplain format that is commonly understood.

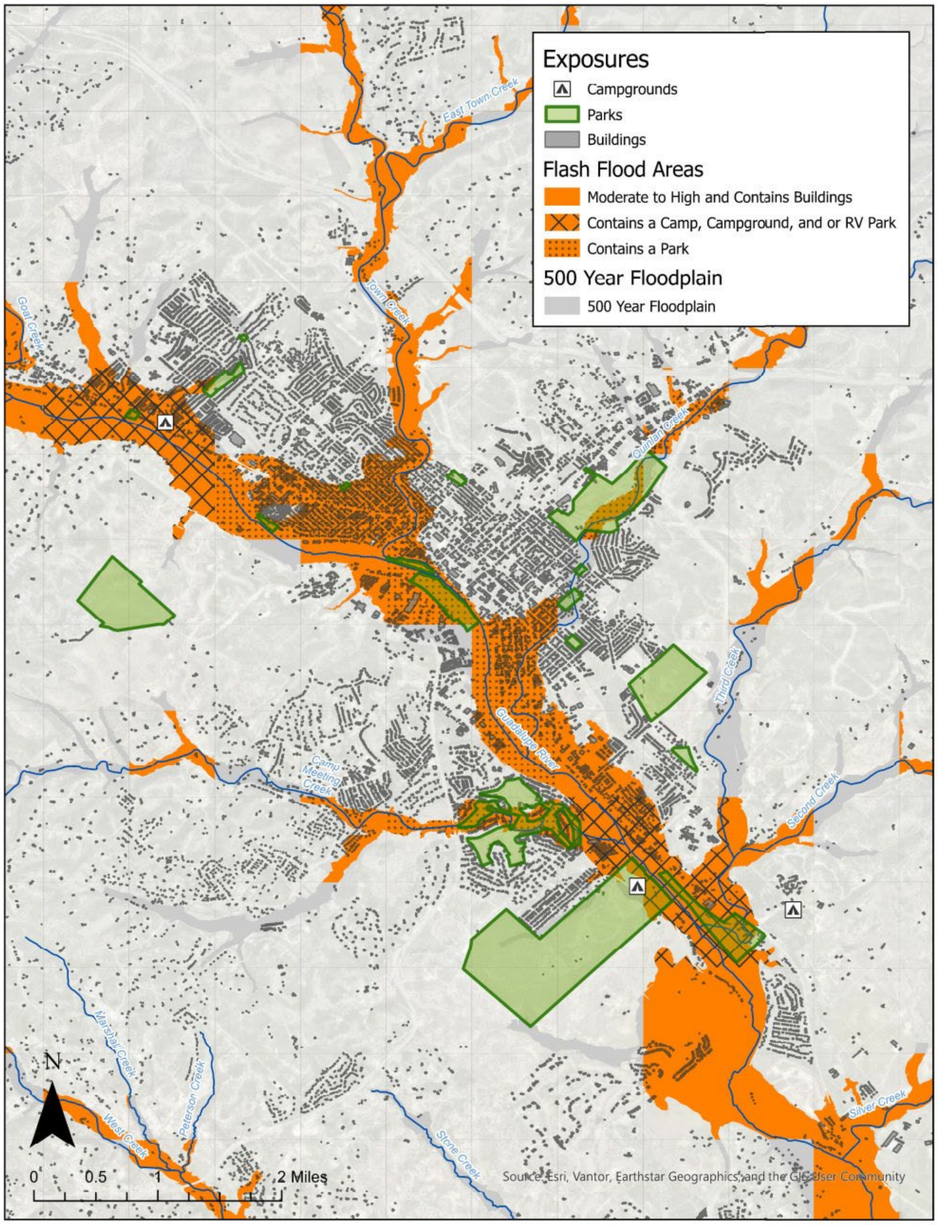


**Figure 6-1: Example Visualization of Provisional FFRA**

The gridded 0.2 percent (500-year) annual chance floodplain format does not undermine the communicated risk. Fragmented floodplains that do not indicate elevated risk can be adjacent to areas identified, due to pixel-based calculations and resolution. In the example in Figure 6-1, the visualization fields identify the reason for consideration for areas that may warrant siren placement. Segments of the floodplain that are not identified as "medium to high" hazard retain the 0.2 percent (500-year) annual chance floodplain visual extent because it does not meet the criteria within that pixel. However, the proximity to high priority pixels provides this detail for a general area being considered. Note that final placement of a siren warning system based upon the provided hazards may also provide audible coverage to some adjacent areas that are not categorized as part of this gridded format, depending on terrain, obstructions, and other factors. See Figure 6-1 for an example in which this occurs. Furthermore, discontinuity of identified areas without direct exposures is a limitation of utilizing the 0.2 percent (500-year) annual chance floodplain as a visual extent. This is due to using data that is pixel based, and it is not reasonable to be able to attribute the stream source or origination of produced floodplains without uncertainty. Nevertheless, this method maintains the analysis driven data integrity of the product for stakeholders to make informed decisions and provide additional local knowledge to help determine siren placement.

Table 6-1 below indicates the number of provisional FFRA miles using the USGS National Hydrography Dataset (NHD) flowlines for 30 counties.

**Table 6-1. Provisional FFRA stream miles.**

| County | Provisional FFRA Miles | Total Stream Miles | Provisional FFRA Percentage |
|---|---|---|---|
| Bandera | 380 | 2,167 | 17.6 |
| Bexar | 876 | 2,443 | 35.9 |
| Burnet | 284 | 2,757 | 10.3 |
| Caldwell | 222 | 1,403 | 15.8 |
| Coke | 32 | 2,061 | 1.6 |
| Comal | 300 | 1,241 | 24.2 |
| Concho | 62 | 1,686 | 3.7 |
| Edwards | 188 | 4,958 | 3.8 |
| Gillespie | 338 | 2,672 | 12.7 |
| Guadalupe | 413 | 1,765 | 23.4 |
| Hamilton | 72 | 1,490 | 4.9 |
| Kendall | 302 | 1,680 | 17.9 |
| Kerr | 431 | 2,515 | 17.2 |
| Kimble | 247 | 2,662 | 9.3 |
| Kinney | 172 | 2,536 | 6.8 |
| Lampasas | 111 | 1,658 | 6.7 |
| Llano | 215 | 2,664 | 8.1 |
| Mason | 219 | 2,557 | 8.6 |
| Maverick | 154 | 3,204 | 4.8 |
| McCulloch | 118 | 2,438 | 4.9 |
| Menard | 104 | 1,733 | 6.0 |
| Real | 252 | 1,789 | 14.1 |
| Reeves | 2 | 2,529 | 0.1 |
| San Saba | 189 | 2,524 | 7.5 |
| Schleicher | 49 | 1,988 | 2.4 |

| County | Provisional FFRA Miles | Total Stream Miles | Provisional FFRA Percentage |
|---|---|---|---|
| Sutton | 110 | 2,759 | 4.0 |
| Tom Green | 201 | 2,468 | 8.2 |
| Travis | 703 | 2,533 | 27.7 |
| Uvalde | 446 | 3,142 | 14.2 |
| Williamson | 644 | 2,607 | 24.7 |
| Total for 30 Counties | 7,839 | 70,629 | 11.1 |

These numbers may overestimate stream mileage expectations where there are multiple parallel stream sources within a single floodplain, as shown in the figure below.

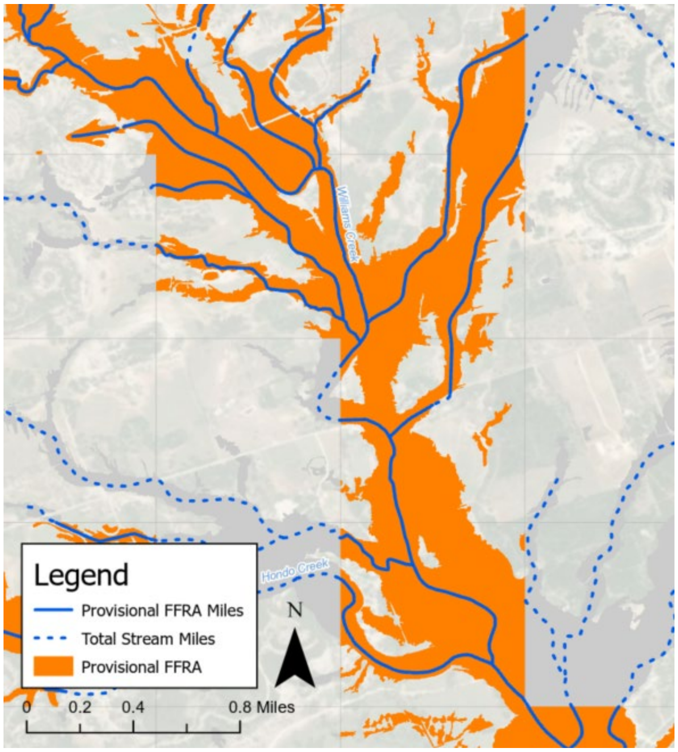


**Figure 6-2. Parallel Stream Mileage**

These results and resulting flash flood risk areas reflect technical screening only and have not yet received community input. For more information and recommendations, refer to Appendix E.

# 7. Limitations

The project team developed this flash flood hazard assessment at a regional scale appropriate for identifying general patterns across the 30-county study area and enabling timely access to grant funding authorized by SB5. As a regional-scale mapping efforts, this analysis provides a comprehensive first assessment (in this case capturing major flash flood risk patterns) while recognizing that no regional study can capture every site-specific factor (such as, in this case, terrain features, localized drainage patterns, or individual property conditions). Attempting to resolve every fine-scale detail would have delayed communities' access to critical, life-saving funding and warning system deployment. Accordingly, base hazard factors generally calculated at 30-meter resolution were resampled to 1km resolution using GIS smoothing and averaging methods to ensure consistency across the study area and timely project delivery.

The Flash Flood Hazard Index methodology combines multiple peer-reviewed factors using the Analytic Hierarchy Process (AHP), with factor selection and weighting informed by extensive literature review and expert interpretation. Although the relative importance of individual factors may vary across local contexts, the team conducted a thorough pairwise comparison for each hazard factor to understand their contributing importance so that appropriate weights could be determined. The resulting Flash Flood Hazard Index (FFHI) values were further validated using multiple data sources including historical flood reports, documented damages, and available HEC-RAS 2D model outputs—recognizing that no single source dataset provides complete or perfectly accurate flash flood information.

This product serves as an effective screening tool that identifies broad flash flood risk patterns and provides communities with an initial, comprehensive assessment for prioritizing outdoor warning siren placement. The mapping establishes regional context and supports resource allocation across the 30-county area. The project team recognizes that local emergency managers and officials possess valuable knowledge of specific flooding patterns and community conditions. Communities are encouraged to enhance this regional assessment with local knowledge, field observations, and site-specific considerations when making final siren placement decisions. This combined approach balances statewide methodological consistency with local expertise, ensuring that community-specific needs are addressed while enabling timely access to program funding without unnecessary delay.

## Project Schedule

The technical approach used within this study was tailored to be consistent with the desire to enable timely access to grant and program funding authorized by SB5. The BLE models are valuable tools that have been leveraged in this study, but future analyses could help utilize them to their full capabilities. With that in mind, the team is confident that the method and weights for hazard calculation are well-supported through the literature, leading to a well-supported provisional product that considers the eventual goal of the product to support the need for outdoor warning siren systems.

## Riverine Flash Flooding Target

While the hazard dataset has comprehensive coverage for the 30-county area, the end product is tailored specifically to target flash flood-prone areas along rivers, streams, channels, or other waterways that may warrant sirens (and may not fully capture localized or pluvial flooding mechanisms). Because of this specialized project target, it should not be concluded that areas with a low FFHI won't experience flash flooding. It is important to note that, given extreme rainfall intensity, hazardous flash flooding can occur at any location, including but not limited to street flooding, low-lying urban areas, and localized drainage areas.

## Analytic Hierarchy Process Method

Considering the time constraints and comprehensive evaluations of plausible practices supported by peer-reviewed literature, the AHP method was reviewed and selected for the project. The method's performance is influenced by the nature and quality of the input data. While the input data were reviewed rigorously by the project team, it is possible for uncertainty to persist due to inherent limitations. The weights established for the hazard layer are based on the literature review, but expert interpretation is still needed for incorporation of the flashiness index developed by Saharia et al., 2017 as a hazard input factor. To address this limitation, a sensitivity analysis for the flashiness index was conducted.

## Spatial Resolution of Product

The methodology used in this study was selected to provide timely access to grant funding authorized by Senate Bill 5 (SB5) while delivering sufficient accuracy for a regional analysis of this scale. The methodology is implemented using distributed computing techniques and applied on a 1-kilometer grid resolution. This resolution was selected based on the accuracy and resolution of the underlying input datasets, which support a minimum grid cell size of 1 kilometer, while providing sufficient spatial detail to support the multi-factor flash flood hazard methodology used in this study.

At this regional scale, the 1-kilometer grid resolution does not capture all sub-kilometer variations in flash flood conditions that may be influenced by localized topography, small drainage features, or site-specific infrastructure. Accordingly, the results are intended to identify stream reaches and adjacent areas that are prone to flash flooding where people, property, infrastructure, or other assets may be impacted. Areas exhibiting flash flood hazard, but lacking exposure are not identified as flash flood risk areas for purposes of this analysis, and no outdoor warning sirens are implied in such locations. Local jurisdictions are encouraged to use site-specific information and local knowledge to further refine siren placement within the identified flash flood risk areas, as appropriate.

## Existing Conditions

This analysis reflects historical and current conditions and does not account for future changes in land use, watershed modification, or precipitation patterns. Flash flood risk may increase over time as conditions change.

## Role of the Study and Local Refinement

This study provides a foundational, first-phase assessment of flash flood risk across the 30-county study area, intended to support statewide consistency and timely implementation of the requirements established under Senate Bill 3 (SB3) and Senate Bill 5 (SB5). The resulting Flash Flood Risk Areas (FFRA) identify locations where flash flood hazard coincides with the presence of people, property, infrastructure, or other assets that may be impacted, and therefore represent areas that may warrant further consideration for outdoor warning sirens.

The datasets leveraged in this study represent the best spatial data available at the time of this study, as described in Appendix B. Exposure data may be limited in the building footprints, campground locations, and park footprints captured, according to source data limitations. Where area extents were not provided for historic flood events and campgrounds, spatial variability was considered with a 1,460-foot (500-meter) proximity from the point location.

Local drainage infrastructure, including storm sewers, culverts, channel improvements, and roadway crossings, is not explicitly represented. These features can significantly alter local flash flood behaviour and should be considered during local review. Exposure estimates may underrepresent transient, seasonal, or informal outdoor populations (e.g., special events, river recreation, temporary camps) that are not captured in available datasets.

The Flash Flood Risk Areas (FFRA) mapping is not intended to replace local planning, engineering judgment, or site-specific evaluation. Rather, it is designed to inform and support subsequent, locally led decision-making. Local jurisdictions are encouraged to incorporate site-specific data, field observations, historical experience, and community knowledge to further refine siren placement within the identified flash flood risk areas, as appropriate. This phased approach balances statewide consistency with local expertise and ensures that final siren placement decisions reflect both regional risk patterns and community-specific conditions.

# 8. Takeaways

This workflow offers a clear, consistent way to identify flash flood risk areas within the 0.2 percent annual chance floodplain where outdoor warning siren systems may be warranted. It uses definitions the public can understand, data public agencies trust, and validation that strengthens confidence. As data improves, weights and thresholds can be revisited to keep the products relevant.

## Key Deliverables

This study produced the following deliverables supporting the TWDB responsibilities outlined in SB3:

1. A geospatial dataset delineating flash flood-prone areas where outdoor warning siren systems may be warranted.
2. Supporting GIS layers, including building footprints, camps, parks, and the FFHI at 1-km resolution.
3. Technical documentation of methodology, data sources, validation procedures, and analytical decisions provided.
4. An interactive dashboard enabling review of results, validation evidence, and exposure characteristics by county and stream reach.

## Next Steps

The technical foundation provided by the results can be refined through continued coordination with stakeholders and additional analysis. Below are some suggestions for future analysis updates.

- Conduct rate of rise analyses (water surface or streamflow) at stream gages for extreme events. Additionally, rate of rise analyses can be conducted using outputs from unsteady or 2D BLE flood models. Time series of water surface elevations or streamflow from flood models for various return periods can supplement the analyses using streamflow gages.
- Extract lag time (time difference between center of mass of precipitation and center of mass of flow hydrograph) from 2D models. Lag times are a good indicator of flash flooding. Readily available 2D models can be leveraged to extract lag time for various return periods.
- Incorporate additional BLE models for other watersheds when the 100-year, 24-hour storm results are readily available for 2D modeling to ensure BLE models of similar type are used consistently across the entire study area and confirm validation.
- Assess high intensity, short duration storms. Typical BLE models include return periods with longer durations such as 24 hours. Existing 2D BLE models can be supplemented with shorter duration storms such as 100-year, 6-hour, and 10-year, 6-hour.
- Include more complex meteorological forcing methods such as storm shifting of historic flash flood events and Monte Carlo simulations. While short duration storms, such as 100-year, 6-hour storms, may be appropriate for small and mid-size streams, they may not be appropriate to assess flash flooding potential for large rivers.
- Incorporate future updates to source exposure datasets. Quality of assessment of exposure (property and population) and subsequent assessment of flash flood risk are dependent on the accuracy of these datasets. These datasets include building footprints, their characteristics, and camp and parks sites and associated structure and recreational locations where people congregate and explore. These foundational datasets should be improved and maintained over time as the ground conditions change.
- Integrate post-flood high water mark survey data from future events to enhance validation.
- Investigate whether this methodology should be expanded to other flash flood-prone regions of Texas.
- Develop automated update procedures as new building footprint data are released.
- Consider detailed delineation of high-risk population areas—including campgrounds, RV parks, community parks, youth camps, other camps (business, religious, etc.), and popular recreation trails—as additional

datasets become available. The current analysis focuses on readily available datasets to support timely completion of the study.

# Appendix A. Literature Review & Analysis

## Goals and Outcomes

A review of over 30 published studies and journal articles was conducted to identify various methods and factors appropriate for use in conducting flash flood risk assessments. This literature review process helped inform the methodology chosen for this effort, the basis for selecting and processing the input factors, and the validation procedures. Literature was reviewed to identify predominant methods used to assess flash flood hazard. Prior studies identified a range of approaches for integrating multiple input factors into composite hazard or risk products, commonly through multi-criteria weighting methodology or machine learning techniques. In general, these methods work by applying individual weights for each input factor to determine the combined effect of the inputs. The common multi-criteria methods identified during the literature review process are presented in Table A-1, Table A-2, Table A-3, and Table A-4—these tables summarize the findings from the literature including technical methods, hazard factors, exposure factors, and validation information, respectively.

## List of Publications Reviewed

- Methods to establish flash flood-prone hazard areas: (Abedi et al., 2022; Ahmadalipour & Moradkhani, 2019a; Al-Rawas et al., 2024; Aroca-Jiménez et al., 2022; Band et al., 2020a; Brand, 1975; Bui et al., 2019; Chowdhury, 2024a; Costache, 2019a, 2019b; Costache, Hong, et al., 2019; Costache, Pham, et al., 2019; Costache et al., 2020, 2022; Darwish, 2023; Duan et al., 2022; Elghouat et al., 2024; Elmahdy et al., 2020; Elsadek & Almaliki, 2024; Forte et al., 2025; F. He et al., 2025; Hoang & Liou, 2024; Janizadeh et al., 2019; Ke et al., 2025; Khajehei et al., 2020; Khodaei et al., 2025; Khosravi et al., 2016a, 2016b; Kocsis et al., 2022; Lin et al., 2020; Majeed et al., 2023; Popa et al., 2019; Riaz & Mohiuddin, 2025; Saharia et al., 2017a; Shafapour Tehrany et al., 2019; Shawky & Hassan, 2023; Singh & Pandey, 2021; Talha et al., 2019; Tariq et al., 2022; Wahba et al., 2024; Waqas et al., 2021; Wilkho et al., 2025a; Zhuang et al., 2026).

- Investigation of vulnerability to flood hazards: (Ali & Nelson, 2025; Cikmaz et al., 2025; Shrestha et al., 2025; Tikuye et al., 2025).

- Flash flood-focused studies: (Abedi et al., 2022; Ali & Nelson, 2025; Band et al., 2020b; Bui et al., 2019; Chowdhury, 2024a; Cikmaz et al., 2025; Costache, 2019c, 2019a; Costache et al., 2022; Costache, Pham, et al., 2019; Costache & Zaharia, 2017a; Elghouat et al., 2024; X. He et al., 2024; Hoang & Liou, 2024; Khodaei et al., 2025; Kocsis et al., 2022; Majeed et al., 2023; Popa et al., 2019; Riaz & Mohiuddin, 2025; Shafapour Tehrany et al., 2019; Shawky & Hassan, 2023; Shrestha et al., 2025; Singh & Pandey, 2021; Talha et al., 2019; Tariq et al., 2022; Tikuye et al., 2025; Wahba et al., 2024; Waqas et al., 2021; Zhuang et al., 2026; Zulhisham & Sadek, 2023).

- Citations with hazard factors: (Abedi et al., 2022; Ali & Nelson, 2025; Band et al., 2020b; Bui et al., 2019; Chowdhury, 2024a; Cikmaz et al., 2025; Costache, 2019c, 2019a; Costache et al., 2022; Costache, Pham, et al., 2019; Costache & Zaharia, 2017a; Elghouat et al., 2024; X. He et al., 2024; Hoang & Liou, 2024; Khodaei et al., 2025; Kocsis et al., 2022; Majeed et al., 2023; Popa et al., 2019; Riaz & Mohiuddin, 2025; Shafapour Tehrany et al., 2019; Shawky & Hassan, 2023; Shrestha et al., 2025; Singh & Pandey, 2021; Talha et al., 2019; Tariq et al., 2022; Tikuye et al., 2025; Wahba et al., 2024; Waqas et al., 2021; Zhuang et al., 2026; Zulhisham & Sadek, 2023).

Studies such as Saharia et al., 2017 have established methods for determining flashy responses without considering the potential flooding impacts. Early work by Beard (1975) and subsequent flashiness-based indices highlight that flash flood risk is strongly influenced by frequency of extreme events compared to more frequent flows at a given location, a perspective that captures both channel response and human vulnerability to flooding. While this relative flashiness concept provides important context, it was not considered directly relevant here because it requires long-term, high-quality gaged flow records that are either unavailable or spatially inconsistent across the study domain—making this approach unsuitable for a fully distributed flood risk susceptibility framework.

## Methods found in Literature Review

Literature was reviewed to identify predominant methods used to assess flash flood hazard. Prior studies identified a range of approaches for integrating multiple input factors into composite hazard or risk products, commonly through multi-criteria weighting methodology or machine learning techniques. In general, these methods work by applying individual weights for each input factor to determine the combined effect of the inputs. The common multi-criteria methods identified during the literature review process are presented in Table A-1 with the method selected for this initiative shaded in light blue.

**Table A-1. Multi-criteria weighting methods from literature**

| Method | Strengths / Applications | Limitations | Typical Data Used | Related References |
|---|---|---|---|---|
| Multi Criteria Decision Analysis (MCDA) | Transparent, reproducible, defendable, widely used in regulatory contexts, variable weighting, easy to communicate to agencies | Subjective factor selection and weighting, assumes linear and independent criteria, sensitive to normalization and scaling. | DEM, TWI, soil, LULC | (Costache, Pham, et al., 2019; Elsadek & Almaliki, 2024) |
| Analytic Hierarchy Process (AHP) | Transparent variable weighting, defendable, flexible, widely used in regulatory hazard-mapping applications, easy to communicate to agencies | Relies on expert judgement in pairwise comparisons, assumes independence of one criterion with respect to others, weight sensitivity increases with the number of factors. | DEM, TWI, soil, LULC | (Lin et al., 2020; Majeed et al., 2023) |
| Weights of Evidence (WoE) | Handles non-linear spatial relationships | Requires reliable flood inventory data, assumes conditional independence between factors, limited extrapolation beyond historical events. | DEM-derived data, LULC, soil | (Chowdhury, 2024a; Kocsis et al., 2022) |
| GIS Weighted Overlay Index | Fast, interpretable, suitable for statewide comparison | Fixed or arbitrary weights, sensitive to class breaks and thresholds with limited representation of process interactions. | Standardized terrain, LULC, soil | FEMA NRI Documentation (2020) |

## Hazard Factors: Literature Details

These input factors represent the hazard criteria that were used to establish flash flood-prone areas within the methodological framework. The frequency of specific hazard factors with respect to the number of published studies, out of the thirty reviewed, using those factors in their analyses is presented in Figure A-1.

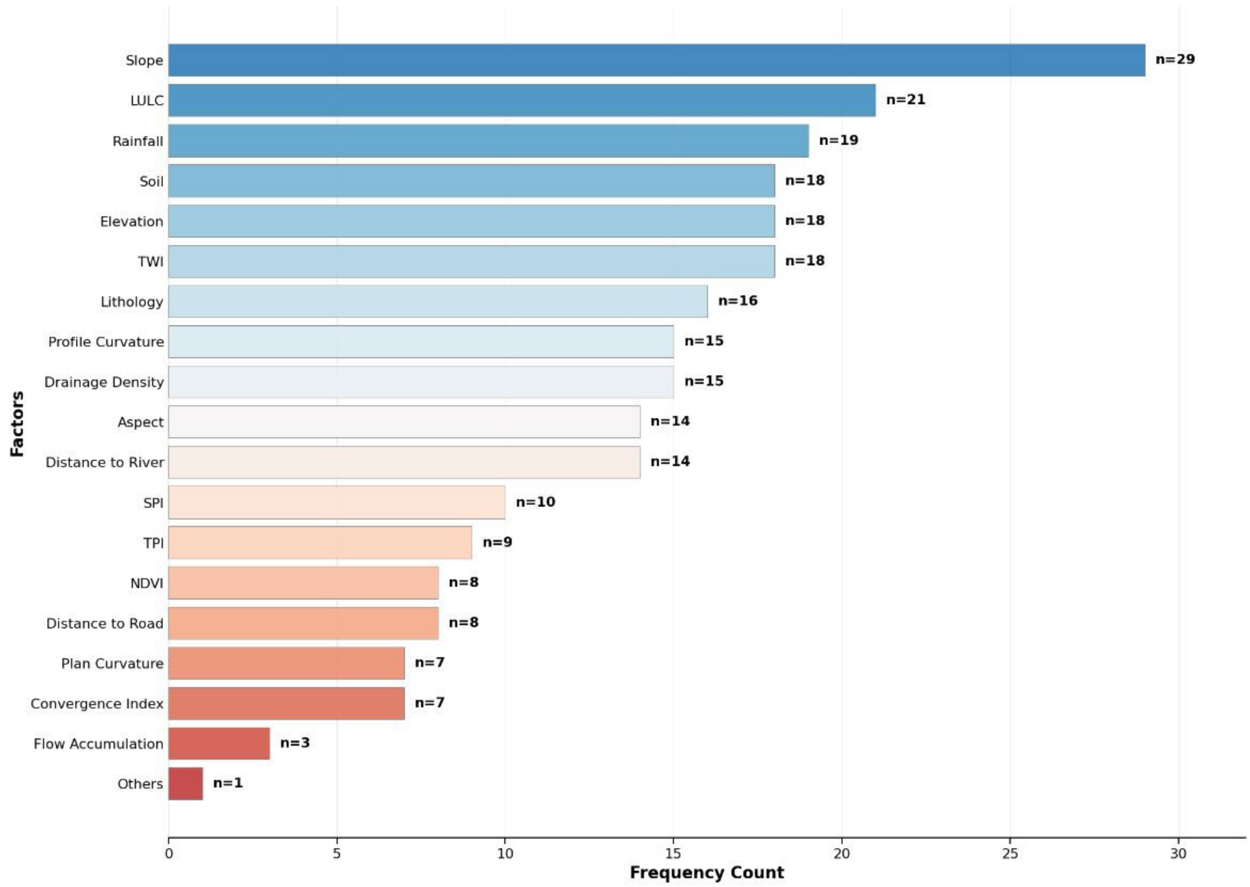


**Figure A-1. Frequency of occurrence of hazard factors in published literature**

This figure summarizes the factors present within 30 flash flood-focused studies (Abedi et al., 2022; Ali & Nelson, 2025; Band et al., 2020b; Bui et al., 2019; Chowdhury, 2024a; Cikmaz et al., 2025; Costache, 2019c, 2019a; Costache et al., 2022; Costache, Pham, et al., 2019; Costache & Zaharia, 2017a; Elghouat et al., 2024; X. He et al., 2024; Hoang & Liou, 2024; Khodaei et al., 2025; Kocsis et al., 2022; Majeed et al., 2023; Popa et al., 2019; Riaz & Mohiuddin, 2025; Shafapour Tehrany et al., 2019; Shawky & Hassan, 2023; Shrestha et al., 2025; Singh & Pandey, 2021; Talha et al., 2019; Tariq et al., 2022; Tikuye et al., 2025; Wahba et al., 2024; Waqas et al., 2021; Zhuang et al., 2026; Zulhisham & Sadek, 2023).

The full list of factors mentioned in the literature review is presented in Table A-2.

**Table A-2. Hazard factors considered**

| Factor | Definition | Relevance to Flash Flooding | Category | Supporting Literature |
|---|---|---|---|---|
| **Distance to River (DR)** | Horizontal distance from a location to stream | Primarily influences inundation (flooding potential) by controlling exposure to channel inundation; does not directly affect flashiness | Hydrologic | (Samanta et al., 2018) |
| **Drainage Density (DD)** | Total drainage length (or stream length) within a specified area above a certain point in the watershed), divided by the drainage area upstream of that point | Primarily influences runoff response (flashy response) by shortening flow paths, also enhances flooding potential by increasing flow convergence towards channels. | Hydrologic | (Elmahdy et al., 2020; Tariq et al., 2022) |
| **Elevation (EL)** | Height of land surface | Controls flood depth (flooding potential); low elevations act as receivers of upstream flash runoff rather than sources of rapid flow | Topographic | (Elghouat et al., 2024; Elmahdy et al., 2020; Saharia et al., 2017a) |
| **Flashiness Index (FL)** | Response of stream to rainfall | Low-Infiltration; rapid runoff response | Hydrologic | (Gannon et al., 2022; Saharia et al., 2017a) |
| **Flow Accumulation (FA)** | Number of areas of upslope cells draining to a given cell | Primarily influences flooding potential by representing spatial convergence and water-depth development, marks locations where rapid runoff transitions into inundation | Hydrologic | (Elmahdy et al., 2020; Hoang & Liou, 2024) |
| **Geology/ Lithology** | Physical composition of underlying rocks | Influences runoff generation and flashy response through permeability and subsurface storage; low permeability units increase flood potential where runoff accumulates | Soil and Sub-surface | (Bui et al., 2019; Kocsis et al., 2022; Kuşcu & Ozdemir, 2024) |

| Factor | Definition | Relevance to Flash Flooding | Category | Supporting Literature |
|---|---|---|---|---|
| **Height Above Nearest Drainage (HAND)** | Vertical elevation difference between each grid cell and its nearest drainage (stream) cell, measured along the downslope flow path | Represents local hydraulic position relative to drainage network; low HAND values indicate proximity to channels and higher susceptibility to rapid inundation during intense rainfall | Topographic/ Hydrologic | (Shawky & Hassan, 2023) |
| **Land Use/ Land Cover (LULC)** | The intended use of each land pixel that gives an indication of the type of surfaces present | Primarily influences flashiness through surface runoff and imperviousness; increases flooding potential where runoff is routed into convergent or low-lying areas | Land Surface/ Vegetation | (Shafapour Tehrany et al., 2019; Costache, Pham, et al., 2019; Rashidiyan & Rahimzadegan, 2024) |
| **Maximum Short –Duration Rainfall (1-3-24h)** | Peak rainfall measured over short interval | Short bursts of extreme rainfall trigger flash flood timing and magnitude | Climatic/ Rainfall Forcing | (F. He et al., 2025) |
| **Normalized Difference Vegetation Index (NDVI)** | Remote-sensing index representing vegetation health | Primarily influences runoff generation and flashy response by regulating interception and surface roughness | Land Surface/ Vegetation | (Swain et al., 2020; Elghouat et al., 2024; F. He et al., 2025) |
| **Plan Curvature (PLC)** | Curvature along contours | Primarily controls flow convergence and depth accumulation (flooding potential); only indirectly influences flashiness by focusing rapid runoff into localized flow paths. | Geomorphic | (Costache, Pham, et al., 2019; Wahba et al., 2024) |
| **Profile Curvature (PRC)** | Curvature along flow direction (Valley/Ridge) | Controls flow acceleration and deceleration along slopes (flashy response), secondarily affects flooding potential where flow slows and locally thickens | Geomorphic | (Costache, Pham, et al., 2019; Wahba et al., 2024) |

| Factor | Definition | Relevance to Flash Flooding | Category | Supporting Literature |
|---|---|---|---|---|
| **Relief and Aspect** | Elevation Difference; Direction of slope face | Relief controls elevation gradients and flow paths that influence runoff velocity and direction (flashy response), while aspect affects moisture and energy balance; flood hazard increases where rapid downslope flow converges in lower-relief channelized areas | Topographic | (Kocsis et al., 2022; Singh & Pandey, 2021; Tikuye et al., 2025) |
| **Slope (SL)** | Local terrain slope defined as the maximum rate of elevation change in each pixel | Primarily controls runoff velocity and response time (flashy response); steep slopes generate rapid overland flow | Topographic | (Costache & Zaharia, 2017b, 2017b; Elmahdy et al., 2020; Tariq et al., 2022) |
| **Soil Type/ Texture/ Curve Number (CN)** | Determine permeability, infiltration rate and runoff generation | Primarily influences runoff generation and flashy response by controlling infiltration capacity | Soil and Sub-surface | (Popa et al., 2019; Costache, Pham, et al., 2019; Kuşcu & Ozdemir, 2024) |
| **Stream Power Index (SPI)** | Potential of Erosion Power | Primarily influences runoff intensity and erosive energy (flashy response); contributes to flooding potential where high-energy flow becomes confined and convergent | Topographic-Hydrologic | (Liuzzo et al., 2019; Chowdhury, 2024b; Wahba et al., 2024) |
| **Topographic Position Index (TPI)** | Difference between a cell's elevation and the mean elevation of its surrounding cells | Primarily influences flooding potential by distinguishing topographic lows and valleys from ridges; low TPI areas favor flow concentration and depth accumulation | Topographic-Hydrologic | (Costache, Pham, et al., 2019; Alam et al., 2021; Khodaei et al., 2025) |
| **Topographic Wetness Index (TWI)** | Describes how water accumulates and how easily it infiltrates | Primarily influences flooding potential by identifying areas prone to saturation and water retention; does not directly control runoff speed | Topographic-Hydrologic | (Khosravi et al., 2016a; Costache, Pham, et al., 2019; Shahabi et al., 2021)(Khosravi et al., 2016a; Costache, Pham, et al., 2019; Shahabi et al., 2021)Costache et al. |

| Factor | Definition | Relevance to Flash Flooding | Category | Supporting Literature |
|---|---|---|---|---|
| | | | | 2019; Kaya & Koc 2023 |
| **Total Annual Precipitation (RF)** | Total amount of rain received over entire year | Primarily influences overall water availability and baseline flood potential, does not directly control event-scale runoff flashiness | Climatic/ Rainfall Forcing | (Saharia et al., 2017a; Carvalho et al., 2022; F. He et al., 2025) |

The factors listed in Table A–3 are a subset selected as reasonably representing the factors influencing flash flood hazard (with light blue shaded rows indicated factors that were ultimately selected for this study). These factors were further analyzed to determine suitability for this study based on relevance to flash flooding and data availability. Some factors that other literature considered explicitly, including land use/land cover (LULC) and soil type or texture, were only used within calculations for other factors, such as Curve Number (CN), in this study.

**Table A-3: Hazard factors considered from literature.**

| Factors considered |
|---|
| Distance to River (DR) |
| Drainage Density (DD) |
| Elevation (EL) |
| Flashiness Index (FL) |
| Flow Accumulation (FA) |
| Geology/ Lithology |
| Height Above Nearest Drainage (HAND) |
| Land Use/ Land Cover (LULC) |
| Maximum Short –Duration Rainfall |
| Normalized Difference Vegetation Index (NDVI) |
| Plan Curvature (PLC) |
| Profile Curvature (PRC) |
| Relief and Aspect |
| Slope (SL) |
| Soil Type/Texture |
| Curve Number (CN) |
| Stream Power Index (SPI) |
| Topographic Position Index (TPI) |
| Topographic Wetness Index (TWI) |
| Precipitation/Rainfall (RF) |

## Exposure Factors from Literature

The exposure factors identified in the literature are summarized in Table A-4, with factors ultimately selected for this study shaded in light blue. Distance to critical infrastructure was another relevant consideration, as proximity influences accessibility to emergency services such as fire stations or hospitals. However, incorporating this factor would require structure-level, network-based accessibility analysis, which is outside of the scope of this study.

**Table A-4. Exposure factors from literature.**

| Factor | Definition | Relevance to Flash Flooding | Supporting Literature |
|---|---|---|---|
| **Distance to Critical Infrastructure** | Proximity to essential facilities like hospitals and emergency response centers | Longer distances may delay emergency response and evacuation | (Ajtai et al., 2023; FEMA, 2020) |
| **Building Count/ Building Density** | Number of buildings per unit area, representing the spatial concentration of the built environment and exposed structures | Areas with high building density experience amplified flood impacts due to the concentration of exposed assets, reduced evacuation efficiency, and increased obstruction of overland flow pathways, which collectively intensify damage and emergency response challenges during short-duration, high-intensity flood events | (Fernandez et al., 2016) |
| **Population Density** | Number of people living in an area per unit area | Higher density indicates areas with larger numbers of potentially exposed people | (Yosri et al., 2024, Wang et al., 2023, Tate et al., 2021) |

## Validation Criteria from Literature Review

A range of validation information documented in prior flash flood hazard studies is summarized in Table A-5, with those utilized in this study shaded in light blue. Historical flood inventories, FEMA and TWDB BLE model results, and records of socio-economic losses and fatalities were directly utilized for validation purposes. Streamflow records were indirectly considered through the Flashiness Index. Expert knowledge and interviews, post-event field surveys, remote sensing-derived flood inundation maps, and social media or crowdsourced data were not considered further here, as they often require event-specific data collection, extensive post-processing, or long lead times that were not feasible within the study schedule.

**Table A-5: Validation information from literature**

| **Factor** | **Definition** | **Relevance to Flash Flooding** | **Supporting Literature** |
|---|---|---|---|
| **Expert Knowledge & Interviews** | Qualitative validation through interviews with local landowners, farmers, or municipal experts | Locals confirm if the hotspots align with their lived experience | (Tascón-González et al., 2020; Wang et al., 2023) |

| Factor | Definition | Relevance to Flash Flooding | Supporting Literature |
|---|---|---|---|
| **Historical Flood Inventories** | Compiled datasets of past flood locations (points or polygons) | Provides the ground truth for validation for floods as well as flash floods | (Abedi et al., 2022));(Band et al., 2020a); (Bui et al., 2019); (Cikmaz et al., 2025); (Costache, ; Shahabi et al., 2021; Tikuye et al., 2025); |
| **Hydrological & Streamflow Data** | Time-series data from river gages measuring stage and discharge | Validates the hydrological response to floods or flash floods | (Holko et al., 2011; Khajehei et al., 2020) |
| **Hydrologic and Hydraulic (H&H) Modeling Data and Results** | H&H modeling results based on prior flash flood events | Validates the hydrological response to flash floods | (Holko et al., 2011; Khajehei et al., 2020) |
| **Post-Event Field Surveys** | On-site data collection conducted immediately after a specific flood event to map high-water marks or sediment deposits | Provides the actual event-based data for validation of flood extents | (Forte et al., 2025; Ke et al., 2025; Kocsis et al., 2022; Shafapour Tehrany et al., 2019; Talha et al., 2019) |
| **Remote Sensing Flood Inundation Maps** | High-resolution aerial photography or satellite imagery of events used to identify associated flood extents | Provides snapshots of actual flood footprint | (Costache et al., 2020; Costache, Pham, et al., 2019) |
| **Social Media and Crowdsourcing** | Geotagged user-generated content from social media platforms | Validates the timing and location of flash floods where gages are sparse | Zhuang et al., 2026) |
| **Socio-Economic Loss and Fatalities** | Records of monetary loss, insurance claims, or fatalities associated with specific flood events | Validates the location of loss of life or impacts to property from floods or flash floods | (Sharif et al., 2012; Terti et al., 2017; Ahmadalipour & Moradkhani, 2019b; Tellman et al., 2020; Wang et al., 2023; Ajtai et al., 2023; Abdrabo et al., 2023; X. He et al., 2024; Hoang & Liou, 2024; Wilkho et al., 2025b) (Sharif et al., 2012; Terti et al., 2017; Ahmadalipour & Moradkhani, 2019b; Tellman et al., 2020; Wang et al., 2023; Ajtai et al., 2023; Abdrabo et al., 2023; X. He et al., 2024; Hoang & Liou, 2024; Wilkho et al., 2025b) |

# Appendix B. Data Collection and Processing

After determining what factors are needed for the flash flood risk methodology, the associated data is required. The data collection and processing efforts start with the gathering of general spatial data, hazard data, exposure data, and validation data. Data selection prioritized consistency, spatial coverage, and applicability to a regional-scale analysis. The subsections below describe the primary data categories used in the study, followed by discussion of derived datasets and data processing steps applied to prepare inputs for the selected analytical method.

## Data for Hazard Identification

The datasets needed to develop hazard related factors gathered for the project are shown in Table B-1.

**Table B-1. Hazard data**

| Dataset / Index | Source / Repository | Analytical Role | Notes / SB 3 Relevance |
|---|---|---|---|
| **Digital Elevation Model (DEM)** | USGS (LiDAR, 30m); released February 2025; downloaded November 2025 | Base for hydrologic terrain modeling, watershed delineation | Defines drainage geometry and headwater flash flood behavior |
| **Land Use / Land Cover (LULC)** | USGS National Land Cover Dataset (NLCD) 2021; released July 2023; downloaded November 2025 | Distinguishes built vs. natural surfaces | Integrates human alteration effects |
| **Precipitation** | NOAA Atlas 14 100-year, 24-hour gridded; released September 2018; downloaded November 2025 | Climatic hazard driver | Needed for storm intensity-frequency context |
| **Soil Hydrologic Groups / Drainage** | USDA NRCS gSSURGO version 2.4; released August 2020; downloaded November 2025 | Controls infiltration and runoff ratio | Distinguishes flood-prone vs. absorbent landscapes |

## Exposure Input Data

**Table B-2. Exposure data.**

| Dataset / Index | Source / Repository | Data Resolution/Type |
|---|---|---|
| **Building Data** | TWDB; released February 2025; downloaded November 2025 | Polygon shapefile of building footprints to determine exposed buildings/property as locations of known exposure and a proxy for transient populations |

| Dataset / Index | Source / Repository | Data Resolution/Type |
|---|---|---|
| **TWDB Floodplain Quilt (2024)** | TWDB ; released January 2025; downloaded November 2025 | 0.2 percent (500-year) annual chance floodplain utilized for mapping extents and for calculating the number of exposed buildings |
| **Location of Camps and Recreation Vehicle (RV) Parks in Texas** | TWDB; sourced from Kampgrounds of America (KOA) campground, Texas Association of Campground Owners (TACO), Texas Parks and Wildlife Department (TPWD), National Park Service (NPS), Texas Department of State Health Services (DSHS), and Texas Public Affairs (TPA); compiled December 2025; downloaded December 2025 | Point shapefile compiled from addresses provided to TWDB, obtained from website listings, or obtained from REST/API services. |
| **Parks** | Texas Parks and Wildlife Department (TPWD) Land and Water Resources Conservation and Recreation Plan (LWRCRP) Statewide 2012 Inventory Data; released October 2022, downloaded January 2026 | Polygon shapefile of park footprint |
| **Location of Historic Flash Flood Events in Texas** | NOAA Storm Events Database (SED) with recorded fatalities, injuries, or monetary building damages, downloaded February 2026 | CSV file converted to point shapefile using location coordinates |
| **Base Level Engineering (BLE) HEC-RAS 2D Model Output (e.g., DV)** | FEMA- and TWDB-developed BLE | Source resolution is variable, resampled to 30-meters; 500-year, 24-hour storm for processed urban watersheds |

The historic flash flood events in Texas from the NOAA Storm Events Database (SED) are shown in Figure B-1 below. These events evaluated in this study have recorded fatalities, injuries, or monetary building damages to prioritize events with recorded exposures. These events include the flash flooding events related to the July 4, 2025 episode and other fatal or damaging flash flooding episodes dating back to 2001.

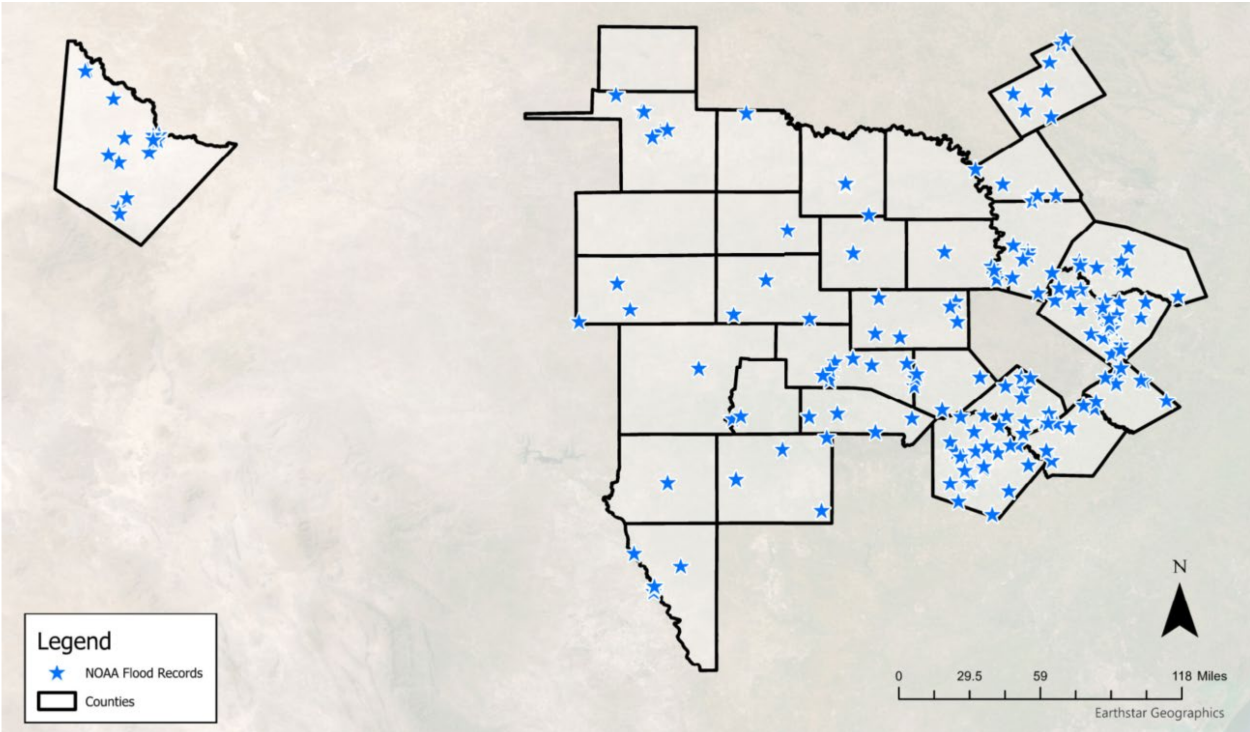


**Figure B-1. Historic flash flood events from NOAA SED**

## Validation and QA/QC Data

To ensure the quality of the product and to ensure that weighting applied to hazard index estimations were reasonable, validation was conducted for the generated hazard and exposure layers utilizing the data found in Table B-2 and Table B-3, respectively.

**Table B-2. Hazard validation data**

| Dataset / Index | Source / Repository | Data Resolution/Type |
|---|---|---|
| **Base Level Engineering (BLE) HEC-RAS 2D Model Output (e.g., DV)** | FEMA- and TWDB-developed BLE | Source resolution is variable, extracted at 300-meters and resampled to 1km; 100-year, 24-hour storm |

For the exposure layer, critical facilities locations (shown in Table B-3) are verified to be included within the RFPG buildings layer.

**Table B-3. Exposure validation data.**

| Dataset / Index | Source / Repository | Data Resolution/Type |
|---|---|---|
| **Critical Facilities** | TWDB | Point shapefile |

In addition to the datasets described above, some other data were initially downloaded and assessed for use but subsequently excluded for various reasons. Data from the NOAA Severe Hazards Analysis & Verification Experiment (SHAVE) and USGS flood events data were excluded due to data sparsity. Flow gages, stream gages, high water marks, and storm event data from the Texas Storm Study may correlate to floods but could not be directly attributed to flash floods. Archived NWS Flash Flood Warning polygons provide information on prior events but do not provide the spatial resolution necessary to identify areas of higher risk, due to often being county-wide warnings and at finest resolution cover approximately 20% of the county.

## General Data Processing

Watershed-scale processing was performed for each HUC-8 watershed using the standardized 1km grid. During early runs, boundary artifacts were observed near watershed edges because some 1km cells only partially intersected the watershed polygon. Including these partial edge cells can mix conditions from inside and outside the watershed and introduce artificial boundary effects in derived indices and maps. To address this, a strict containment mask was applied, retaining only 1km cells whose full footprints were entirely contained within the analysis domain for computing indices. To ensure continuity in exported GeoTIFFs and interactive maps, a complementary intersection-based mask was then applied during raster output, writing only cells intersecting the target domain and assigning zero values to remaining interior cells rather than generating no data. This combined masking strategy reduces cross-boundary mixing, mitigates internal edge discontinuities, and produces spatially coherent watershed-level products.

## Derived Data & Data Processing for Hazard

Many input factors rely on data that are based on or derived from other datasets, while some only must be processed. Table B-4 summarizes the derived data developed for this study. These derived layers are intended to represent hydrologic conditioning and terrain controls on rapid runoff generation and flooding propensity in a consistent manner across the study area. To assess flash flood susceptibility, several topographic and hydrological conditioning factors were derived from the source datasets—such as Digital Elevation Model (DEM), land use, and soils using the spatial analysis capabilities of ArcGIS Pro. All the processing was done using the NAD 1983 (2011) Texas Centric Mapping System Albers (Meters) projection system.

To ensure continuity of drainage pathways delineated, the DEM was first clipped to the study area boundary and hydrologically conditioned using the Fill Sink tool of ArcGIS Spatial Analyst Tools. Utilizing the filled DEM from the previous step, the flow direction was derived using the Flow Direction tool in ArcGIS. The flow direction tool uses an eight-direction (D8) algorithm to encode the direction at each cell. The output from the flow direction tool becomes the input for the next step, which is flow accumulation. The Flow Accumulation tool quantifies the number of upstream cells contributing or draining to a given cell. Finally, utilizing the flow accumulation grid, a drainage network (e.g., stream raster) was delineated using a flow accumulation threshold of 1,000 cells. These initially derived data form the basis for other factors.

Details on the data processing for each factor identified for use in this analysis are provided below.

### *Curve Number*

The use of Curve Number (CN) is established in the literature, and its numerical value eliminates the potential need for subjective judgements to fit the underlying categorical data (i.e., land use/land cover and soil type) into numerical values. The Curve Number values were also normalized from 0-1 using an inverse hyperbolic sine function.

### *Flashiness Index*

The flashiness index, denoted by $\phi$ is used in this study to quantify the tendency of a watershed to generate rapid and high-magnitude runoff responses following intense rainfall. It reflects how quickly streamflow rises above critical threshold relative to basin size and response time and serves as an indicator of flash flood severity. The flashiness index for basin *i* and flood event *j* is defined as,

$$\Phi_{ij} = \frac{Q_{ij}^{(p)} - Q_{ij}^{(a)}}{A_i\, T_{ij}}$$

where $Q_{ij}^{(p)}$ is the peak discharge for event j in basin I, $Q_{ij}^{(a)}$ is the corresponding National Weather Service (NWS) action stage discharge (e.g., where a mitigation action is needed), $A_i$ is the basin area, and $T_{ij}$ is the flooding rise time for event j. The NWS Action Stage for river flooding is the water level (stage) where the NWS and local partners start mitigation actions for potential minor flooding, indicating where a rising stream warrants caution as water may become a nuisance or cause minor impacts, requiring preparation like monitoring or property protection before significant damage occurs, which is often indicated by a specific gauge height (stage) that corresponds to a certain discharge or flow rate. In this study, the flashiness index was normalized using an inverse hyperbolic sine function to reduce skewness and improve comparability with other index inputs, resulting in a dimensionless value between 0 and 1, with higher values indicating flashier hydrologic responses.

### *Height Above Nearest Drainage (HAND)*

This was calculated based on the DEM and the DEM-based stream raster grid. Unlike absolute elevation, which reflects regional topography, HAND captures the relative vertical position of a location with respect to its local drainage network. This makes HAND more directly linked to flash flooding and runoff processes than elevation, as areas with low HAND values are hydraulically closer to channels and more prone to flood hazard regardless of their absolute elevation.

$$\mathrm{HAND}(x, y) = Z_{\mathrm{DEM}}(x, y) - Z_{\mathrm{drainage}}(x_d, y_d)$$

Where, $Z_{\mathrm{DEM}}(x, y)$ = elevation of the cell, $Z_{\mathrm{drainage}}(x_d, y_d)$ = elevation of the nearest drainage

It was derived using the flow distance tool with the distance type = "Vertical", based on a flow direction raster, and a stream raster defined from flow accumulation greater than 1,000 cells. The 30m raster was resampled to a 1-km grid using bilinear interpolation, multiplied by (-1), and normalized using an inverse hyperbolic sine function. The units for HAND in this study are meters.

### *Flow Accumulation (FA)*

Flow accumulation is derived from the DEM-based flow direction grid using the eight-direction flow routing algorithm and represents the number of upstream grid cells contributing flow to a given cell. Mathematically, flow accumulation at cell $i$ is defined as $FA_i = \sum_{\{j \in upstream\}} 1$

Where, the summation counts each upstream cell j that drains to cell i. Thus, the equation above express flow accumulation as a cell count of contributing upstream area. The 30-m flow accumulation raster was resampled to a 1km grid using bilinear interpolation and normalized using an inverse hyperbolic sine transformation.

### *Slope (SL)*

While basin slope represents the average slope for an entire basin, a spatially varied slope surface is required to perform raster-based calculations. Therefore, terrain slope was selected over other slopes for this study. Moreover, the influence of upstream basin area and slope are incorporated through the inclusion of additional factors: the Topographic Wetness Index (TWI) and Stream Power Index (SPI). Slope was calculated using the Slope ArcGIS Spatial Analyst tool, which uses Horn's algorithm to calculate the vector magnitude of slope in x and y directions in a window of 3 cells x 3 cells (e.g., 90m x 90m neighborhood), the default range and a best practice established through the literature. Slope was calculated as a dimensionless number (radians). The 30m slope raster was resampled to a 1km grid using bilinear interpolation and then normalized using the inverse hyperbolic sine function. Mathematically,

$$\beta = \tan^{-1}\left(\sqrt{\left(\frac{\partial z}{\partial x}\right)^2 + \left(\frac{\partial z}{\partial y}\right)^2}\right)$$

Where, z is the elevation, and $\frac{\partial z}{\partial x}$ and $\frac{\partial z}{\partial y}$ are the elevation gradient in the x- and y-directions, respectively.

### *Distance to River (DR)*

Horizontal distance to drainage is computed using the flow distance tool with the "Horizontal" option in ArcGIS. This calculates the downslope flow-path distance from each cell to the nearest stream cell delineated using accumulation threshold of 1,000. The 30m raster was resampled to 1-km grid using bilinear interpolation, multiplied by (-1), and normalized using the inverse hyperbolic sine function. The unit in this study for distance to drainage was meters.

### *Drainage Density (DD)*

Drainage density is calculated locally using focal statistics (or moving window analysis) rather than as a basin-wide metric. First, a moving neighborhood of 33x33 30-meter cells, which approximately aligns with the end goal of 1-kilometer pixels, is applied to the binary stream raster using the ArcGIS Focal Statistics (SUM) to count stream cells within the neighborhood. Drainage density is then computed as the ratio of total stream length to total area within the window using the raster calculation tool in ArcGIS. The 30m raster was resampled to a 1km grid using bilinear interpolation method and then normalized using the inverse hyperbolic sine function. The unit for this calculation is $m^{-1}$ or $m/m^2$. Mathematically,

$$D_d = \frac{N_s}{w^2 \cdot r}$$

where $N_s$ is the number of stream cells in the neighborhood, w is neighborhood size in cells, and r is pixel size in meters.

### *Profile Curvature (PRC)*

Profile curvature is computed using the curvature tool in ArcGIS. The raw DEM (unfilled) was used in this calculation to preserve natural micro-topographic features such as small depressions and slope breaks that influence surface flow routing. The 30m raster was resampled to a 1km grid using bilinear interpolation, multiplied by -1, and normalized using the inverse hyperbolic sine function. The unit for this curvature is $m^{-1}$.
Mathematically,

$$k_{profile} = \frac{\partial^2 z}{\partial s^2}$$

where ∂z = change in slope, ∂s = change in distance in meters along the steepest slope direction.

### *Plan Curvature (PLC)*

Plan curvature is derived from the digital elevation model using the Curvature tool in ArcGIS. The 30m raster was resampled to a 1km grid using bilinear interpolation, multiplied by (-1), and normalized using the inverse hyperbolic sine function. The unit for this curvature is $m^{-1}$.
Mathematically,

$$k_{plan} = \frac{\partial^2 z}{\partial n^2}$$

Where, ∂z = change in slope, ∂n = change in distance perpendicular to the slope direction.

### *Topographic Position Index (TPI)*

TPI was calculated based on DEM. The neighborhood radius of 16 cells was used to calculate TPI, as this area represents approximately the 1-kilometer end goal. The 30m raster was resampled to a 1km grid using bilinear interpolation, multiplied by (-1), and normalized using the inverse hyperbolic sine function. The unit for TPI in this study is meters.
Mathematically,

$$TPI = z_i - \overline{z_{window}}$$

### *Topographic Wetness Index (TWI)*

TWI was calculated following the Beven-Kirkby formulation using flow accumulation and slope. The flow accumulation was added with +1 to avoid zero contributing area and undefined value returned from ln(0). The 30m raster was resampled to a 1km grid using bilinear interpolation method and then normalized using the inverse hyperbolic sine function. TWI is a dimensionless number. Mathematically,

$$TWI = \ln\left(\frac{A_s}{\tan(\beta)}\right)$$

where, $A_s$ = specific catchment area in square meters, $\beta$= slope in radians

For processing within ArcGIS, the formula is applied as:

$$TWI = \ln\left(\frac{(FA\ +\ 1)\,.\,r}{\tan(\beta)}\right)$$

Where, FA = flow accumulation, r = pixel size in square meters.

### *Stream Power Index (SPI)*

The 30m raster was resampled to a 1km grid using bilinear interpolation method and then normalized using an inverse hyperbolic sine function. The units for SPI are $m^2/m$ or meters (m). Mathematically,

$$SPI = A_s \cdot \tan(\beta)$$

Where, $A_s$ is specific catchment area in square meters and tan(β) is slope in radians

For processing within ArcGIS, the formula is applied as:

$$A_s\ = \frac{(flow\ accumulation)\ x\ Area\ of\ a\ pixel}{width\ of\ a\ pixel}$$

$$A_s = (flow\ accumulation)\ x\ \frac{length\ of\ pixel\ x\ width\ of\ pixel}{width\ of\ a\ pixel}$$

$$A_s = (flow\ accumulation\ x\ length\ of\ a\ pixel)$$

Where $A_s$ = Flow accumulation x pixel size

### *Rainfall (RF)*

Rainfall data were obtained from NOAA Atlas 14 in raster format for depth. The original pixel values are stored as scaled integers, with precipitation depths in inches multiplied by a factor of 1,000. To recover rainfall values in physical units, the raster was divided by 1,000. The resulting rainfall depths were then normalized using the hyperbolic arc sine transformation to support comparison across the study area.

**Table B-4. Derived data.**

| Dataset / Index | Source / Repository | Analytical Role | Notes / SB 3 Relevance |
|---|---|---|---|
| **Curve Number** | Derived from LULC and hydrologic soil type data using the SCS TR-55 method | Represents spatial runoff potential | Higher Curve Number (CN) values indicate higher surface runoff potential, contributing to increased flash flood susceptibility, used without antecedent moisture condition to maintain consistency across events. |
| **Distance to Drainage** | Derived from stream raster using flow distance tool of ArcGIS Spatial Analyst Tools | Horizontal distance (Euclidean distance) of a cell to the nearest stream indicates more hazard to flash flood | Helps quantify the risk based on the proximity to streams or rivers. |
| **Drainage Density** | Derived from stream network and window of 33 x 33 cells using ArcGIS Spatial Analyst Focal Statistics and Raster Calculator tools | Quantifies the local concentration of stream channels per unit area | Higher drainage density indicates higher risk of flash flood. |
| **Flashiness Index** | Obtained from (Saharia et al., 2017a) | Represents the flashy nature of landscape | High flashiness index indicates higher risk of flash flood and flashier response |

| Dataset / Index | Source / Repository | Analytical Role | Notes / SB 3 Relevance |
|---|---|---|---|
| **Flow Accumulation** | Derived from Flow Direction raster using ArcGIS Spatial Analyst Flow Accumulation tool | Number of upstream contributing cells | Identifies concentrated flow paths and potential channel initiation zones. |
| **Plan Curvature** | Derived from DEM using ArcGIS Spatial Analyst Curvature tool with option "Plan" | Computes curvature perpendicular to slope direction | Identifies flow convergence and divergence zones. |
| **Profile Curvature** | Derived from DEM using ArcGIS Spatial Analyst Curvature tool with option "Profile" | Computes curvature along direction of maximum slope. | Controls flow acceleration, erosion, and deposition potential |
| **Rainfall** | Obtained from NOAA Atlas 14 and processed with minor processing | Represents 100-yr, 24-hr rainfall values | Higher rainfall indicates higher runoff potential |
| **Slope** | Derived from 30m DEM using ArcGIS Spatial Analyst Slope tool | Controls runoff velocity and flow direction | Strong predictor of flash flood intensity in steep basins |
| **Stream Power Index** | Derived from Flow Accumulation and Slope using ArcGIS Spatial Analyst Raster Calculator tool with a pixel size of 30m | Indicates erosive energy and& peak flow hazard | Prioritizes high-impact hazard corridors |
| **Topographic Position Index** | Derived from 30m DEM using ArcGIS Spatial Analyst TPI tool with a radius of 16 cells | Distinguishes ridge/valley and channel confinement | Helps locate flash flood routing corridors |
| **Topographic Wetness Index** | Derived from Flow Accumulation and Slope using ArcGIS Spatial Analyst Raster Calculator tool with a pixel size of 30m | Identifies runoff concentration/saturation zones | Useful for detecting flood-triggering accumulation pockets |

## Derived Data and Data Processing for Validation

### *BLE Models Outputs for Hazard Validation*

Spatial results for water depth and flow velocity were obtained from the BLE model outputs for the 100-year, 24-hour flood simulations. The depth-velocity product was computed at every time step over the full duration of the simulation by extracting depth and velocity grids separately, then multiplying them using the Raster Calculator tool in ArcGIS. The maximum value of this depth-velocity product across the entire time series was then identified for each 300-m pixel and compiled into a single raster, referred to as the DV raster. This raster was used for validation purposes.

# Appendix C. Methods Review, Evaluation, and Implementation

## Hazard Identification & Validation

Hazard factors that were not included in the analysis are Lithology (geological index), Convergence Index, Land use/land cover, NDVI, and aspect because these variables either provide redundant information with the selected factors parameters or offer limited additional value for the study region. Land use/land cover, soil type, lithology information, and vegetation metrics such as seasonal and mean NDVI were not used directly, as their combined influence on hydrology is represented through the Curve Number. The Curve Number integrates characteristics such as surface conditions, infiltration capacity, and vegetation effects into a single, well-established index. In this study, Curve Number was derived using the hydrologic soil group (HSG), which reflects infiltration capacity and subsurface permeability influenced by underlying lithology. Aspect was excluded because its contribution to runoff potential is largely embedded within slope and elevation and including it as a separate factor would introduce redundancy. The Convergence Index, which describes flow concentration across the terrain, was not included because its hydrologic role is effectively captured by the Topographic Wetness Index (TWI) and flow accumulation layers that are already part of the analysis. Geology was not explicitly included as a separate factor because its primary hydrologic influence in this study area—namely shallow bedrock and low effective infiltration capacity—is already implicitly represented through the Hydrologic Soil Group (HSG)–based Curve Number framework.

## Decision-Making Framework: Analytic Hierarchy Process (AHP)

The relative importance of each factor was interpreted based on the weights reported across the 30 peer-reviewed studies. For factors appearing in multiple studies, the median value was used as an indicator of its influence, as shown in Figure C-1 below. This approach minimized the effects of outliers and reduced bias introduced by individual methodologies and study regions to provide a more representative measure of how strongly each factor is emphasized in existing research.

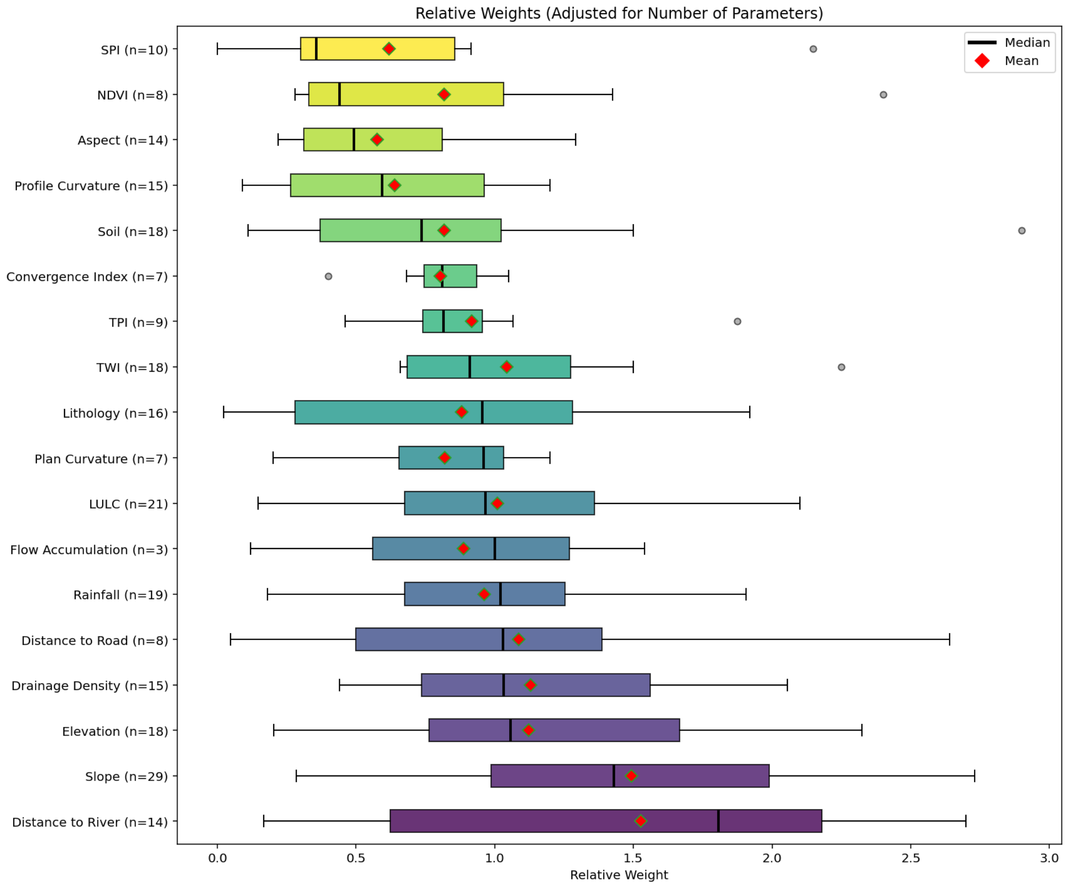


**Figure C-1. Ranked weighting of factors from literature**

These literature-inferred weights of importance values were then used to inform the pairwise comparison process in the AHP framework.

First, the median relative importance values (shown in Table C-1) for the selected factors were normalized by dividing each value by the sum of all selected factors. Ratios between the normalized weights were then computed to evaluate the relative dominance of one factor over another. For example, the normalized importance of distance to river relative to slope yielded a ratio of approximately 1.26—indicating slightly higher importance.

**Table C-1. Median and normalized relative weights of selected factors**

| Parameters Used | Median Relative Weight | Normalized Relative Weights |
|---|---|---|
| Distance to River | 1.8073 | 0.15 |
| Slope | 1.43 | 0.12 |
| Height Above Nearest Drainage | 1.0558 | 0.09 |
| Drainage Density | 1.0331 | 0.09 |
| Rainfall | 1.02 | 0.09 |

| **Parameters Used** | **Median Relative Weight** | **Normalized Relative Weights** |
| --- | --- | --- |
| Flow Accumulation | 1 | 0.08 |
| Plan Curvature | 0.96 | 0.08 |
| Topographic Wetness Index | 0.9102 | 0.08 |
| Curve Number | 0.85085 | 0.07 |
| Topographic Position Index | 0.816 | 0.07 |
| Profile Curvature | 0.5928 | 0.05 |
| Stream Power Index | 0.3577 | 0.03 |
| **Total** | **11.83375** | **1.0** |

Because the Analytic Hierarchy Process framework requires discrete comparison values, these continuous ratios were translated into a structured comparison framework applying Saaty's fundamental scale (Saaty, 1977) summarized in Table C-2. This scale assigns numerical values to the relative importance between two factors, ranging from 1 (equal importance) to 9 (extreme importance), with intermediate values used when the preference falls between major categories. Ratios close to unity were assigned a value of 1, reflecting similar importance, while progressively larger ratios were mapped to higher integer values. The reciprocal of each value was assigned for the inverse comparison to ensure reciprocal consistency across the pairwise comparison matrix, with intermediate values used when the preference falls between major categories.

**Table C-2. AHP weighting scale.**

| Definition | AHP Scale |
| --- | --- |
| Equal Importance | 1 |
| Moderate Importance | 3 |
| Strong Importance | 5 |
| Very Strong Importance | 7 |
| Extreme Importance | 9 |
| Intermediate Values | 2,4,6,8 |

Using this procedure, a complete pairwise comparison matrix was constructed for all selected conditioning factors (Table C-3). The matrix reflects patterns of relative importance consistently reported across multiple studies rather than relying solely on subjective judgement or assumptions from a single methodology. The matrix was then column-normalized and the final weight of each factor was calculated as the average of its normalized value across all columns.

An additional consideration in the study was the inclusion of the flashiness index from Saharia et al., 2017. Since none of the reviewed literature incorporated flashiness within the Analytic Hierarchy Process or other common weighting approaches, a sensitivity analysis was used to integrate this factor. Although existing flood-hazard studies provide extensive guidance on the relative importance of conditioning factors, they do not explicitly incorporate a flashiness index in their weighting methodologies. Flashiness based analysis indicates that the slope and curve number exert a direct and comparable influence on runoff response (Saharia et al., 2017b)—so, these two parameters were assigned equal relative importance with respect to flashiness.

For all remaining parameters, to avoid bias toward flashiness driven controls, the influence of the flashiness index was constrained to the median range of literature reported importance. Parameters such as elevation, drainage density, rainfall characteristics, and flow accumulation consistently exhibited median importance across the reviewed studies and were therefore treated equivalently in the pairwise comparison matrix. Their relative importance with respect to other factors was used as a surrogate for constructing the Analytic Hierarchy Process comparisons for their flashiness, ensuring the balanced representation of both runoff flashiness and flooding potential. The pairwise judgement was populated to form the Analytic Hierarch Process pairwise comparison matrix for the hazards as shown in Table C-3.

**Table C-3. Pairwise comparison matrix for hazard factors.**

| Factor* | DR | SL | FL | HAND | DD | RF | FA | PLC | TWI | CN | TPI | PRC | SPI |
|---|---|---|---|---|---|---|---|---|---|---|---|---|---|
| DR | 1 | 1 | 2 | 2 | 2 | 2 | 2 | 2 | 2 | 2 | 2 | 3 | 5 |
| SL | 1 | 1 | 1 | 1 | 1 | 1 | 1 | 2 | 2 | 2 | 2 | 2 | 4 |
| FL | 0.50 | 1 | 1 | 1 | 1 | 1 | 1 | 1 | 1 | 1 | 1 | 2 | 3 |
| HAND | 0.50 | 1 | 1 | 1 | 1 | 1 | 1 | 1 | 1 | 1 | 1 | 2 | 3 |
| DD | 0.50 | 1 | 1 | 1 | 1 | 1 | 1 | 1 | 1 | 1 | 1 | 2 | 3 |
| RF | 0.50 | 1 | 1 | 1 | 1 | 1 | 1 | 1 | 1 | 1 | 1 | 2 | 3 |
| FA | 0.50 | 1 | 1 | 1 | 1 | 1 | 1 | 1 | 1 | 1 | 1 | 2 | 3 |
| PLC | 0.50 | 0.50 | 1 | 1 | 1 | 1 | 1 | 1 | 1 | 1 | 1 | 1 | 2 |
| TWI | 0.50 | 0.50 | 1 | 1 | 1 | 1 | 1 | 1 | 1 | 1 | 1 | 1 | 2 |
| CN | 0.50 | 0.50 | 1 | 1 | 1 | 1 | 1 | 1 | 1 | 1 | 1 | 1 | 2 |
| TPI | 0.50 | 0.50 | 1 | 1 | 1 | 1 | 1 | 1 | 1 | 1 | 1 | 1 | 2 |
| PRC | 0.33 | 0.50 | 0.50 | 0.50 | 0.50 | 0.50 | 0.50 | 1 | 1 | 1 | 1 | 1 | 2 |
| SPI | 0.20 | 0.25 | 0.33 | 0.33 | 0.33 | 0.33 | 0.33 | 0.50 | 0.50 | 0.50 | 0.50 | 0.50 | 1 |

** Note: Distance to Rivers (DR); Slope (SL); Flashiness Index (FL); Height Above Nearest Drainage (HAND); Drainage Density (DD); Rainfall (RF); Flow Accumulation (FA); Plan Curvature (PLC); Topographic Wetness Index (TWI); Curve Number (CN); Topographic Position Index (TPI); Profile Curvature (PRC); Stream Power Index (SPI);*

After the pairwise comparison matrix is complete, the weights are calculated. The priorities in the Analytic Hierarchy Process can be derived using various methods (Ishizaka & Lusti, 2006), but the precise method has not been shown to impact the overall weights significantly. Thus, the eigenvector method was selected for normalization. For the derivation of the final weights, the pairwise comparison matrix is:

$$A = [a_{ij}]$$

Then the final weight vector for the different parameters, $w = (w_1, w_2, \ldots., w_n)^T$ is obtained as the principal eigen vector of A. This is written as,

$$Aw = \lambda_{\max w}$$

where, $\lambda_{max}$ is the maximum eigenvalue of A.

The eigenvector $w$ is then normalized so that the weights sum to 1:

$$w_i^* = \frac{w_i}{\sum_{k=1}^{n} w_k}\ , i = 1, \ldots, n$$

and the normalized vector $w^* = (w_1^*, \ldots \ldots, w_n^*)$ gives the final weight for each factor used in the Analytic Hierarchy Process.

The resulting normalized and final weights obtained as the principal eigenvector of the matrix are shown in Table C-4. This process provides a consistent method for converting qualitative and literature-informed assessment into quantitative weights for mapping the flash flood hazard.

**Table C-4. Normalized comparison matrix for hazard factors.**

| Factor* | DR | SL | FL | HAND | DD | RF | FA | PLC | TWI | CN | TPI | PRC | SPI | **Weights/ Normalized Comparison Matrix** |
|---|---|---|---|---|---|---|---|---|---|---|---|---|---|---|
| DR | 0.14 | 0.10 | 0.16 | 0.16 | 0.16 | 0.16 | 0.16 | 0.14 | 0.14 | 0.14 | 0.14 | 0.15 | 0.14 | **0.14** |
| SL | 0.14 | 0.10 | 0.08 | 0.08 | 0.08 | 0.08 | 0.08 | 0.14 | 0.14 | 0.14 | 0.14 | 0.10 | 0.11 | **0.11** |
| FL | 0.07 | 0.10 | 0.08 | 0.08 | 0.08 | 0.08 | 0.08 | 0.07 | 0.07 | 0.07 | 0.07 | 0.10 | 0.09 | **0.08** |
| HAND | 0.07 | 0.10 | 0.08 | 0.08 | 0.08 | 0.08 | 0.08 | 0.07 | 0.07 | 0.07 | 0.07 | 0.10 | 0.09 | **0.08** |
| DD | 0.07 | 0.10 | 0.08 | 0.08 | 0.08 | 0.08 | 0.08 | 0.07 | 0.07 | 0.07 | 0.07 | 0.10 | 0.09 | **0.08** |
| RF | 0.07 | 0.10 | 0.08 | 0.08 | 0.08 | 0.08 | 0.08 | 0.07 | 0.07 | 0.07 | 0.07 | 0.10 | 0.09 | **0.08** |
| FA | 0.07 | 0.10 | 0.08 | 0.08 | 0.08 | 0.08 | 0.08 | 0.07 | 0.07 | 0.07 | 0.07 | 0.10 | 0.09 | **0.08** |
| PLC | 0.07 | 0.05 | 0.08 | 0.08 | 0.08 | 0.08 | 0.08 | 0.07 | 0.07 | 0.07 | 0.07 | 0.05 | 0.06 | **0.07** |
| TWI | 0.07 | 0.05 | 0.08 | 0.08 | 0.08 | 0.08 | 0.08 | 0.07 | 0.07 | 0.07 | 0.07 | 0.05 | 0.06 | **0.07** |
| CN | 0.07 | 0.05 | 0.08 | 0.08 | 0.08 | 0.08 | 0.08 | 0.07 | 0.07 | 0.07 | 0.07 | 0.05 | 0.06 | **0.07** |
| TPI | 0.07 | 0.05 | 0.08 | 0.08 | 0.08 | 0.08 | 0.08 | 0.07 | 0.07 | 0.07 | 0.07 | 0.05 | 0.06 | **0.07** |
| PRC | 0.05 | 0.05 | 0.04 | 0.04 | 0.04 | 0.04 | 0.04 | 0.07 | 0.07 | 0.07 | 0.07 | 0.05 | 0.06 | **0.05** |
| SPI | 0.03 | 0.03 | 0.03 | 0.03 | 0.03 | 0.03 | 0.03 | 0.03 | 0.03 | 0.03 | 0.03 | 0.02 | 0.03 | **0.03** |

*Note: Distance to Rivers (DR); Slope (SL); Flashiness Index (FL); Height Above Nearest Drainage (HAND); Drainage Density (DD); Rainfall (RF); Flow Accumulation (FA); Plan Curvature (PLC); Topographic Wetness Index (TWI); Curve Number (CN); Topographic Position Index (TPI); Profile Curvature (PRC); Stream Power Index (SPI);*

After obtaining the preliminary weights from the pairwise comparison matrix, the internal consistency of the judgement was evaluated using Saaty's Consistency Index (CI) and Consistency Ratio (CR). The CI measures the degree to which the pairwise comparisons are logically coherent and free from contradictory pairwise comparisons assigned within the Analytic Hierarchy Process framework. The CI is computed from the maximum eigenvalue of the comparison matrix, while the Consistency Ratio compares the Consistency Index against the expected inconsistency of a randomly generated matrix of the same order. A Consistency Ratio value below 0.10 is generally considered acceptable.

In the study, the pairwise comparison matrix yielded a Consistency Index of 0.047 and a Consistency Ratio of 0.011, indicating a high level of internal consistency in the judgement structure. This confirms that the weighting scheme is methodologically sound and suitable for aggregation within the Analytic Hierarchy Process framework. This physical relevance of the selected factors and the resulting flash flood hazard patterns is evaluated independently through comparison with hydrologic reasoning along with the weights comparison from prior literature.

## *Sensitivity Analysis of the Flashiness Index Weight*

The resulting distribution of flashiness weight (Figure C-2) is unimodal and approximately symmetric, indicating a stable representation of flashiness within the weighting framework. The mean flashiness weight was (7.98 percent), closely aligned with the value adopted in the final Analytic Hierarchy Process weights (8 percent), with the 5$^{th}$ and 95$^{th}$ percentile bounds ranging from 6.27 percent to 9.79 percent. The relatively narrow spread of this distribution suggests that the assigned importance of flashiness is robust to reasonable variations in pairwise judgements and is not overly sensitive to individual comparisons.

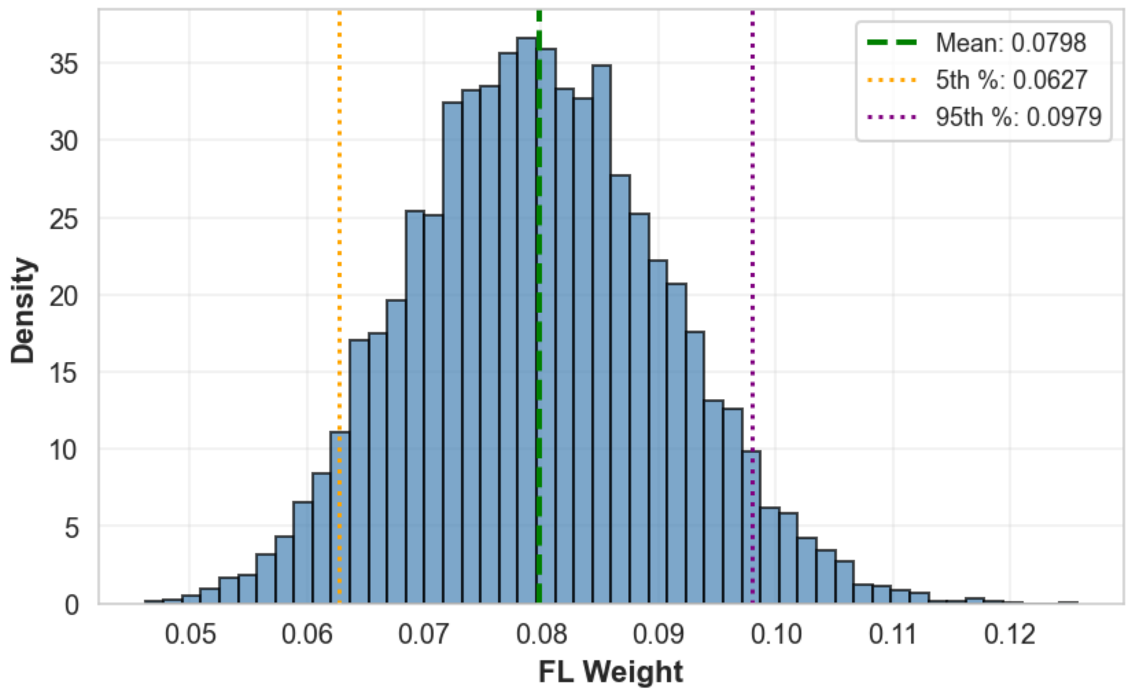


**Figure C-2. Distribution of weights of the flashiness**

## *Hazard Index Calculation*

After finalizing the weights for hazard factors as shown in Table C-5, the hazard index is generated.

**Table C-5. Hazard index weights**

| Factor* | **Weight** |
|---|---|
| Distance to River (DR) | **14.35%** |
| Slope (SL) | **10.75%** |
| Flashiness Index (FL) | **7.86%** |
| Height Above Nearest Drainage (HAND) | **7.86%** |
| Drainage Density (DD) | **7.86%** |
| Rainfall (RF) | **7.86%** |
| Flow Accumulation (FA) | **7.86%** |
| Plan Curvature (PLC) | **6.88%** |
| Topographic Wetness Index (TWI) | **6.88%** |
| Curve Number (CN) | **6.88%** |
| Topographic Position Index (TPI) | **6.88%** |

| Factor* | Weight |
|---|---|
| Profile Curvature (PRC) | **5.20%** |
| Stream Power Index (SPI) | **2.88%** |

Mathematically, the hazard index was performed using a weighted sum using the calculated weights to six decimal points.

Example maps of the hazard index for the Upper Guadalupe and Brady Creek watersheds are shown in Figure C-3 and Figure C-4, respectively.

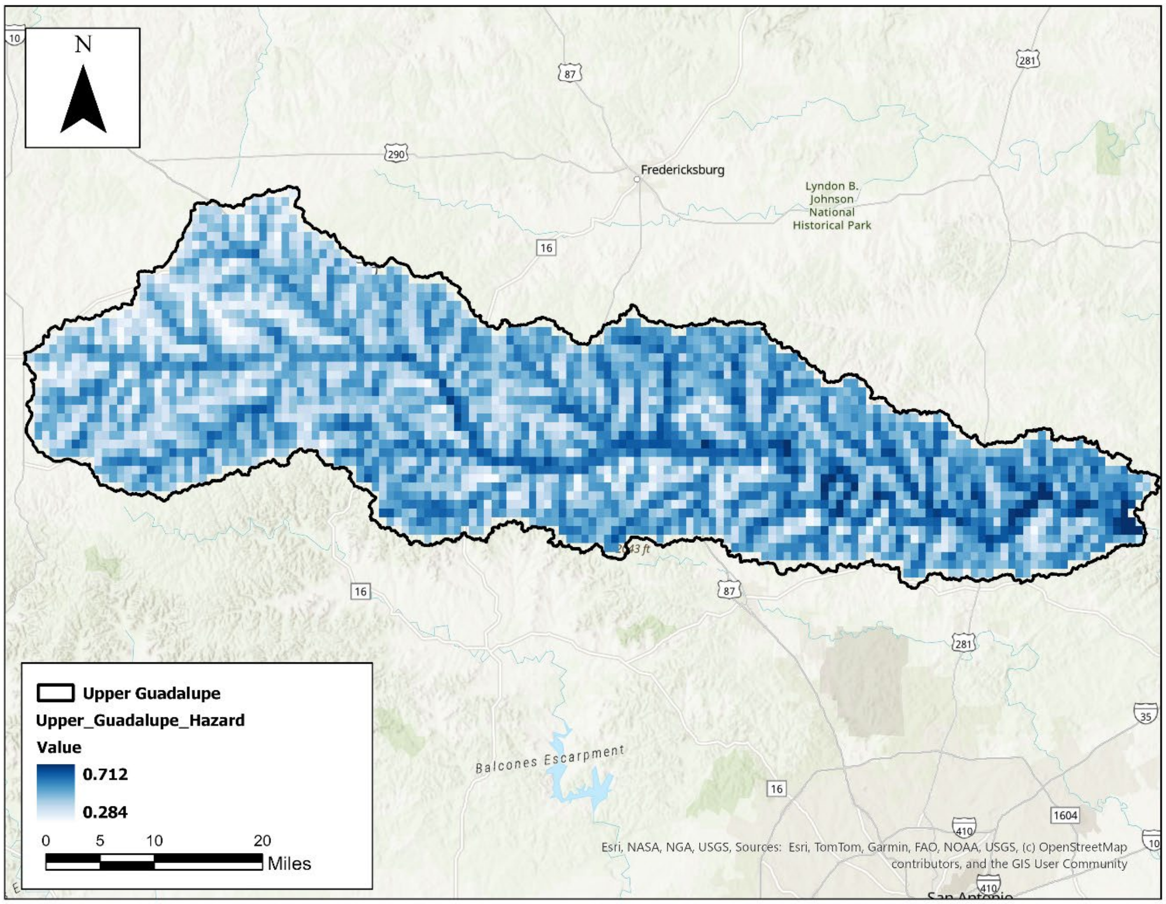


**Figure C-3. Draft hazard index for the Upper Guadalupe watershed**

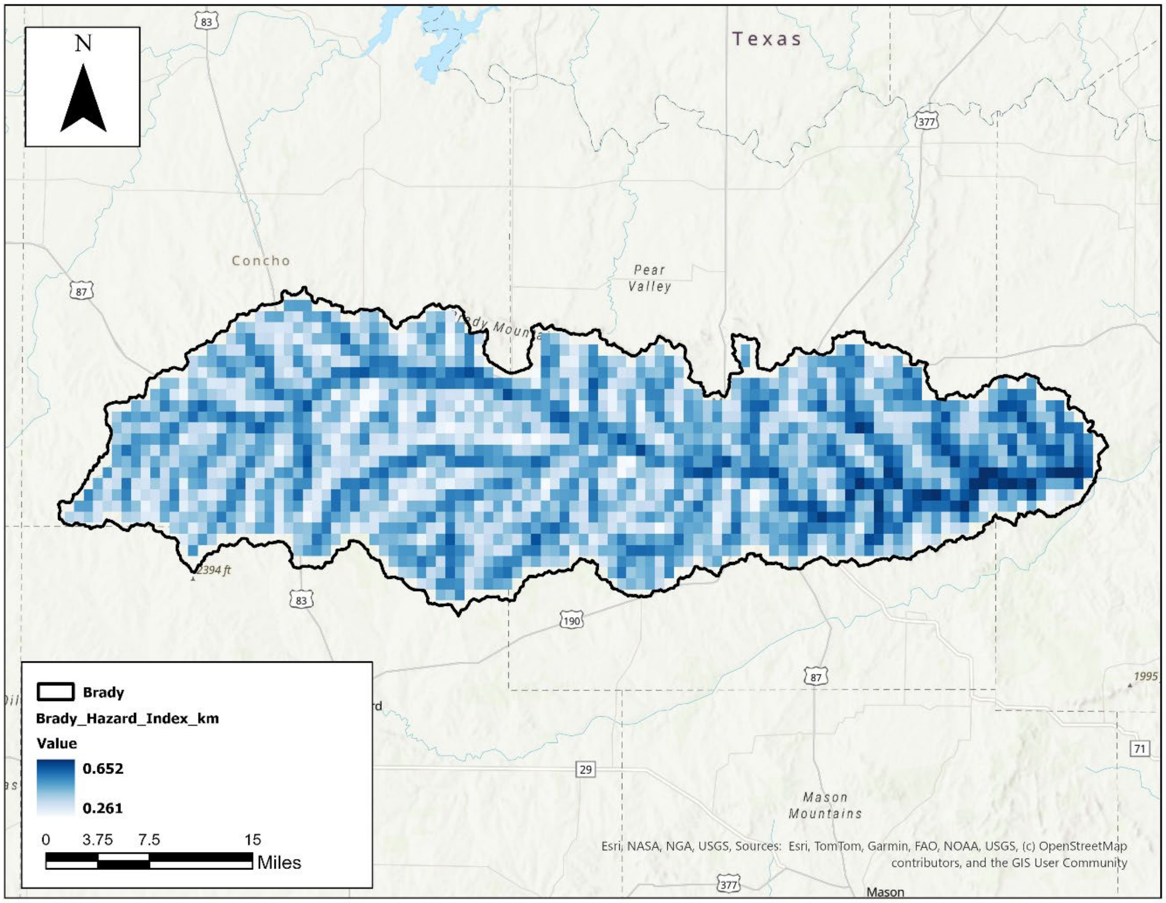


**Figure C-4. Draft hazard index for the Brady Creek watershed**

## Hazard Validation

### *Watershed DV Validation*

Validation based on the 100-year, 24-hour event was performed for 22 watersheds according to availability and ease of accessing the results directly. Example validation results for the Upper Guadalupe for the 100-year, 24-hour storm is presented in Figure C-5, with other AUC values given in Table C-6. The purpose of the ROC analysis is not to identify an optimal classification threshold or to achieve a specific target AUC, but rather to evaluate whether the AHP-based hazard index provides meaningful spatial discrimination between relatively hazardous and non-hazardous locations. Validation against the 100-year 24-hour rainfall scenario produced an acceptable AUC of 0.671 reflecting moderate but meaningful discriminatory ability. This difference is expected given the inherent limitations of the validation datasets, including the nature of the observed event and the conservative spatially distributed characteristics of the design-storm based hazard validation datasets. The AUC values exceeding 0.5 indicate performance better than random assignment and demonstrate that the framework is effective at screening-level identification and prioritization of areas prone to high-impact flooding, rather than precise event prediction. Accordingly, AUC values are interpreted diagnostically and comparatively to recognize the imperfect nature of the validation data.

An example map is presented in Figure C- for the Upper Guadalupe watershed, displaying the depth-velocity raster from the HEC-RAS 2D 100-year, 24-hour model results according to the flood severity classifications detailed above.

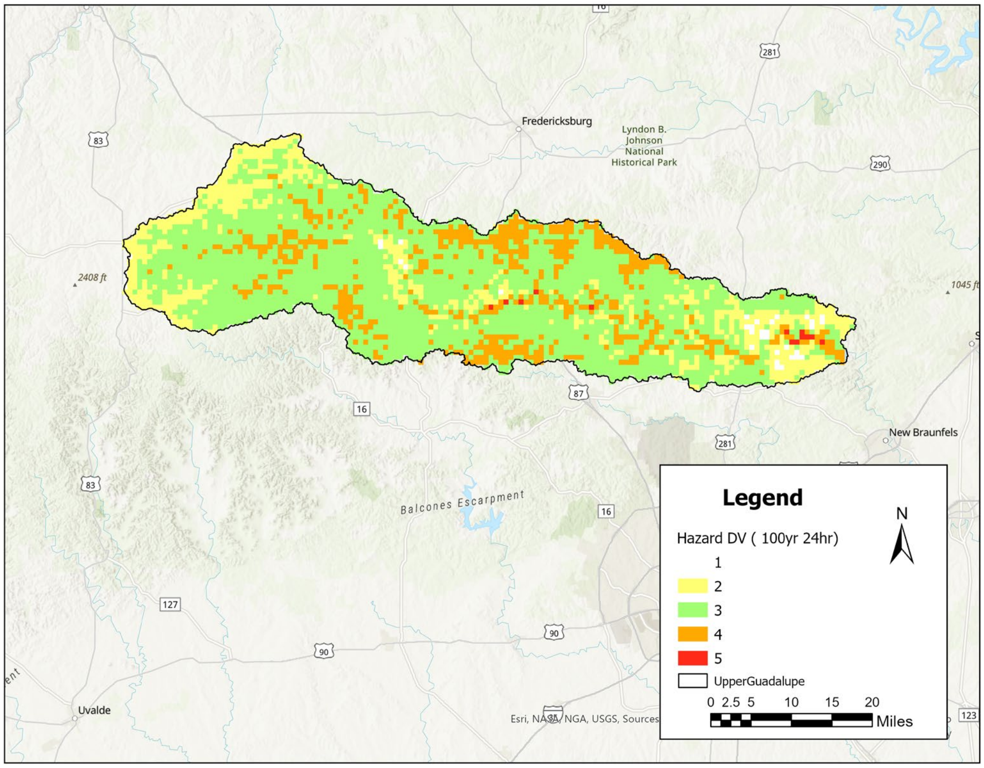


**Figure C-5. Categorical depth-velocity layer example using the Upper Guadalupe watershed**

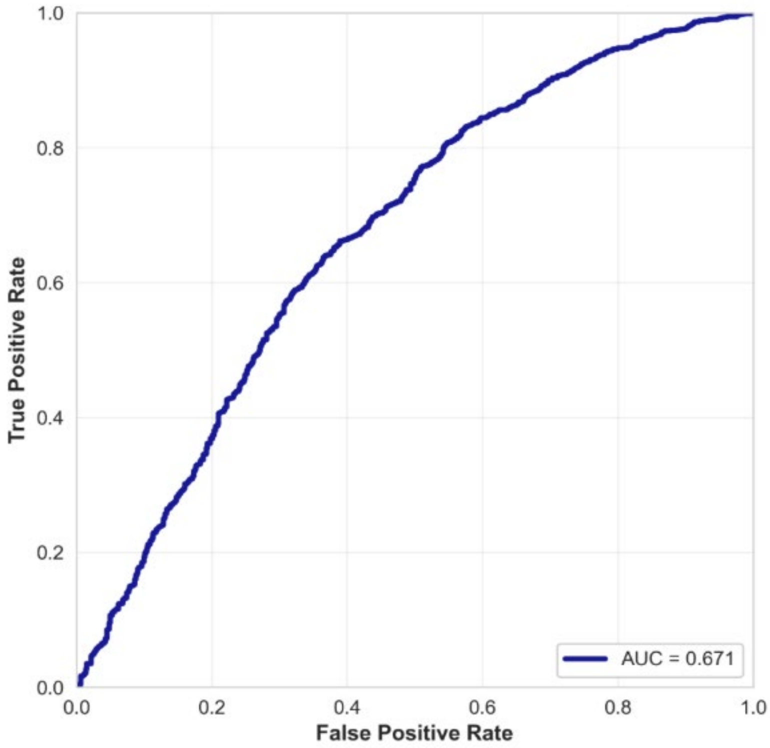


**Figure C-6. Draft upper Guadalupe watershed 100-year, 24-hour hazard validation**

The spatial comparison shows a strong agreement between the AHP-derived hazard index and the hydraulically based depth-velocity hazard classification from the BLE models, with higher hazard index values consistently concentrated along the main channel and hydraulically-connected floodplain areas where DV hazard classes are elevated. The visual correspondence is supported by the ROC analysis for the Brady watershed which yields an AUC value of 0.81 and indicates good discriminatory performance of the Analytic Hierarchy Process (Figure C-7).

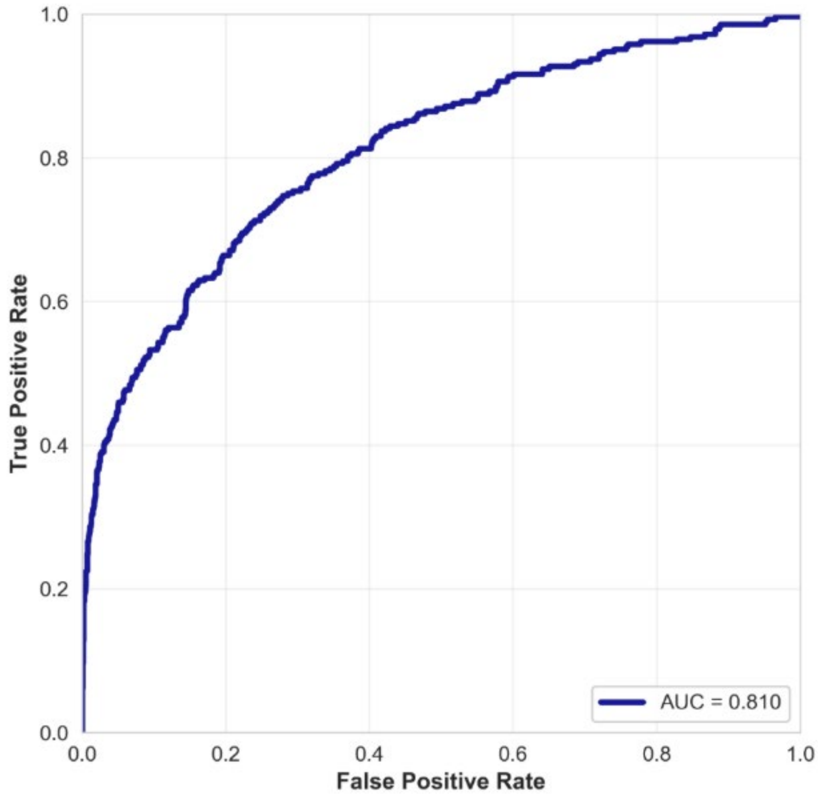


**Figure C-7. Draft Brady watershed 100-year, 24-hour hazard validation.**

**Table C-6. Watershed depth-velocity validation for AUC values.**

| Watershed | AUC |
|---|---|
| Austin Travis | 0.6 |
| Bosque | 0.77 |
| Brady | 0.81 |
| Cibolo | 0.69 |
| Concho | 0.81 |
| Cowhouse | 0.73 |
| Elm Sycamore | 0.55 |
| Hondo | 0.62 |
| Leon | 0.76 |
| Lower Pecos Red Bluff Reservoir | 0.74 |
| Lower San Antonio | 0.85 |
| Middle Colorado | 0.69 |
| North Bosque | 0.69 |
| Nueces Headwaters | 0.66 |
| Salt Draw | 0.58 |
| San Ambrosia Santa Isabel | 0.59 |
| San Gabriel | 0.8 |

| Watershed | AUC |
|---|---|
| San Saba | 0.64 |
| South Llano | 0.59 |
| Toyah | 0.52 |
| Upper San Antonio | 0.71 |
| Upper Guadalupe | 0.67 |

# Appendix D. Independent Validation

The Independent Validation/Quality Control Process provides a structured set of checks to ensure that the computed Flash Flood Hazard Index (FFHI) and Exposure Factors behave consistently, align with real-world physical processes, and reflect development patterns and historical impacts. The goal is to detect modeling errors, incorrect data inputs, spatial discontinuities, processing failures, or conceptual inconsistencies.

Validation Inputs required for Quality Control:

- FFHI raster (flow velocity, depth, or combined hazard metric)
- Exposure raster (structure density, critical facilities, land use, etc.)
- Watershed boundaries (HUC-8, HUC-10, HUC-12) from the Watershed Boundary Data Set
- County boundaries from the U.S. Census
- Building footprint datasets from Microsoft Bing or FEMA USA Structures
    - Alternatively, or additionally, address points from the U.S. Census or commercial providers like TomTom.
- Underlying imagery and contour data, for example, the USGS National Map Imagery Topo WMS layer
- Optionally, USGS flood gage locations and data, NOAA rain gages and data

Assumptions:

- All data layers were harmonized to a common projection, resolution, and coordinate system
- Symbolization thresholds were consistent across regions being compared

The Independent Validation lists the review processes, shows sample review comments, and related details. Unless otherwise stated, these are visual checks performed by loading the datasets into GIS, symbolizing them for ease of review, and then panning through. Following specific streams from headwaters to outlet is useful in detecting anomalies. Later checks in the process include review between watersheds for consistency in the output ranges.

# Appendix E. Flash Flood Risk Areas

## Final Product

The product delivered, provisional Flash Flood Risk Areas (FFRA), highlights areas that potentially warrant siren placement through a hierarchy of criteria, based on flash flood hazard and exposure to flooding. This product is visualized using the 0.2 percent (500-year) annual chance floodplain spatial data from the TWDB 2024 Flood Quilt with attribution at 1km resolution of associated hazard and exposure data. Pixels from the 0.2 percent (500-year) annual chance floodplain are identified with an elevated flash flood risk, according to the hierarchy of hazard and exposure criteria, as shown below.

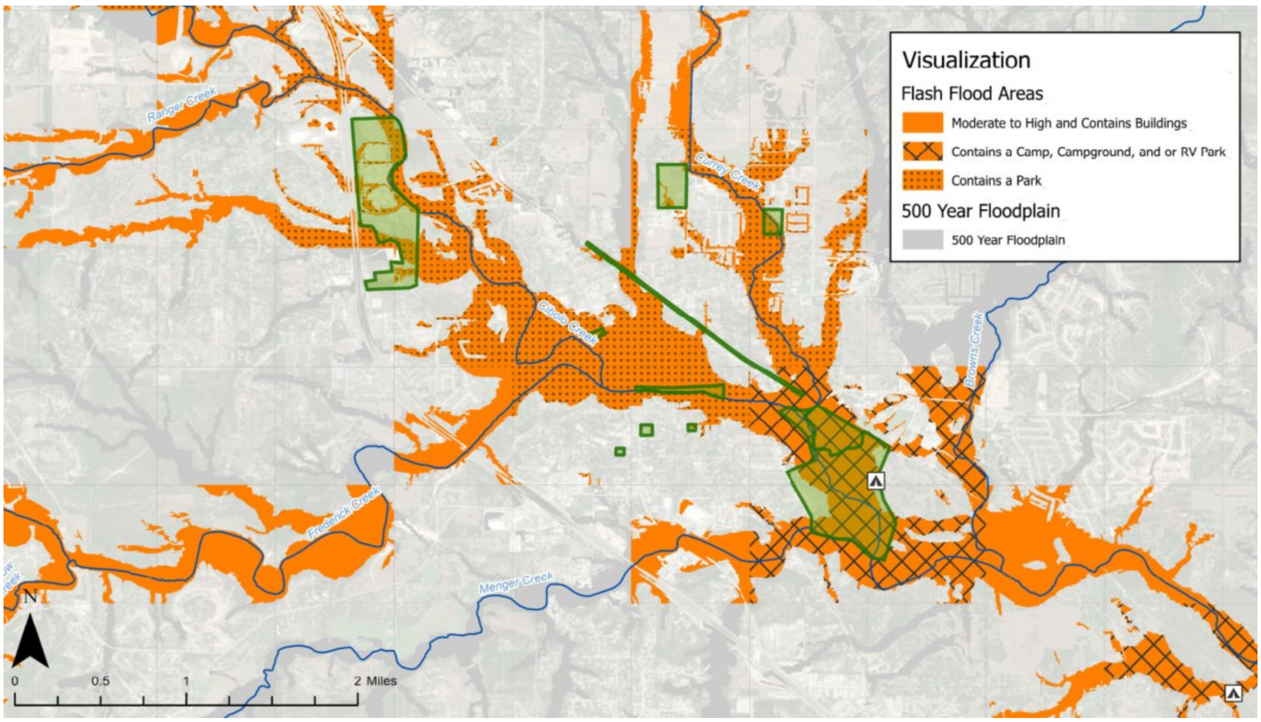


**Figure E-1: Data visualization example**

## Public Viewer

It is recommended to publish a simplified dataset of the provisional Flash Flood Risk Areas product for the public viewer to provide communities with the most useful fields for identifying and refining priority areas that may warrant sirens. See the Product Details section of this Appendix for more detailed information related to fields that may assist in refining priority areas. A simple attribution field for visualizing the dataset is provided and described in this Appendix to identify priority flash flood risk areas that may warrant sirens. Additional fields described in this section provide background information for the areas that are considered a flash flood risk and help establish the priority of concern. With this information, stakeholders can identify recommended areas of siren placement.

## Full Delivery

The full Flash Flood Risk Areas product is packaged in a geodatabase with relational mapping between input data, index results, and the 0.2 percent (500-year) annual chance floodplain shapefile. Its metadata specifies the units, inputs, and process for generating each attribute. A symbology layer file is provided as a visual aid for representing the visualization field, as depicted in Figure E-1. The polygon provided is not simplified and is intended for usage on geospatial viewing software. Additional documentation will be provided that is associated to the full database to give users a clear linkage between attribute fields and associated metadata. This data is intended for higher level users than the Public Viewer dataset and has additional attributes and details. The simplified public data viewer will still be provided within this database for use in spatial viewing platforms if preferred over the more detailed dataset.

## Communicating Risk

The public viewer and full delivery dataset packages provide the necessary details to make informed decisions relative to warning siren placement. The 0.2 percent (500-year) annual chance floodplain provides a widely accepted dataset in which extreme flooding can be reasonably measured.  The public viewer dataset allows for identification of high priority areas within 0.2 percent (500-year) annual chance floodplain, and aids in optimizing placement that stays outside this extent.

The pixelation of the 0.2 percent (500-year) annual chance floodplain does not undermine the communicated risk. Segmented floodplains can correspond to the size of areas with elevated flash flood risk. In the example below, the visualization fields identify higher priority hazards and exposures that warrant siren placement. Fragments of the floodplain are not identified as high hazard or high exposure because the pixel does not meet the criteria, but the proximity to a high priority pixel provides this detail. It is assumed that a siren warning system based upon the provided hazards would provide audible coverage to any adjacent pixel that is not categorized as part of this fragmentation. Therefore, it is reasonable to not manually decide floodplain connectivity based on source of stream. This maintains the analysis-driven data integrity of the product for stakeholders to make informed decisions.

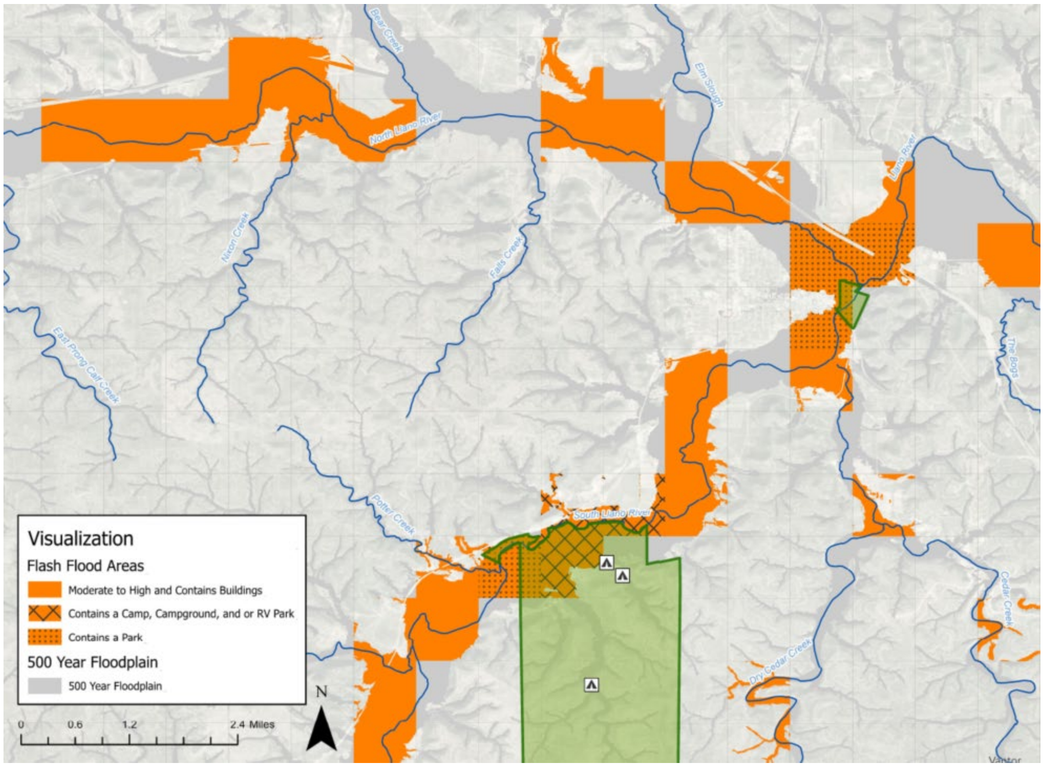


**Figure E-2: Pixelation example**

## Factors for Consideration

The following section is used to describe the factors considered for identifying Flash Flood Risk Areas criteria.

### *Mapping Output*

The Flash Flood Risk Areas product is visualized using the 0.2 percent (500-year) annual chance floodplain spatial data from the TWDB 2024 Flood Quilt with attribution at 1km resolution of associated hazard and exposure data.

- **0.2 Percent (500-Year) Annual Chance Floodplain** – The spatial qualities of the 0.2 percent (500-year) annual chance floodplain provide a justifiable and widely accepted dataset in which extreme flooding can be reasonably measured. This layer provides a spatial footprint in which evaluations are to occur within or near. Hazard thresholds are necessary to further distinguish higher and lower flash flood hazard, but overall spatial footprint is high priority for location identification. The 0.2 percent (500-year) annual chance floodplain from the TWDB 2024 Flood Quilt is the compilation of National Flood Hazard Layer data, Base Level Engineering (BLE) data, and cursory floodplain data.

### *Hazard Source*

Hazard is evaluated in the FFRA product through the flash flood hazard index and historic flood events with recorded exposures, through the NOAA Storm Events Database (SED). The flash flood hazard index identifies potential for flash flooding through the evaluation of watershed physical and meteorological characteristics, as described in Section 4. Historic flood events with recorded exposures identify areas where people have been exposed to flooding, which may indicate potential for severe flooding to recur.

#### Flash Flood Hazard Index

The flash flood hazard index was developed as a relative value based on various factors for comparison across the study area. Thus, selection of a hazard threshold was necessary to establish “high” and “moderate” values.

- **Hazard > 0.54** – This establishes a threshold for “high hazard” based on the median hazard value from DV-based validation for Flood Severity Class 5.
- **0.54 > Hazard > 0.525** – This establishes a threshold for “moderate hazard” based on the median hazard value from DV-based validation for Flood Severity Class 4.

#### Historic Flood Events

Historic flood events identify areas where flooding has occurred and may recur. The NOAA Storm Events Database (SED) is used to identify flash flood hazards with recorded exposures. Only flash flood records that have instances of recorded fatalities, injuries, or building damages are evaluated in order to prioritize areas with historical flash flood exposures, with the assumption that it is likely to recur again in the future.

- **NOAA Flash Flood Record** - The NOAA Storm Events Database does not capture the area extent of flash flood events; therefore, the potential outdoor exposure for NOAA flash flood records is indicated within a 1,460-foot (500-meter) proximity of the event location to account for the spatial variability of where flooding may have occurred

### *Exposure Source*

Two types of exposure were considered:  potential outdoor exposure locations and buildings. Potential outdoor exposure locations can indicate where people may congregate outdoors. Since the purpose of outdoor warning sirens is to notify people who may be outdoors, these locations were included as areas that may warrant outdoor warning sirens, given a hazard threshold was met. Building footprints delineate the spatial extents of where people may be expected, as it is assumed the spatial location is known and unlikely to change. The filtering criteria for the two types of exposure are given below:

#### Potential Outdoor Exposure

Outdoor warning sirens are designed for use in outdoor spaces, but full-coverage datasets depicting all areas of known and potential outdoor exposure are not available. Thus, we have considered potential outdoor exposure areas separately from the building-based exposure to provide for this scenario. The threshold of 1460 ft (500 m) proximity to the 0.2 percent (500-year) annual chance floodplain is used to set the extent of inclusion for outdoor exposures where area extents are not provided. This is considered reasonable because the provided outdoor exposure datasets do not discern for spatial variability of where people may be positioned relative to the point location. This inclusion helps provide conservative risk assessment to avoid loss of life in areas of likely but unknown whereabouts of individuals. The following are described as outdoor exposures:

- **Campgrounds** - These are areas that congregate people in large concentration, but the spatial whereabouts are uncertain and change frequently. Therefore, the potential outdoor exposure for campgrounds is indicated within a 1,460-foot (500-meter) proximity of the campground location to account for the spatial variability and transience of campgrounds.
- **Parks** - The congregation of people in the outdoor environment is likely to be in or around the delineated extent of the parks.

#### Known Exposure: Buildings

- Buildings are considered a known exposure type. As these are a fixed position, typically people will be within or around the footprint of the structure. Therefore, it is justifiable to only consider buildings if within the 0.2 percent (500-year) annual chance floodplain. Buildings – Any building type that contains at least one building within the 0.2 percent (500-year) annual chance floodplain warrants inclusion as it is assumed these building type will typically be occupied to some extent by a person or incur increased damages from a flash flood event. Additional fields are provided to aid communities in refining priority areas with building characteristics, including building and population counts by zoning classification.

### *Waterbodies*

Waterbodies are areas that are identified to have a large area of flat backwater conditions, typically upstream of major dams or reservoirs. Major waterbodies were identified from the National Hydrography Dataset Plus dataset. Waterbodies with an area larger than 1 square kilometer were identified for exclusion from this study. Streams impacted by these major waterbodies are typically heavily regulated, and lakes impacted by these major waterbodies would exhibit slower rate of rise in a storm event that may not result in flash flood conditions The hydraulic nature of these areas drastically reduces the risk of flash flooding to be catastrophic. This is because in areas like this, the flood level largely becomes volume based. Typical flash flood precipitation events are not long volumetric storm events and would have minimal impact on waterbody areas. Therefore, it is deemed reasonable to exclude these areas based upon the provided assumption.

## Methodology

The final spatial dataset is provided based on the 0.2 percent (500-year) annual chance floodplain from the TWDB 2024 Flood Quilt. All criteria and information set forth are spatially relative to this layer but are attributed at 1km resolution of associated hazard data. Isolated polygons of flooding within the 1km resolution are evaluated independently for meeting the criteria described below.

### *Criteria*

A well-defined criterion is essential for identifying risk to fulfil the purpose within the project and to aid in providing a product that is captured consistently and effectively. The criterion described below allows for a categorization data standard that removes ambiguity, aligns stakeholders on the source of risk, and helps differentiate the product for visualization and understanding. The following, in accordance with TWDB, will enable informed decision making to support the identification of potential locations of outdoor flash flood warning systems.

1) Included moderate to high hazard campgrounds
    a) Where flash flood hazard index >= 0.525 and within 1,460-foot (500-meter) proximity of campground location
2) Included moderate to high hazard parks
    a) Where flash flood hazard index >= 0.525 and overlaps park footprint
3) Included moderate to high hazard buildings
    a) Where flash flood hazard index >= 0.525 and overlaps building footprint
    b) Or within 1,460-foot (500-meter) proximity of NOAA flash flood record and overlaps building footprint
4) Excluded waterbody influence due to reduced risk from hydraulics dynamics

Additional justification and more detailed discussion of these criteria can be found within the Factors for Consideration section of this Appendix.

## Product Details

The product generated as part of this project allows for varied levels of detail for pre-described queries. The three major fields of query are provided under the status, criteria, and visualization fields of the datasets attribute table. These pre-determined queries are utilized to avoid any misinterpretation of the provided product due to the complex queries necessary to categorize the information according to the user's preference or topic of concern. Each of these three fields serves a purpose according to the user's familiarity with the product and allows for rapid viewing with associated packaged .lyr files for quick generation of symbology.

### *Status Field*

This attribute is to provide the simplest dataset for viewing for quick analysis of locations that may be considered in or out of the described criteria.

1) Include: Identifies polygon extent that meets the described inclusion criteria
2) Exclude: Identifies polygon extents that were excluded from further analysis due to the exclusion criteria
3) N/A: Identifies polygon extent that never meets inclusion criteria

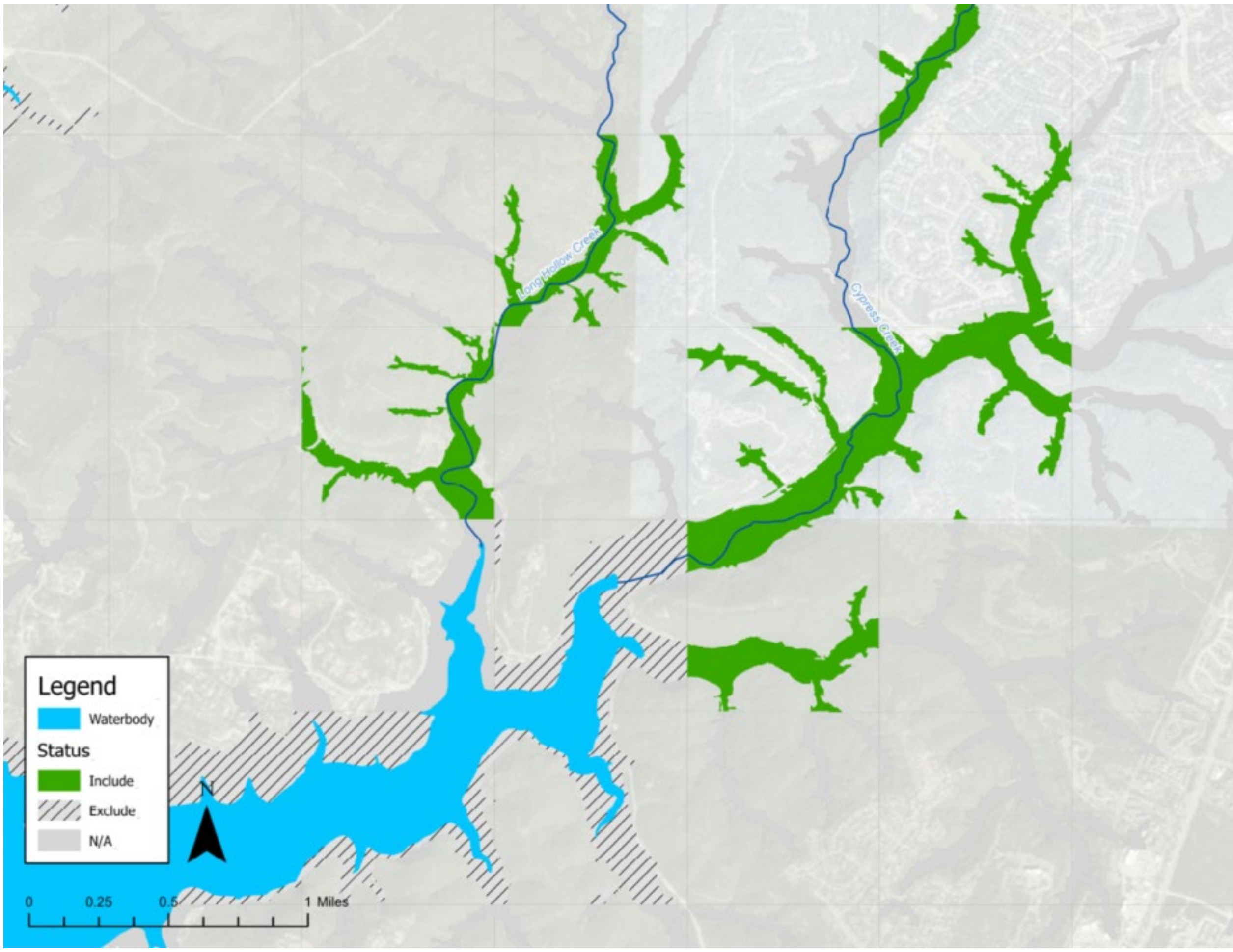


**Figure E-3: Status field example**

## *Criteria Field*

This attribute is to provide clarity to the dataset of why a given section of polygon is attributed as included, excluded, or N/A from the status field. (1-5) are indicative of being included, (6) are indicated of being excluded, and (7) is the remainder of the 0.2 percent (500-year) annual chance floodplain that would be considered N/A.

1) Near campground and hazard >= 0.525
2) Near park and hazard >= 0.525
3) Near NOAA flood record and hazard >= 0.525 and buildings in 500-year floodplain
4) Building in 500-year floodplain and hazard >= 0.54
5) Building in 500yr floodplain and hazard >= 0.525Remove for waterbody
6) Near NOAA flood record and hazard >= 0.525 and no buildings in 500-year floodplain (areas not included in priority areas but provided if relevant to community interests)
7) N500-year floodplain with buildings (areas not included in priority areas but provided if relevant to community interests)
8) 500-year floodplain (areas not previously categorized by criteria)

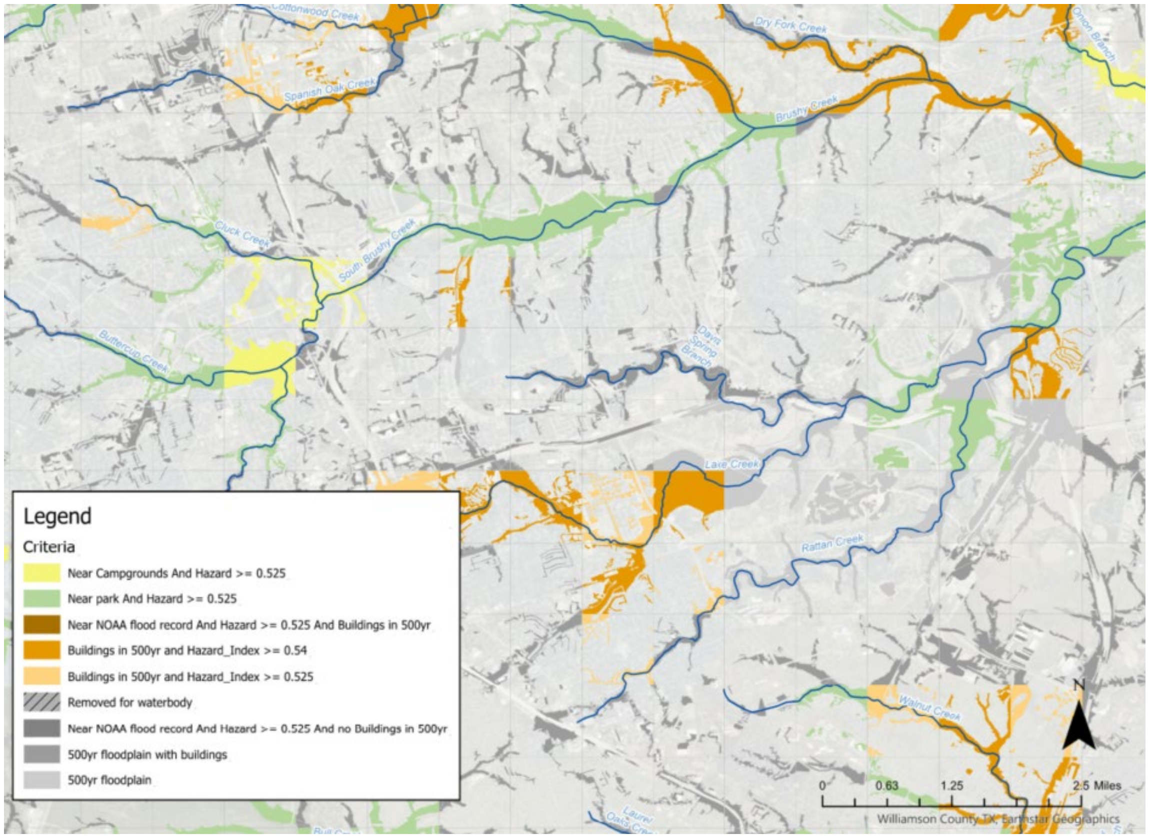


**Figure E-4: Criteria field example**

## *Visualization Field*

This attribute is to establish a priority of concern based upon the exposure source. All other data that does not fall into these prioritization levels are indicated as the 0.2 percent (500-year) annual chance floodplain.

1) Contains a Camp, Campground and or RV Park
2) Contains a Park
3) Moderate to High and Contains Buildings
4) 500-year Floodplain

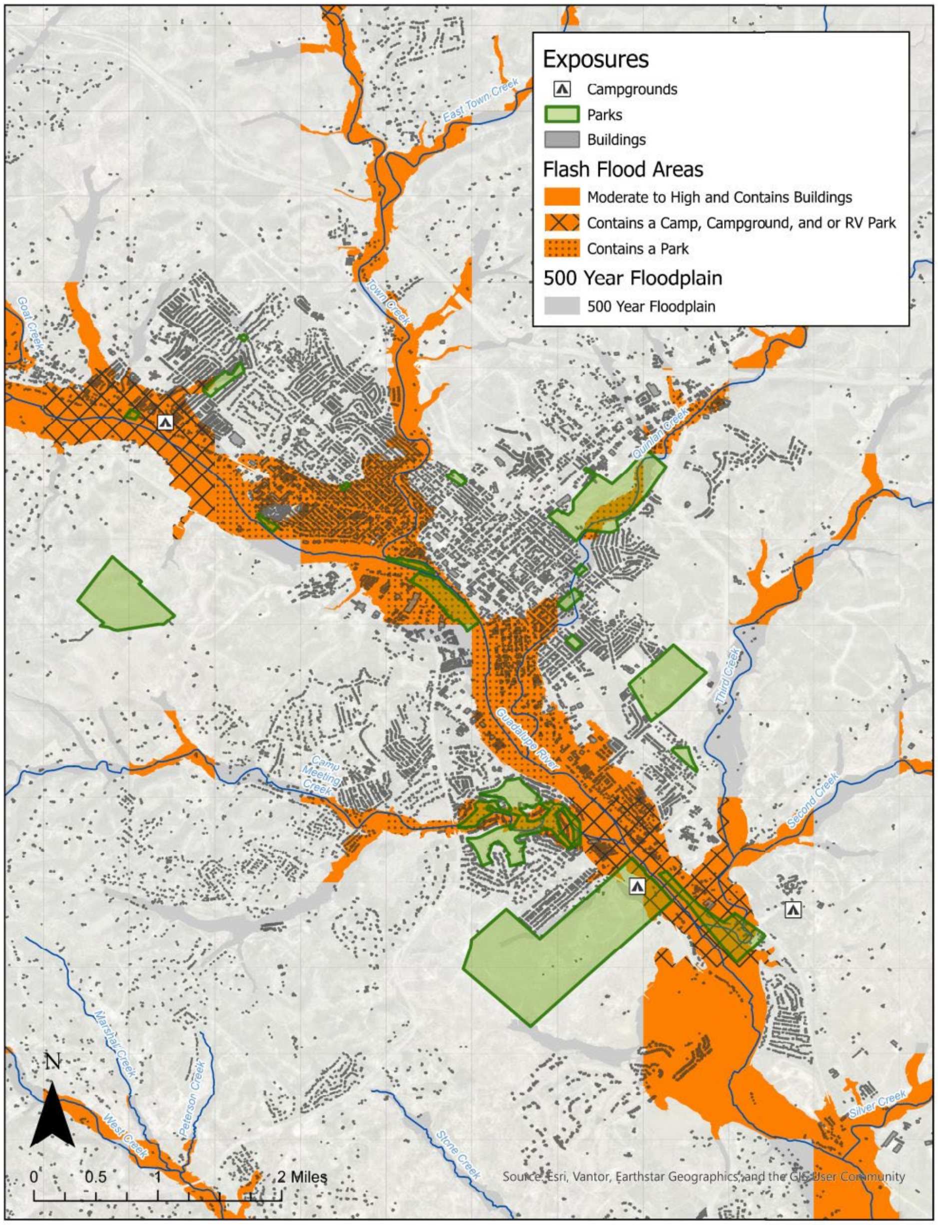


**Figure E-5: Visualization field example**

### *Other*

Many additional attributes are stored within the geospatial polygons beyond those identified above. These are provided to allow for a more robust dataset that can be queried according to user preference to further refine priority areas.

Additional fields include building counts by zoning classification, building population count, and median depth-velocity (DV) flood severity category from Base Level Engineering (BLE) models, where available, at building centroids.

# Appendix F. References


1. Abdrabo, K. I., Kantoush, S. A., Esmaiel, A., Saber, M., Sumi, T., Almamari, M., Elboshy, B., & Ghoniem, S. (2023). An integrated indicator-based approach for constructing an urban flood vulnerability index as an urban decision-making tool using the PCA and AHP techniques: A case study of Alexandria, Egypt. *Urban Climate*, *48*, 101426. https://doi.org/10.1016/j.uclim.2023.101426
2. Abedi, R., Costache, R., Shafizadeh-Moghadam, H., & Pham, Q. B. (2022). flash flood susceptibility mapping based on XGBoost, random forest and boosted regression trees. *Geocarto International*, *37*(19), 5479–5496. https://doi.org/10.1080/10106049.2021.1920636
3. Ahmadalipour, A., & Moradkhani, H. (2019 A data-driven analysis of flash flood hazard, fatalities, and damages over the CONUS during 1996–2017. *Journal of Hydrology*, *578*, 124106. https://doi.org/10.1016/j.jhydrol.2019.124106
4. Ajtai, I., Ştefănie, H., Maloş, C., Botezan, C., Radovici, A., Bizău-Cârstea, M., & Baciu, C. (2023). Mapping social vulnerability to floods. A comprehensive framework using a vulnerability index approach and PCA analysis. *Ecological Indicators*, *154*, 110838. https://doi.org/10.1016/j.ecolind.2023.110838
5. Alam, A., Ahmed, B., & Sammonds, P. (2021). Flash flood susceptibility assessment using the parameters of drainage basin morphometry in SE Bangladesh. *Quaternary International*, *575–576*, 295–307. https://doi.org/10.1016/j.quaint.2020.04.047
6. Ali, A. A. B., & Nelson, J. (2025). Integrative Multi-Criteria Geospatial Modeling for Assessing Compound Flood-Contamination Risks in Vulnerable Communities. *Environmental Processes*, *12*(4), 58. https://doi.org/10.1007/s40710-025-00803-0
7. Al-Rawas, G., Nikoo, M. R., & Al-Wardy, M. (2024). A review on the prevention and control of flash flood hazards on a global scale: Early warning systems, vulnerability assessment, environmental, and public health burden. *International Journal of Disaster Risk Reduction*, *115*, 105024. https://doi.org/10.1016/j.ijdrr.2024.105024
8. Aroca-Jiménez, E., Bodoque, J. M., García, J. A., & Figueroa-García, J. E. (2022). Holistic characterization of flash flood vulnerability: Construction and validation of an integrated multidimensional vulnerability index. *Journal of Hydrology*, *612*, 128083. https://doi.org/10.1016/j.jhydrol.2022.128083
9. Band, S. S., Janizadeh, S., Chandra Pal, S., Saha, A., Chakrabortty, R., Melesse, A. M., & Mosavi, A. (2020a). Flash Flood Susceptibility Modeling Using New Approaches of Hybrid and Ensemble Tree-Based Machine Learning Algorithms. *Remote Sensing*, *12*(21), 3568. https://doi.org/10.3390/rs12213568
10. Band, S. S., Janizadeh, S., Chandra Pal, S., Saha, A., Chakrabortty, R., Melesse, A. M., & Mosavi, A. (2020b). Flash Flood Susceptibility Modeling Using New Approaches of Hybrid and Ensemble Tree-Based Machine Learning Algorithms. *Remote Sensing*, *12*(21), 3568. https://doi.org/10.3390/rs12213568
11. Beard, L. R. (1975). *Generalized evaluation of flash flood potential*.
12. Bui, D. T., Tsangaratos, P., Ngo, P.-T. T., Pham, T. D., & Pham, B. T. (2019). Flash flood susceptibility modeling using an optimized fuzzy rule based feature selection technique and tree based ensemble methods. *Science of The Total Environment*, *668*, 1038–1054. https://doi.org/10.1016/j.scitotenv.2019.02.422
13. Carvalho, R. de C. F., Moreira, T. R., Souza, K. B. de, Costa, G. A., Zanetti, S. S., Barbosa, K. V., Filho, C. B. C., Miranda, M. R., Guerra Filho, P. A., Santos, A. R. dos, Ramalho, A. H. C., Ferreira, E. S. A., Araújo, E. F., Neves, F. P. das, Lima, J. F. V. de, Moreau, J. S., Belan, L. L., Aguiar, M. O., Gorsani, R. G., … Santos, A. R. dos. (2022). GIS-Based Approach Applied to Study of Seasonal Rainfall Influence over Flood Vulnerability. *Water*, *14*(22), 3731. https://doi.org/10.3390/w14223731
14. Chowdhury, Md. S. (2024). Flash flood susceptibility mapping of north-east depression of Bangladesh using different GIS based bivariate statistical models. *Watershed Ecology and the Environment*, *6*, 26–40. https://doi.org/10.1016/j.wsee.2023.12.002
15. Cikmaz, B. A., Yildirim, E., & Demir, I. (2025). Flood susceptibility mapping using fuzzy analytical hierarchy process for Cedar Rapids, Iowa. *International Journal of River Basin Management*, *23*(1), 1–13. https://doi.org/10.1080/15715124.2023.2216936
16. Costache, R. (2019a). flash flood Potential assessment in the upper and middle sector of Prahova river catchment (Romania). A comparative approach between four hybrid models. *Science of The Total Environment*, *659*, 1115–1134. https://doi.org/10.1016/j.scitotenv.2018.12.397

17. Costache, R. (2019b).  flash flood Potential Index mapping using weights of evidence, decision Trees models and their novel hybrid integration. *Stochastic Environmental Research and Risk Assessment*, *33*(7), 1375–1402. https://doi.org/10.1007/s00477-019-01689-9
18. Costache, R. (2019c).  flash flood Potential Index mapping using weights of evidence, decision Trees models and their novel hybrid integration. *Stochastic Environmental Research and Risk Assessment*, *33*(7), 1375–1402. https://doi.org/10.1007/s00477-019-01689-9
19. Costache, R., Hong, H., & Pham, Q. B. (2020). Comparative assessment of the flash flood potential within small mountain catchments using bivariate statistics and their novel hybrid integration with machine learning models. *Science of The Total Environment*, *711*, 134514. https://doi.org/10.1016/j.scitotenv.2019.134514
20. Costache, R., Hong, H., & Wang, Y. (2019). Identification of torrential valleys using GIS and a novel hybrid integration of artificial intelligence, machine learning and bivariate statistics. *CATENA*, *183*, 104179. https://doi.org/10.1016/j.catena.2019.104179
21. Costache, R., Pham, Q. B., Sharifi, E., Linh, N. T. T., Abba, S. I., Vojtek, M., Vojteková, J., Nhi, P. T. T., & Khoi, D. N. (2019).  flash flood Susceptibility Assessment Using Multi-Criteria Decision Making and Machine Learning Supported by Remote Sensing and GIS Techniques. *Remote Sensing*, *12*(1), 106. https://doi.org/10.3390/rs12010106
22. Costache, R., Trung Tin, T., Arabameri, A., Crăciun, A., Ajin, R. S., Costache, I., Reza Md. Towfiqul Islam, A., Abba, S. I., Sahana, M., Avand, M., & Thai Pham, B. (2022).  flash flood hazard using deep learning based on H2O R package and fuzzy-multicriteria decision-making analysis. *Journal of Hydrology*, *609*, 127747. https://doi.org/10.1016/j.jhydrol.2022.127747
23. Costache, R., & Zaharia, L.  flash flood potential assessment and mapping by integrating the weights-of-evidence and frequency ratio statistical methods in GIS environment – case study: Bâsca Chiojdului River catchment (Romania). *Journal of Earth System Science*, *126*(4), 59. https://doi.org/10.1007/s12040-017-0828-9
24. Darwish, K. (2023). GIS-Based Multi-Criteria Decision Analysis for Flash Flood Hazard and Risk Assessment: A Case Study of the Eastern Minya Watershed, Egypt. *The 7th International Electronic Conference on Water Sciences*, 87. https://doi.org/10.3390/ECWS-7-14315
25. Duan, L., Liu, C., Xu, H., Huali, H., Liu, H., Yan, X., Liu, T., Yang, Z., Liu, G., Dai, X., Zhang, D., Fu, X., Liu, X., & Lu, H. (2022). Susceptibility Assessment of Flash Floods: A Bibliometrics Analysis and Review. *Remote Sensing*, *14*(21), 5432. https://doi.org/10.3390/rs14215432
26. Elghouat, A., Algouti, A., Algouti, A., Baid, S., Ezzahzi, S., Kabili, S., & Agli, S. (2024). Integrated approaches for flash flood susceptibility mapping: Spatial modeling and comparative analysis of statistical and machine learning models. A case study of the Rheraya watershed, Morocco. *Journal of Water and Climate Change*, *15*(8), 3624–3646. https://doi.org/10.2166/wcc.2024.726
27. Elmahdy, S., Ali, T., & Mohamed, M. (2020). Flash Flood Susceptibility Modeling and Magnitude Index Using Machine Learning and Geohydrological Models: A Modified Hybrid Approach. *Remote Sensing*, *12*(17), 2695. https://doi.org/10.3390/rs12172695
28. Elsadek, W. M., & Almaliki, A. H. (2024). Integrated hydrological study for flash flood assessment using morphometric analysis and MCDA based on hydrological indices—Al-Sail Al-Kabir, KSA. *Natural Hazards*, *120*(7), 6853–6880. https://doi.org/10.1007/s11069-024-06450-2
29. Federal Emergency Management Agency (FEMA). (2025). Guidance for Flood Risk Analysis and Mapping: Flood Depth and Analysis Grids. https://www.fema.gov/sites/default/files/documents/fema_guidance_riverine_mapping_and_floodplain_boundaries_nov2024.pdf
30. Fernandez, P., Mourato, S., & Moreira, M. (2016). Social vulnerability assessment of flood risk using GIS-based multicriteria decision analysis. A case study of Vila Nova de Gaia (Portugal). *Geomatics, Natural Hazards and Risk*, *7*(4), 1367–1389. https://doi.org/10.1080/19475705.2015.1052021
31. Forte, G., De Falco, M., Santo, A., Gautam, D., & Santangelo, N. (2025). Flash flood impacts and vulnerability mapping at catchment scale: Insights from southern Apennines. *Engineering Geology*, *350*, 107988. https://doi.org/10.1016/j.enggeo.2025.107988
32. Gannon, J. P., Kelleher, C., & Zimmer, M. (2022). Controls on watershed flashiness across the continental US. *Journal of Hydrology*, *609*, 127713. https://doi.org/10.1016/j.jhydrol.2022.127713
33. Hawkesbury-Nepean Floodplain Management Strategy Steering Committee. (2024). Designing Safer Subdivisions: Guidance on Subdivision Design in Flood Prone Areas.

https://www.ses.nsw.gov.au/sites/default/files/2024-02/subdivision_guidelines.pdf
34. He, F., Liu, S., Mo, X., & Wang, Z. (2025). Interpretable flash flood susceptibility mapping in Yarlung Tsangpo River Basin using H2O Auto-ML. *Scientific Reports*, *15*(1), 1702. https://doi.org/10.1038/s41598-024-84655-y
35. He, X., Fang, Y., Wang, B., & Huang, X. (2024). Towards a verifiable, uncertainty-controlled assessment of the spatiotemporal dynamics of social vulnerability to flash floods. *Ecological Indicators*, *166*, 112323. https://doi.org/10.1016/j.ecolind.2024.112323
36. Hoang, D.-V., & Liou, Y.-A. (2024). Assessing the influence of human activities on flash flood susceptibility in mountainous regions of Vietnam. *Ecological Indicators*, *158*, 111417. https://doi.org/10.1016/j.ecolind.2023.111417
37. Holko, L., Parajka, J., Kostka, Z., Škoda, P., & Blöschl, G. (2011). Flashiness of mountain streams in Slovakia and Austria. *Journal of Hydrology*, *405*(3–4), 392–401. https://doi.org/10.1016/j.jhydrol.2011.05.038
38. Ishizaka, A., & Lusti, M. (2006). How to derive priorities in AHP: A comparative study. *Central European Journal of Operations Research*, *14*(4), 387–400. https://doi.org/10.1007/s10100-006-0012-9
39. Janizadeh, S., Avand, M., Jaafari, A., Phong, T. V., Bayat, M., Ahmadisharaf, E., Prakash, I., Pham, B. T., & Lee, S. (2019). Prediction Success of Machine Learning Methods for Flash Flood Susceptibility Mapping in the Tafresh Watershed, Iran. *Sustainability*, *11*(19), 5426. https://doi.org/10.3390/su11195426
40. Ke, X., Wang, N., Xiu, Y., Dong, Z., & Wang, T. (2025). A flash flood susceptibility prediction and partitioning method based on GeoDetector and random forest. *Stochastic Environmental Research and Risk Assessment*, *39*(4), 1377–1404. https://doi.org/10.1007/s00477-025-02922-4
41. Khajehei, S., Ahmadalipour, A., Shao, W., & Moradkhani, H. (2020). A Place-based Assessment of Flash Flood Hazard and Vulnerability in the Contiguous United States. *Scientific Reports*, *10*(1), 448. https://doi.org/10.1038/s41598-019-57349-z
42. Khodaei, H., Nasiri Saleh, F., Nobakht Dalir, A., & Zarei, E. (2025). Future flood susceptibility mapping under climate and land use change. *Scientific Reports*, *15*(1), 12394. https://doi.org/10.1038/s41598-025-97008-0
43. Khosravi, K., Pourghasemi, H. R., Chapi, K., & Bahri, M. (2016). Flash flood susceptibility analysis and its mapping using different bivariate models in Iran: A comparison between Shannon's entropy, statistical index, and weighting factor models. *Environmental Monitoring and Assessment*, *188*(12), 656. https://doi.org/10.1007/s10661-016-5665-9
44. Kocsis, I., Bilașco, Ștefan, Irimuș, I.-A., Dohotar, V., Rusu, R., & Roșca, S. (2022). Flash Flood Vulnerability Mapping Based on Flash Flood Potential Index (FFPI) Using GIS Spatial Analysis Case Study: Valea Rea Catchment Area, Romania. *Sensors*, *22*(9), 3573. https://doi.org/10.3390/s22093573
45. Kuşcu, İ., & Ozdemir, H. (2024). Flood susceptibility analysis of settlement basins on a provincial scale using inventory flood data. *Environmental Earth Sciences*, *84*(1), 15. https://doi.org/10.1007/s12665-024-11988-2
46. Lin, K., Chen, H., Xu, C.-Y., Yan, P., Lan, T., Liu, Z., & Dong, C. (2020). Assessment of flash flood risk based on improved analytic hierarchy process method and integrated maximum likelihood clustering algorithm. *Journal of Hydrology*, *584*, 124696. https://doi.org/10.1016/j.jhydrol.2020.124696
47. Liuzzo, L., Sammartano, V., & Freni, G. (2019). Comparison between Different Distributed Methods for Flood Susceptibility Mapping. *Water Resources Management*, *33*(9), 3155–3173. https://doi.org/10.1007/s11269-019-02293-w
48. Majeed, M., Lu, L., Anwar, M. M., Tariq, A., Qin, S., El-Hefnawy, M. E., El-Sharnouby, M., Li, Q., & Alasmari, A. (2023). Prediction of flash flood susceptibility using integrating analytic hierarchy process (AHP) and frequency ratio (FR) algorithms. *Frontiers in Environmental Science*, *10*, 1037547. https://doi.org/10.3389/fenvs.2022.1037547
49. Painter, M. A., Shah, S., Alexandre, G., Khalid, F., Prudencio, W., Chisty, M. A., Tormos-Aponte, F., & Wilhelmi, O. (2023). *A systematic scoping review of the Social Vulnerability Index as applied to natural hazards*. In Review. https://doi.org/10.21203/rs.3.rs-2978301/v1
50. Popa, M. C., Peptenatu, D., Drăghici, C. C., & Diaconu, D. C. (2019). Flood Hazard Mapping Using the Flood and flash flood Potential Index in the Buzău River Catchment, Romania. *Water*, *11*(10), 2116. https://doi.org/10.3390/w11102116

51. Rashidiyan, M., & Rahimzadegan, M. (2024). Investigation and Evaluation of Land Use–Land Cover Change Effects on Current and Future Flood Susceptibility. *Natural Hazards Review*, *25*(1), 04023049. https://doi.org/10.1061/NHREFO.NHENG-1854
52. Riaz, R., & Mohiuddin, Md. (2025). Application of GIS-based multi-criteria decision analysis of hydro-geomorphological factors for flash flood susceptibility mapping in Bangladesh. *Water Cycle*, *6*, 13–27. https://doi.org/10.1016/j.watcyc.2024.09.003
53. Saaty, T. L. (1977). A scaling method for priorities in hierarchical structures. *Journal of Mathematical Psychology*, *15*(3), 234–281. https://doi.org/10.1016/0022-2496(77)90033-5
54. Saharia, M., Kirstetter, P.-E., Vergara, H., Gourley, J. J., Hong, Y., & Giroud, M. (2017). Mapping Flash Flood Severity in the United States. *Journal of Hydrometeorology*, *18*(2), 397–411. https://doi.org/10.1175/JHM-D-16-0082.1
55. Samanta, S., Pal, D. K., & Palsamanta, B. (2018). Flood susceptibility analysis through remote sensing, GIS and frequency ratio model. *Applied Water Science*, *8*(2), 66. https://doi.org/10.1007/s13201-018-0710-1
56. Shafapour Tehrany, M., Kumar, L., & Shabani, F. (2019). A novel GIS-based ensemble technique for flood susceptibility mapping using evidential belief function and support vector machine: Brisbane, Australia. *PeerJ*, *7*, e7653. https://doi.org/10.7717/peerj.7653
57. Shahabi, H., Shirzadi, A., Ronoud, S., Asadi, S., Pham, B. T., Mansouripour, F., Geertsema, M., Clague, J. J., & Bui, D. T. (2021). Flash flood susceptibility mapping using a novel deep learning model based on deep belief network, back propagation and genetic algorithm. *Geoscience Frontiers*, *12*(3), 101100. https://doi.org/10.1016/j.gsf.2020.10.007
58. Sharif, H. O., Hossain, Md. M., Jackson, T., & Bin-Shafique, S. (2012). Person-place-time analysis of vehicle fatalities caused by flash floods in Texas. *Geomatics, Natural Hazards and Risk*, *3*(4), 311–323. https://doi.org/10.1080/19475705.2011.615343
59. Shawky, M., & Hassan, Q. K. (2023). Geospatial Modeling Based-Multi-Criteria Decision-Making for Flash Flood Susceptibility Zonation in an Arid Area. *Remote Sensing*, *15*(10), 2561. https://doi.org/10.3390/rs15102561
60. Shrestha, S., Dahal, D., Poudel, B., Banjara, M., & Kalra, A. (2025). Flood Susceptibility Analysis with Integrated Geographic Information System and Analytical Hierarchy Process: A Multi-Criteria Framework for Risk Assessment and Mitigation. *Water*, *17*(7), 937. https://doi.org/10.3390/w17070937
61. Singh, G., & Pandey, A. (2021). Flash flood vulnerability assessment and zonation through an integrated approach in the Upper Ganga Basin of the Northwest Himalayan region in Uttarakhand. *International Journal of Disaster Risk Reduction*, *66*, 102573. https://doi.org/10.1016/j.ijdrr.2021.102573
62. Smith, G. P., Davey, E. K., and Cox, R. J. (2014) Flood Hazard. UNSW Australia Water Research Laboratory Technical Report 2014/07. https://www.aidr.org.au/media/2334/wrl-flood-hazard-techinical-report-september-2014.pdf
63. Swain, K. C., Singha, C., & Nayak, L. (2020). Flood Susceptibility Mapping through the GIS-AHP Technique Using the Cloud. *ISPRS International Journal of Geo-Information*, *9*(12), 720. https://doi.org/10.3390/ijgi9120720
64. Talha, S., Maanan, M., Atika, H., & Rhinane, H. (2019). PREDICTION OF FLASH FLOOD SUSCEPTIBILITY USING FUZZY ANALYTICAL HIERARCHY PROCESS (FAHP) ALGORITHMS AND GIS: A STUDY CASE OF GUELMIM REGION IN SOUTHWESTERN OF MOROCCO. *The International Archives of the Photogrammetry, Remote Sensing and Spatial Information Sciences*, *XLII-4/W19*, 407–414. https://doi.org/10.5194/isprs-archives-XLII-4-W19-407-2019
65. Tariq, A., Yan, J., Ghaffar, B., Qin, S., Mousa, B. G., Sharifi, A., Huq, Md. E., & Aslam, M. (2022). Flash Flood Susceptibility Assessment and Zonation by Integrating Analytic Hierarchy Process and Frequency Ratio Model with Diverse Spatial Data. *Water*, *14*(19), 3069. https://doi.org/10.3390/w14193069
66. Tascón-González, L., Ferrer-Julià, M., Ruiz, M., & García-Meléndez, E. (2020). Social Vulnerability Assessment for Flood Risk Analysis. *Water*, *12*(2), 558. https://doi.org/10.3390/w12020558
67. Tellman, B., Schank, C., Schwarz, B., Howe, P. D., & De Sherbinin, A. (2020). Using Disaster Outcomes to Validate Components of Social Vulnerability to Floods: Flood Deaths and Property Damage across the USA. *Sustainability*, *12*(15), 6006. https://doi.org/10.3390/su12156006
68. Terti, G., Ruin, I., Anquetin, S., & Gourley, J. J. (2017). A Situation-Based Analysis of Flash Flood Fatalities in the United States. *Bulletin of the American Meteorological Society*, *98*(2), 333–345. https://doi.org/10.1175/BAMS-D-15-00276.1

69. Texas Water Development Board (TWDB). (2024). 2024 State Flood Plan. https://www.twdb.texas.gov/flood/planning/sfp/2024/doc/SFP-2024.pdf?d=9190
70. Tikuye, B. G., Ray, R. L., Abeysingha, N. S., & Gurau, S. (2025). Integrating multi-criteria decision analysis and geospatial data for flood susceptibility mapping in Texas, USA. *Progress in Disaster Science*, *28*, 100462. https://doi.org/10.1016/j.pdisas.2025.100462
71. Wahba, M., Essam, R., El-Rawy, M., Al-Arifi, N., Abdalla, F., & Elsadek, W. M. (2024). Forecasting of flash flood susceptibility mapping using random forest regression model and geographic information systems. *Heliyon*, *10*(13), e33982. https://doi.org/10.1016/j.heliyon.2024.e33982
72. Wang, W., Kim, D., Han, H., Tak Kim, K., Kim, S., & Soo Kim, H. (2023). Flood risk assessment using an indicator based approach combined with flood risk maps and grid data. *Journal of Hydrology*, *627*, 130396. https://doi.org/10.1016/j.jhydrol.2023.130396
73. Waqas, H., Lu, L., Tariq, A., Li, Q., Baqa, M. F., Xing, J., & Sajjad, A. (2021). Flash Flood Susceptibility Assessment and Zonation Using an Integrating Analytic Hierarchy Process and Frequency Ratio Model for the Chitral District, Khyber Pakhtunkhwa, Pakistan. *Water*, *13*(12), 1650. https://doi.org/10.3390/w13121650
74. Wilkho, R. S., Gharaibeh, N. G., & Chang, S. (2025). A GIS-based tool for dynamic assessment of community susceptibility to flash flooding. *Journal of Flood Risk Management*, *18*(1), e13049. https://doi.org/10.1111/jfr3.13049
75. Zhuang, Y., Gong, T., Fang, J., Shen, D., Tang, W., Lin, S., Chen, X., & Zhang, Y. (2026). Integrating social media data and machine learning methods for flash flood susceptibility mapping in China. *Journal of Hydrology*, *664*, 134397. https://doi.org/10.1016/j.jhydrol.2025.134397
76. Zulhisham, N. A., & Sadek, E. S. S. M. (2023). Employing the Flash Flood Potential Index (FFPI) with Physical Environmental Factors in Baling, Kedah through GIS Analysis. *International Journal of Geoinformatics*, *19*(5), 19–29. https://doi.org/10.52939/ijg.v19i5.